WARMINGUP

Innovatief Duurzaam Warmtecollectief

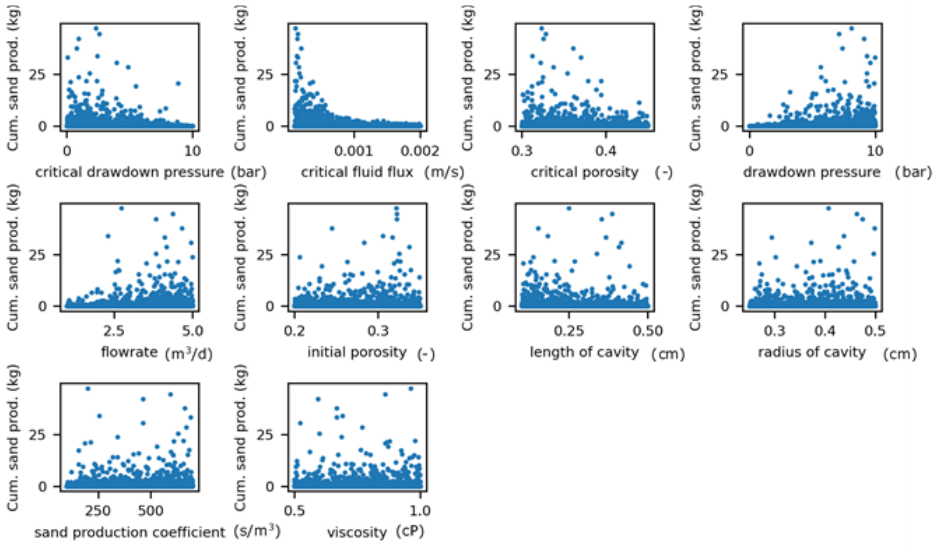

Sand production in shallow geothermal applications

Limit, control, handle

door

E. Peters, D. Dinkelman, D. van Nimwegen, P. Shoeibi Omrani

6 oktober 2022

Sand production in shallow geothermal applications

E. Peters, D. Dinkelman, D. van Nimwegen, P. Shoeibi Omrani
6 oktober 2022

Dit project is uitgevoerd als onderdeel van het Innovatieplan WarmingUP. Dit is mede mogelijk gemaakt door subsidie van de Rijksdienst voor Ondernemend Nederland (RVO) in het kader van de subsidieregeling Meerjarige Missiegedreven Innovatie Programma's (MMIP), bij RVO bekend onder projectnummer TEUE819001.
WarmingUP geeft invulling aan MMIP-4 – Duurzame warmte en koude in gebouwde omgeving en levert daarmee een bijdrage aan Missie B – Een CO_2-vrije gebouwde omgeving in 2050.

Projectnummer
060.43190/01.01.01

Keywords
Sand production, completions, erosion, Brussels Sand

Jaar van publicatie
2022

Meer informatie
Lies Peters

E Lies.peters@tno.nl

Summary

Sand production is a complex process which depends on many aspects of the subsurface and the well completions and operations: in situ stress conditions, consolidation of the sand, size distribution and shape of the particles and the flow velocity of the fluids are important aspects. Three main options to deal with potential sand production where investigated with focus on the relatively shallow formations of the North Sea Groups: limit flow rate/drawdown, control the inflow of particles through completions or handle in the well.

For limitation of the drawdown/flow rate as a sand control method, design criteria that predict the onset of sand production are often used. These criteria indicate that for the very weak rocks (unconsolidated or poorly consolidated) expected in the North Sea groups some form of sand control is required. Thus design criteria based on well bore or perforation stability are not likely to provide useful design criteria. Design criteria limiting the flow rate below the erosion rate are also not likely to be useful: geothermal wells need to operate at considerable rates to be economically viable. To really understand if sand production will be a problem, approaches that can predict the amount of sand production are more useful. However predictive models for both onset and amount of sand produced need to be tuned to the local conditions, which is mostly done using sand production data and experience in existing wells. However, available experience of shallow geothermal production is very limited.

Completions for sand control are mainly different types of screens and gravel packs. The criteria for choosing a particular type of completion are sometimes different for different sources. Clogging of the completions can always be an issue, but some level of clogging can be acceptable before the inflow is significantly affected as the pores in the gravel pack and the screens are typically much larger than the pores in the reservoir. For handling particles in the well, sand hold up and erosion were investigated. Due to the relatively high flow rates in geothermal wells, sand deposition in the well is not likely to be an issue. The risk of erosion is small in the straight sections and the large radius bends. The most likely place for erosion is the ESP, however erosion in the ESP is difficult to simulate and no simple correlations exist.

For the Brussels Sand Mb a detailed analysis was done at the location of Zwijndrecht. For this formation, information was collected in the WarmingUP project. Sand control in the form of metal mesh screens appears to be the most appropriate. Alternatively expandable screens might be an option. There is some disagreement however between the different methods for determining the type of sand control: the sand fraction is reasonably well sorted, but the formation also has a relatively large sub 44 µm fraction. The reasonable sorting typically leads to the advice of a metal-mesh screen. In some methods, the relatively large sub 44 µm fraction leads to the advice of a gravel pack. Due to the relatively large amount of fines, which are predominantly present in the lower parts of the formation, clogging is possibly an issue and some fines will be produced. Careful startup and shutin procedures are required to ensure stability of the formation and the 'natural gravel pack' that will likely develop around the screen. At this point, it is not clear whether a limitation on the flow rate is advisable to avoid clogging of the screens, because it is difficult to determine the risk of clogging of the gravel packs and metal-mesh screens. For the Brussels Sand Mb, the formation productivity/injectivity is not very large and limits due to pressure constraints appear to be more important than due to sand production issues.

Inhoudsopgave

1 Introduction

In the Climate Agreement, it has been agreed that 1.5M houses need to be heated sustainably in 2030. Heating of these houses is currently done using natural gas. Part of these houses will be heated using collective heat networks and geothermal energy is an important source of heat for such networks. Within the WarmingUp project Theme 4, the goal is to accelerate the development and use of geothermal sources for use in urban heat networks. The following 3 main aspects are addressed:

1. Reduction of the geological risk through improved characterisation of the relatively poorly studied shallow subsurface and of marginal reservoirs, fit-for-purpose well designs and integration in heat networks
2. Quantification and control of the risk of induced seismicity and other effects on the environment.
3. Improved performance through optimisation of the production process.

The improved characterisation will primarily be made available via ThermoGIS (thermogis.nl). The goal of ThermoGIS is to present a regional geothermal resource assessment (Vrijlandt, Struijk et al. 2019) to facilitate the use of geothermal resources. In addition to the characterization at national level, three local areas are studied in more detail. The first of these is the area around Zwijndrecht, with the Brussels Sand Member as potential target. Of the shallow formations of Cenozoic age, The Brussels Sand Mb is expected to be one of the most prolific reservoirs and therefore a prime focus in the project. In this report the focus is on sand and/or fines control for geothermal production from the shallow unconsolidated or poorly consolidated formations.

For geothermal production in (shallow) unconsolidated or poorly consolidated formations, the potential production of sand or fines should be taken into account when planning a doublet. If not properly handled sand and/or fines production can have a range of adverse effects such as erosion and clogging of the well and surface facilities and reduced productivity and injectivity. However, unnecessary or inappropriate sand control can increase cost and reduce well productivity over time due to clogging (e.g. (King 2009),(Bellarby 2009)) .

Three main options to deal with potential sand production can be distinguished: limit, control or handle. If the sand production is to be limited, the rate or drawdown at which the wells are produced is limited to such an extent that the sand production is avoided or minimized. For unconsolidated formations, reducing the rate sufficiently to avoid sand production is often not economically feasible. In the second option (control), completions are chosen which control the inflow of sand into the well. These completions can for example be screens or gravel packs. This option means that the resistance to inflow is increased, which is detrimental to the efficiency of the system. In the third option, some sand production is allowed into the well and removed at surface. Sand in the well however, can damage the well, the pump (ESP=Electrical Submersible Pump) and surface equipment. Moreover, separating and removing the sand leads to additional costs. In practice often a combination of methods is used.

Poorly consolidated formations can be found both deep (e.g. the Delft Sandstone up to 2500 m deep) and shallow (e.g. the Brussels Sand at 500 to 800 m depth). The focus here is on shallow, geothermal applications in the North Sea groups between approximately 500 m and 1500 m depth. For this intermediate depth range both methods from shallow and deep applications might be

applicable. The approaches to asses and reduce sand production issues can differ between the ('deep') petroleum industry on the one hand and shallow applications such as the drinking water industry and heat-cold storage (warmte-koude opslag, WKO) on the other hand. For conventional geothermal applications in the Netherlands, generally guidelines for the petroleum industry are followed. However, the shallow geothermal applications considered here are in formations that are not generally used for petroleum production (except at the De Wijk field and offshore A- and B blocks). In addition some of the key characteristics for geothermal production differ from those in the petroleum industry: in particular higher rates and less depletion. Therefore experience from both shallow and deep applications are reviewed in this report and their applicability to shallow geothermal applications is evaluated.

The goal of this report is to:

- Present a literature review of available literature on sand production issues and sand control and management from both deep and shallow applications
- Identify generic solutions for typical conditions found in the North Sea Groups if possible.
- Identify relevant knowledge gaps.
- Apply selected methods to the pilot area of the Brussels Sand near Zwijndrecht if possible (given the limited amount of available data)

The setup of the report is as follows: in Chapter 2, options for limiting sand production by limiting rate or drawdown are investigated (design criteria). These limits can also be used to identify whether sand production is likely to be an issue or not. At the start of the chapter, the process of sand production is discussed. In Chapter 3, methods for controlling sand production using completions are discussed. In Chapter 4 the following is presented: handling sand production in the well and the impact on production and erosion, incl. potential for sanding up of the well. And in Chapter 5, for the Brussels Sand in Zwijndrecht, sand production is estimated and the impact on possible well designs will be discussed.

2 Limit sand production

2.1 The process of sand production

The process of rock failure and sand/fines production is well described in e.g. (Vardoulakis, Stavropoulou et al. 1996), (Rahmati, Jafarpour et al. 2013) or (Van den Hoek, Geilikman 2005). For consolidated rock the first step is failure of the rock and then the failed rock is transported to the well. Rock failure is primarily a mechanical process. The transport/production of the failed sand is directly related to the flow induced strain and can be related to applied drawdown. This explains for a large part the differences in approach for deep and shallow. The rock failure part does not need to be taken into account for unconsolidated sand, since the formation will be weak/failed already and only the transport part is relevant. This also means that initial instability of a well bore is a necessary, but not a sufficient condition. In most cases, some initial sand production (often referred to as transient sand production) can be cleaned from the well. *The important step is to understand if sand production will become a problem and sand control measures are required*. To achieve this, the sand production rate should generally be estimated taking into account the transport. The two processes of failure and transport are interrelated (Vardoulakis, Stavropoulou et al. 1996): sand production reduces the rock strength and thus increases the likelihood for failure. This is reproduced in models predicting the sand production rate and described by the growth of a plastic zone around the well or perforation ((Van den Hoek, Geilikman 2003) and (Fjaer, Holt et al. 2008)).

Failure mechanisms
Failure of rocks in boreholes occurs mostly as shear failure, in particular when considering stability of a cylindrical hole. Many wells in the petroleum industry are however cased and perforated and the sand production occurs at the perforation rather than from the well bore. Thus for sand production also different failure mechanisms can be important as described in (Fjaer, Holt et al. 2008)(e.g. worm-holing, tensile failure). Tensile failure can for example occur at the tip of perforations. A sand production stability diagram ((Morita, N., Whitfill et al. 1989, Morita, N., Whitfill, Massie et al. 1989)) can be created to define safe production conditions based on different failure mechanisms. In such a diagram, also the impact of depletion can be included. For petroleum reservoirs, the depletion caused by production of hydrocarbons destabilizes the formation. This means that many reservoirs that initially do not experience sand production, can start to produce sand later in the field life (see e.g. (Bellarby 2009, Hettema, Andrews et al. 2006)). Around perforations sand arches can improve the stability in weak or unconsolidated formations (section 10.2.4 from (Fjaer, Holt et al. 2008)).

Sand transport
Transport of failed rock is mostly described by considering the hydrodynamic forces on a grain on the surface of the rock or a loose grain ((Vardoulakis, Stavropoulou et al. 1996), (Fjaer, Holt et al. 2008)). Since the transport is assumed to occur in failed rock, the strength of the rock is further ignored. The hydrodynamic forces acting on a particle increase with increasing fluid flow rate and size of the particle. The forces needed to be overcome to transport the particle (assuming the zero rock tensile and cohesive strength for an unconsolidated sand) are determined by the effective axial and tangential stresses on the particle, the coefficient of internal friction and the particle size. (Fjaer, Holt et al. 2008) show that even for a very weak rock the hydrodynamic forces are smaller than the forces needed to move the particle from the rock. The analysis also implies that for larger

depth (and thus higher effective axial and tangential stresses and shear strength), sand and fines are more difficult to remove from an intact matrix of grains (even if they are unconsolidated). This was also shown in the experiments by (Al-Awad, El-Sayed et al. 1999) in which they noticed a decrease in sand production with confining pressures. This in contrast to (Papamichos 2018) who concluded on the basis of experiments that sand production rate increased with the applied stress. The difference is the setup of the experiments: the experiments by Papamichos were representative for perforations in relatively competent rock, whereas (Al-Awad, El-Sayed et al. 1999) analysed the flow through a sand pack under different confining stress. In the setup of (Papamichos 2018), sand and fines are produced from failed rock in a cavity: increasing confinement means increased failure of rock. The setup of (Al-Awad, El-Sayed et al. 1999) is more appropriate for an unconsolidated formation which is produced using a screen or gravel pack in which it is assumed that there are no cavities.

The factors impacting sand production (e.g. (Fjaer, Holt et al. 2008, Bellarby 2009, Khamehchi, Reisi 2015, Veeken, Davies et al. 1991)) related to the formation are:

- Reservoir depth and in-situ stress conditions (including the effects of depletion)
- Reservoir pressure and fluids (gas/oil/water)
- Formation characteristics (strength, cementation, permeability, shape of sand particles and particle size distribution (Fattahpour, Moosavi et al. 2012)).

Factors related to well and operations are:

- Flow conditions: drawdown, flow rate, fluid type, depletion of the reservoir. Not only the steady state flow conditions but also transient effects are important. See for example bean-up guidelines for sand production in (Van den Hoek, Geilikman 2006) and (Wong, Dria et al. 2005).
- Well bore parameters: orientation and diameter (smaller is more stable, which is clear from experiments but not included in many theoretical analysis), completions, perforations

Sand control completions

The discussion of sand production so far was focused on producing sand from a perforation cavity or well bore. However, if we consider a well bore with gravel pack or screen/slotted liner, the situation is very different. Assuming no annular space or an annular space that is filled up (gravel pack or natural gravel pack), sand and fines migration within the formation and completion is important (Wan, Liu et al. 2006). Now the processes of clogging within the pores and openings in the screen or liners need to be considered (Zare-Reisabadi, Safari-Beidokhti 2014, Ahad, Jami et al. 2020). Larger particles cannot move through the narrow pore throats in the formation or the liners. Bridging of particles reduces this even further. Sand retention tests (Ahad, Jami et al. 2020) can be done on completions to determine clogging for given formation characteristics. This is further discussed in Chapter 3.

In shallow applications, the focus for the design criteria is in many cases on clogging risks and design criteria for injection wells and also to some extent for production wells are focused on preventing clogging of the completions (KWR 2011). The maximum injection rate criteria take into account the suspended solids and a specific clogging velocity of the completion (see Section 2.2). For ‘deep’ applications such limits to reduce the flow rate are not common. For injection wells, the water is filtered before injection: the filter size is determined to remove sufficient particles in order to avoid clogging. (De Zwart 2007) presents an overview of the aspects in the subsurface affecting mobilization and deposition of fines for water wells. The author concludes that particle concentration strongly affects clogging and that bridging depends critically on the pore-particle

aspect ratio. Thus higher flow rates can lead to a higher concentration of particles and increased clogging of completions.

Case studies
Several case studies can be found in literature which describe control strategies for sand production. For example (Kjorholt, Joranson et al. 1998) and (Hettema, Andrews et al. 2006) detail the strategy by Statoil, which is based on a combination of modelling and testing wells for an "acceptable sand production rate". Different predictive models are compared to data from the Statfjord Field and different sand production regimes defined in particular for increasing depletion of the field (Hettema, Andrews et al. 2006). (Al-Awad, El-Sayed et al. 1999) presents lessons learned in Saudi oil and gas reservoirs. (Mohd Jamil 2011) present a simple approach for cases with little information based on wave velocity. Applying such strategies or approaches to a new location with little data such as shallow geothermal is difficult, because they are geared towards specific locations and/or companies and often require data which is not available. However, they are useful for defining the steps towards a suitable sand production strategy.

Injectors in unconsolidated formations
Unconsolidated formations are also a risk for injection wells. Even if injection water is filtered and clogging is not an issue, in some wells failure of the formation can be caused by the water hammer effect during emergency or normal shutin. A well-documented case study is the Heidrun field which was presented in several publications (see e.g. (Santarelli, Skomedal et al. 2000) or an overview in www.advntk.com/pwrijip2003/pwri/final_reports/task_5/Statoil%5CHeidrun%5CHeidrun1.htm (access date Aug 2021)). Adjustment of procedures for emergency shutdown and minimum shutdown duration were implemented successfully and no further losses of injectivity were observed. Another case has been presented by Conoco (Morita, Nobuo, Davis et al. 1998), which followed a different approach to solve the problem.

2.2 Design criteria to limit sand production in unconsolidated, shallow applications (up to 500 m depth)

In unconsolidated shallow applications such as groundwater production for drinking water or low temperature aquifer thermal energy storage (ATES), failure of the formation is generally not accounted for. It is assumed that the formation is weak enough for the particles to be transported. Internal and surface particle migration is caused by erosion and transport due to drag forces caused by the fluid velocity. Thus in shallow formations, sand control is generally required. Some form of screen, filter or gravel pack is always installed and the design criteria are based on a maximum production or infiltration rate limited by sand production or clogging (Bloemendal, Lopik et al. 2020).

Drinking water guidelines (~20-200 m depth)
The maximum fluid velocity at the borehole wall (often called 'at the sandface' in petroleum engineering) and flow rate are dependent on the type of aquifer and are therefore highly variable. The aquifers used for drinking water extraction are often shallow (~20-200 m depth) and coarse-grained ((Buik, N., Bakema 2019). For the calculation of the maximum flow velocity at the borehole wall for drinking water extraction wells, the formula of (Sichardt 1928) can be used:

$$v_{max} = \sqrt{K}/15 \qquad (2\text{-}1)$$

v_{max} maximum flow velocity at the borehole wall (m/s)
K hydraulic conductivity of aquifer at 12°C (m/s) , which can be calculated from:

$$K = \frac{\rho_f \cdot g}{\mu} \cdot k_i$$

ρ_f density of fluid (kg/m^3)
g gravitational force (9.81 m/s^2)
μ viscosity of fluid (Pa·s)
k_i intrinsic permeability (m^2)

The relation between v_{max} and K has been found empirically based on hydrological research into a large number of wells. In practice, the formula of (Huisman 1969) is often used. This formula is more conservative (Sichardt formula divided by 2) and takes better into account the length of the filter:

$$v_{max} = \sqrt{K}/30 \qquad (2\text{-}2)$$

These formulas are not scientifically validated. However, it is advised to use the Huisman formula unless better information about the maximum flow rate in the wells is available (van der Schans, Meerkerk 2019).

Infiltration wells (generally referred to as 'injection well' in petroleum engineering) are not necessarily used for drinking water production. If they are used, the maximum velocity is generally based on the guidelines for low temperature aquifer storage (guidelines by NVOE (Nederlandse Vereniging voor Ondergrondse Energie Opslag (nu BodemenergieNL)) (NVOE 2006, IF Technology 2001, Buik, N. A., Willemsen 2002):

$$v_{max} = 1000 \left(\frac{K}{150}\right)^{0.6} \sqrt{\frac{v_v}{2 * MFI_{mea} * U_{eq}}} \qquad (2\text{-}3)$$

v_{max} maximum flow velocity at the borehole wall (m/h)
K hydraulic conductivity (m/d)
v_v specific clogging velocity (m/a)
MFI_{mea} measured Membrane Filter Index (MFI) which is a measure for the amount of suspended particles in groundwater (s/l^2)
U_{eq} equivalent full load hours per year (h/y)
The MFI is the increase of the resistance of the membrane filter per liter of water infiltrated and depends on the pore size of the filter (IF Technology 2001). Generally it is lower than 5 s/l^2.

Low-temperature ATES guidelines (~20-250 m depth)
For the low-temperature ATES systems, the infiltration norm was presented in the previous section (eq. 2-3). The norm for the maximum production flow rate for an ATES system is different from that for drinking water and is given as:

$$v_{max} = K/12 \qquad (2\text{-}4)$$

v_{max} maximum flow velocity at the borehole wall (m/h)
K hydraulic conductivity (m/d)

This production flow velocity norm is applied for a large amount of ATES systems (>> 1.000 systems) and the number of projects that had problems with sand production was small. Some systems experienced sand production, the reason for this is not necessarily exceedance of the

norms but could also be due to the wrong choice in screen, gravel pack etc. This shows that the guidelines are safe, but can also imply a larger flow rate margin (van der Schans, Meerkerk 2019). Specific for storage wells is that the flow direction is reversed every half year, which may affect the clogging potential.

High-temperature ATES (~150-500 m depth)
High-temperature ATES (HT-ATES) systems are often located in fine-grained sandy aquifers, with generally a lower hydraulic conductivity than the aquifers used for LT-ATES and drinking water extraction. Due to the higher temperatures involved, the hydraulic conductivity will not only be dependent on the characteristics of the porous medium (sediment) but also the viscosity and density of the fluid flowing through this porous medium. The viscosity and density are dependent on temperature, and to a lesser extent on pressure and salinity. Therefore the low-temperature NVOE guidelines are adapted for higher temperatures by including viscosity and density in the formula (IF Technology 2012):

$$\text{for production} \quad v_{max} = 7200 * \frac{\rho_f \cdot g}{\mu} \cdot k_i \qquad (2\text{-}5)$$

$$\text{for infiltration} \quad v_{max} = 1000 \left(576 * \frac{\rho_f \cdot g}{\mu} \cdot k_i\right)^{0.6} \sqrt{\frac{v_v}{2 * MFI_{mea} * U_{eq}}} \qquad (2\text{-}6)$$

v_{max} maximum flow velocity at the borehole wall (m/h)
K hydraulic conductivity (m/d)
ρ_f density of fluid (kg/m^3)
g gravitational force (9.81 m/s^2)
μ viscosity of fluid (Pa·s)
k_i intrinsic permeability (m^2)
v_v specific clogging velocity (m/a)
MFI_{mea} measured Membrane Filter Index (s/l^2)
U_{eq} equivalent full load hours per year (h/y)

In fine-grained aquifers, the infiltration velocity is less critical than the production/extraction velocity. Also, the depth of the aquifer has an impact on the maximum flow velocity that can be reached without sand production or clogging. With increasing depth, the stresses on sediment increase due to the overburden and gravity. This causes the loose sand grains to be mobilized less easily. This aspect is not included in the NVOE guidelines, and therefore these guidelines are, in general, too conservative for deeper fine-grained formations.

The HT-ATES pilot study in Middenmeer (NL) (Uitvoeringsteam WINDOW (IF Technology, TNO, Deltares, KWR) 2020) is an example of a deeper located aquifer (360-383 m) that is used for injection and production of hot water. Well tests proved that the flow velocities at the wellbore could be exceeded by at least 2,44 times the current NVOE norms for flow velocity (higher velocities could not be tested due to practical reasons). This suggests that higher flow rates can be reached at higher depths, however, this is based on one pilot and cannot be automatically applied to other regions in the Netherlands. Also, the effect of a higher flowrate on the mobilization of particles and clogging in the long term has to be investigated.

2.3 Criteria for onset of sand production for consolidated applications

For consolidated or semi-consolidated applications, generally first an estimate is made to check whether the rock is likely to fail given the rock strength and in situ stress conditions. This is an

indication that sand production is possible (the onset of sand production). To do this, in many cases a criterion is used which based on a failure model, which evaluates the possible failure of a cylindrical hole (perforation or open hole) in a stress field. This is described in many textbooks (e.g. (Bellarby 2009, Fjaer, Holt et al. 2008)). However, empirical relations are also commonly used. In the following different approaches and criteria for the onset of sand production or to determine whether sand production is required are described below.

Many of the criteria for the onset of sand production take the form of a critical drawdown. Such a criterion can also be used as a design criterion, for example by specifying that the drawdown has to be less than the estimated critical drawdown.

Empirical rules

Empirical rules of thumb to determine whether sand production is required are usually based on sonic velocity or porosity. Examples of different rules of thump are presented in Table 2-1. Several are based on sonic transit time: $\Delta t = 1/V_p$ (Vp is the primary wave velocity). Δt is defined as the time for a compressional wave to travel a distance of 1 ft. (King 2009) presents the most extensive list of possible rules of thumb. (Bellarby 2009) mentions similar numbers of 30% porosity or sonic time larger than 120 μs/ft. (Mohd Jamil 2011) state that for a sonic transit time of more than 90 μs/ft sand prone intervals can be expected. A disadvantage of such rules of thumb is that they are very coarse and need local calibration.

Table 2-1. Examples of empirical rules to determine whether sand control is required.

Variable	Criterion	Source
Sonic transit time	> 90 μs/ft: may need control	(King 2009) (Mohd Jamil 2011)
	> 120 μs/ft: likely to require control	(King 2009) (Bellarby 2009)
Porosity	0.2 – 0.3: may need control	(King 2009)
	> 0.3: likely to require control	(King 2009) (Bellarby 2009)
Reservoir pressure	Rocks below 69 bar (1000 psi) may need sand control	(King 2009)
	Drawdown > 1.7 times compressive formation strength	(King 2009)

When we compare the properties of potential shallow geothermal reservoirs in The Netherlands with these criteria, we can see that the sonic transit time would be about 150 μm/ft with a minimum of around 140 μm/ft. This is based on the velocities from the VELMOD 3.1 model published in (Pluymaekers, Doornenbal et al. 2017) (Figure 2-1) for the North Sea Groups (marked in yellow 'N'). These velocities are close to the velocities for unconsolidated formations (e.g. Figure 1 from (Mukerji, Mavko 2006)). This means that all the formations from the North Sea groups require sand control according to the empirical rules in sonic transit time.

For porosity, a recent petrophysical analysis for the Brussels Sand Mb (Geel, Foeken 2021), showed average effective porosity in the range of 0.25 to 0.3. Total porosity is higher. The best producing intervals generally have a porosity over 0.3, also indicating the requirement for sand control based on the criteria in Table 2-1.

The criteria based on reservoir pressure are not relevant for geothermal, because the aquifer is not depleted like an oil or gas reservoir.

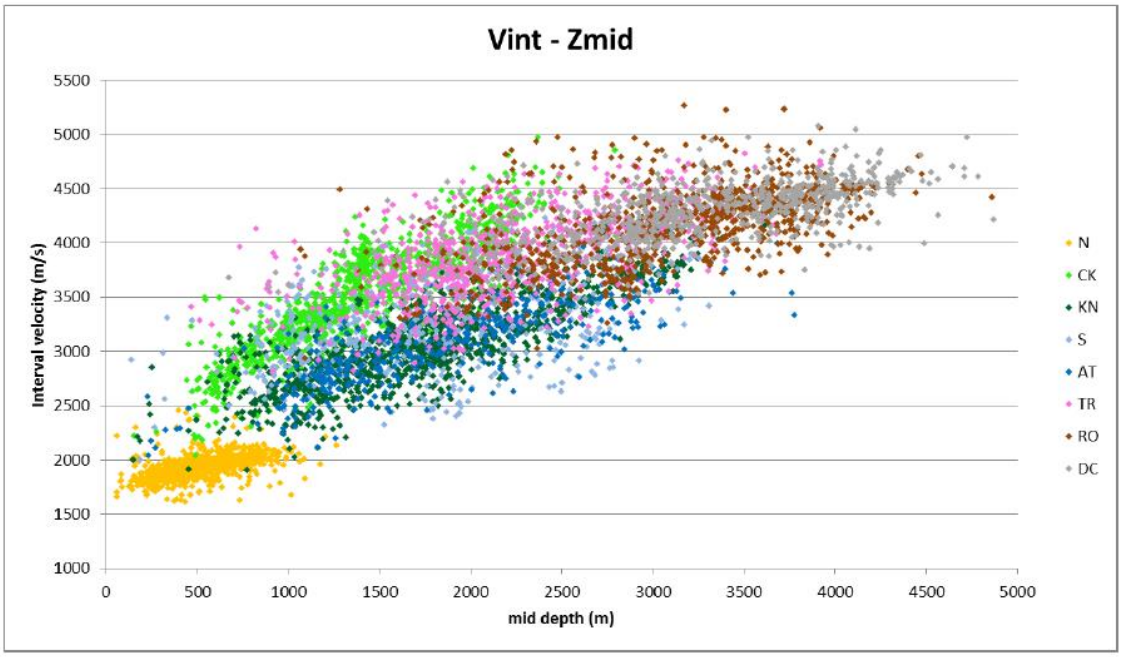

Figure 2-1. Interval velocity vs mid depth for each main lithostratigraphic group (North Sea Groups ('N') are marked in yellow) (source: (Pluymaekers, Doornenbal et al. 2017)).

Analytical failure criteria

Many analytical criteria are available to determine whether sand control could be a problem. Many of the criteria are based on shear failure around a cylindrical hole. The solution of the stresses around the cylindrical hole are usually based on the so-called Kirsch equations (e.g. (Zoback 2007, Fjaer, Holt et al. 2008)). Discussions of different failure criteria can be found in (Bellarby 2009), (Wojciechowski 2018) and (Papamichos 2020). Main difference between different criteria are how the detailed the (anisotropic) stress conditions are taken into account. It is know that these criteria based on shear failure are generally conservative for determining whether sand production is an issue. (Bellarby 2009) discusses possibilities for making the criterion less conservative: for example by taking the smallest difference between the stresses instead of the largest. A general issue with these criteria is that they do not take into account the drag of fluid flow into account and thus are not very good at prediction of sand production will be a problem after the initial burst. Since the required rates in geothermal are mostly very large, this is a serious limitation.

To define a failure criterion for a borehole, the stresses around an open hole in the rock given an anisotropic stress field need to be resolved. This is described in many textbooks, see for example (Zoback 2007) and (Fjaer, Holt et al. 2008) and will not be discussed here. The solutions are generally referred to as the Kirsch equations because they are extensions of the original solution presented by (Kirsch 1898). In Figure 2-2 the tangential stresses around the wall of a horizontal borehole are illustrated here for the a normal faulting regime with borehole axis parallel to the maximum horizontal stress σ_H (S_H in the figure).

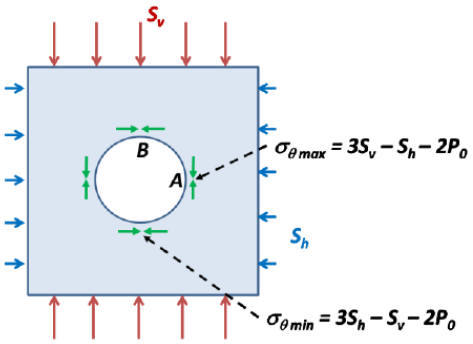

Figure 2-2. Illustration of the Kirsch solution for the tangential stresses around the wall of a horizontal borehole, illustrated here for a normal faulting regime with the borehole parallel to S_H. Source: (Latham, Farsi et al. 2019).

The critical well pressure described by (Bellarby 2009) assumes yielding when the effective tangential stress equals the yield strength of the material (σ_{yield}). For a vertical well in a normal stress regime with $\sigma_v > \sigma_H > \sigma_h$ this becomes:

$$p_{w,cr} = \frac{3\sigma_H - \sigma_h - \sigma_{yield} - Ap_r}{2 - A} \qquad (2\text{-}7)$$

With

$$A = \frac{1 - 2\nu}{1 - \nu}\alpha$$

Where

σ_{yield}: yield strength
σ_v : vertical stress
σ_h : minimum horizontal stress
σ_H : maximum horizontal stress
p_r : reservoir fluid pressure
ν : Poission's ratio
α: Biot's constant

The stresses can be adjusted depending on the orientation of the well or of the stress field. In that case σ_H is replaced by the largest of the stresses and σ_h by the smallest.

(Fjaer, Holt et al. 2008) define a generalised critical drawdown p_d^c as:

$$p_d^c = A1(C_0 - 2\sigma_{is}') + A2 \qquad (2\text{-}8)$$

Where:

σ_{is}' : effective in-situ stress
C_0 : uni-axial compressive strength

A1 and A2 are parameters that depend on the rock properties, but may be estimated from data. For a vertical well, the critical drawdown can be calculated as:

$$p_d^c = (1 - \nu)(C_0 - 3\sigma_H' + \sigma_h') \qquad (2\text{-}9)$$

The prime indicates effective stresses which are calculated here as $\sigma_H' = \sigma_H - p_r$.

(Latham, Farsi et al. 2019) provide an interesting discussion on well bore stability. They define a range in which a bore hole becomes unstable: from 'stable with breakouts' (equivalent to the Mohr Coulomb criterion) to 'unstable'. The criterion for 'unstable' follows (Zoback 2007): "Maintaining initial breakout width to <90° has been suggested as an effective criterion for achieving a desired degree of wellbore stability (Zoback 2007)". This could possibly be interpreted as a range for sand production with three regions: no sand, possible sand production, sand production. A disadvantage is that this also does not include the flow velocity as a factor. Therefore this has not been investigated further.

(Khamehchi, Reisi 2015) propose yet a totally different approach: they propose a sand production prediction method using the ratio of shear modulus to bulk compressibility. This has not further been investigated.

For some conditions a total failure of the formation can occur, which is often referred to as a Bratli-Risnes event. As stated in (Van den Hoek, Geilikman 2003): "According to the well-known Bratli-Risnes criterion, applying a drawdown beyond a specified 'tensile failure' limit leads to cavity collapse and subsequent massive sand production". This can occur for very weakly consolidated or unconsolidated formations in which the cavity does not stabilize after a failure. A Bratli-Risnes type of event occurs in particular during start-up or shut-down procedures and less during (high-rate) production (Van den Hoek, Geilikman 2005).

A different approach is the Drucker-Prager criterion proposed by (Buik, N., Bakema 2019). The major difference is that this criterion is for intact rock and not based on the Kirsch solution for stresses around an open hole. Thus this criterion determines when shear failure is likely to occur in the rock at some distance from the stress disturbance around the well. In that case, the increasing stress on the grains with depth increases the strength and likely reduces sanding in intact formation. This could represent the possibility for sand production from the formation outside of the direct vicinity of the well, in particular for wells without annular space (e.g. gravel packs). In addition the criterion takes into account all three major stress directions. As strength criterion for the formation, the cohesion or cohesive strength is used. The results of this criterion will be shown in Section 2.4.

$$p_d^c = \alpha_D I_1 + k_D - \sqrt{J_2} \qquad (2\text{-}10)$$

Where

$$I_1 = \sigma_1' + \sigma_2' + \sigma_3' \qquad (2\text{-}11)$$

$$J_2 = \tfrac{1}{6}[(\sigma_2' - \sigma_2')^2 + (\sigma_2' - \sigma_2')^2 + (\sigma_2' - \sigma_2')^2] \qquad (2\text{-}12)$$

$$\alpha_D = \frac{2\sin\varphi_f}{\sqrt{3}(3-\sin\varphi_f)} \qquad (2\text{-}13)$$

$$k_D = \frac{6S_0\cos\varphi_f}{\sqrt{3}(3-\sin\varphi_f)} \qquad (2\text{-}14)$$

$\sigma_1', \sigma_2', \sigma_3'$: effective stresses in 3 main directions.
φ_f : angle of internal friction
S_0 : cohesion

For a very weak rock, cohesion is around 1 MPa (10 bar). The friction angle φ_f is taken as 33° in this report (Buik, N., Bakema 2019).

2.4 Comparison of criteria for the Dutch subsurface

A comparison of different criteria for limiting sand production was presented by (Buik, N., Bakema 2019). The authors presented the criteria as a function of hydraulic conductivity. The lowest value considered was 2 m/d. However, the hydraulic conductivity encountered in de formations of the North Sea Groups which are considered for geothermal development are generally below 1 m/d. For example the Brussels Sand near Zevenbergen is estimated to have permeability of 750 mD in the best reservoir layers (Buik, N., Bakema 2019), which is equivalent to 0.7 m/d at the in situ brine conditions. (Geel, Foeken 2021) estimate similar values for permeability for the rest of the Brussels Sand. Therefore here different criteria from sections 2.2 and 2.3 will be compared and it will be analysed how they change with depth for typical Dutch subsurface conditions.

Norms from the drinking water industry were not implemented, because (Buik, N., Bakema 2019) already concluded that they are far too conservative.

2.4.1 Input as a function of depth

To estimate the criteria for limiting sand production, first some input needs to be defined. All calculations were done with a vertical resolution of 50 m.

For the in situ stress conditions the following approximations were used assuming a normal faulting regime.
Lithostatic stress (vertical):

$$\sigma_v = \int_0^D \rho_b(z) g \mathrm{d}z \qquad (2\text{-}15)$$

Where
ρ_b: bulk density of formation, calculated as $(\varphi\rho_r + (1-\varphi)\rho_w)$ with the density of the grains ρ_r=2600 kg/m^3, φ is porosity and ρ_w is density of the brine depending on salinity, pressure and temperature following (Spivey, McCain et al. 2004).

Since it is expected that in shallow un- or poorly consolidated formation, tectonic stress build-up does not play a big role, the minimum in situ stress (σ_h) is approximated by an approach that is suitable for areas with little tectonic influence:

$$\sigma_h = \frac{\nu}{1-\nu}(\sigma_v - p_r) + p_r \qquad (2\text{-}16)$$

where
ν : Poisson's ratio
P_r : fluid pressure in the reservoir
This results in values close to those used for the Dutch subsurface in (De Kler, Neele et al. 2016, Verweij, Simmelink et al. 2012) of $\sigma_h = 0.6\sigma_v$.

For the highly uncertain, intermediate or maximum horizontal stress (σ_H) we assume an isotropic model ($\sigma_H = \sigma_h$)(e.g. (van Eijs 2015)). To check the impact of this assumption also the conservative assumption of an anisotropic stress (in terms of well bore stability) is tested (Bellarby 2009):

$$\sigma_H = \frac{\sigma_v + \sigma_h}{2} \qquad (2\text{-}17)$$

Possion's ratio ν was assumed to increase from 0.24 at surface to 0.29 at 2500 m depth. For Biot's constant α a value of 0.9 was used (Bellarby 2009).

In Figure 2-3 the stresses are plotted as a function of depth.

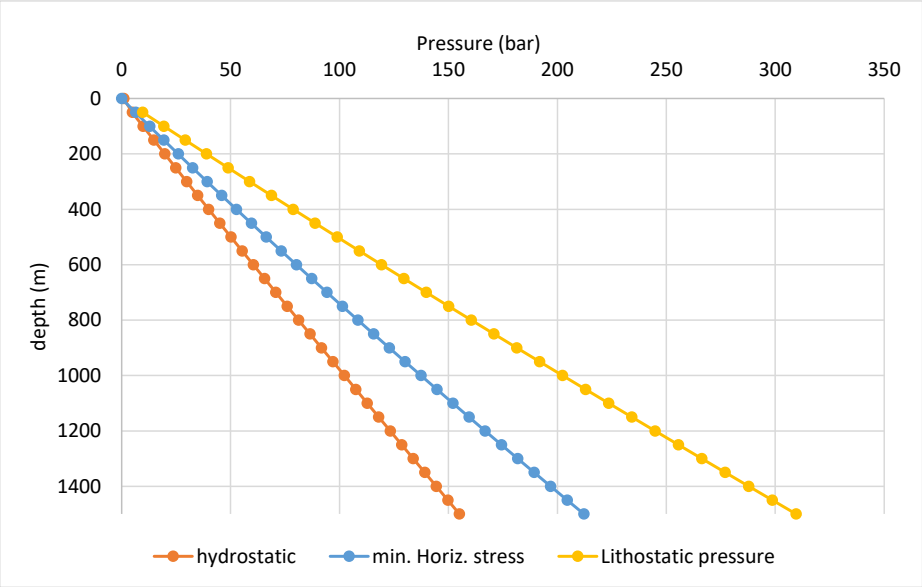

Figure 2-3. Overview of the different stresses as a function of depth

Temperature is assumed to increase with depth according to:

T = 10°C + 0.031 * depth (in m) (2-18)

The brine salinity increase linearly with depth from zero to 15 weight %. Hydrostatic pressure is calculated from the density with depth.

For the (total) porosity in the calculation of the vertical stress gradient, a function changing with depth was used according to Athy's law (Figure 2-4):

$$\varphi = \varphi_0 e^{-a*depth} \quad (2\text{-}19)$$

With φ_0=0.4 and a = 0.32E-3.

For the failure criteria different strength characteristics are used: yield strength, uni-axial compressive strength (C_0 or UCS) and cohesive strength (S_0). (Bellarby 2009) advises results from TWC (Thick Wall Cylinder) experiments as the most representative strength for failure of boreholes. The values have to be adjusted to the hole size however, where smaller holes (such as perforations) are stronger than larger holes.
It is difficult to define the strength of typical Paleogene and Neogene formations. In general formation strength increases with depth due to increasing normal stress and due to compaction and diagenesis. For unconsolidated sediments, shear strength τ increases with effective confining or normal stress σ'_N as:

$$\tau = S_0 + \sigma'_N \tan\theta \quad (2\text{-}20)$$

Where S_0 is cohesion and θ is the friction angle. Due to compaction and diagenesis the increase will be more. Two cases are simulated: one in which the increase in strength is purely the increase in shear strength due to normal stress (with S_0 = 1 bar and θ = 30°) and a second one in which the rock strength increases. A rather arbitrary increase in yield strength was assumed which reaches

around 300 bar (30 MPa) at a depth of 1500 m, which is in line with a weak sandstone. This change over depth is illustrated in Figure 2-4. In addition, a case will be shown for a rock with a constant yield strength of 50 bar (5 MPa) with depth which is representative for a weakly consolidated rock.

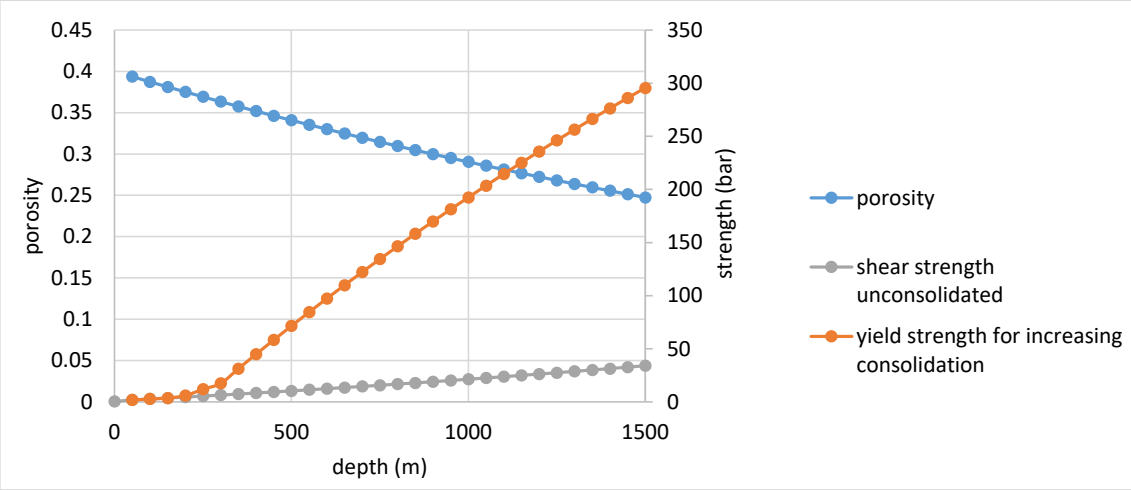

Figure 2-4. Porosity, shear strength for unconsolidated formation due to effective normal stress (no compaction included) and yield strength increasing with depth due to consolidation and cementation.

2.4.2 Results

ATES norms

For the high temperature ATES norms (eq. 5) a case was calculated for a constant permeability of 750 mD. The maximum flow velocity on the borehole wall is translated to a maximum drawdown using a diameter of 0.15 m and reservoir diameter of 1000 m with the inflow equation for inflow into a fully-penetrating vertical well (Dake 1983). Figure 2-5 shows the hydraulic conductivity K as a function of depth for k=750 mD due to the changes in viscosity and density. Figure 2-6 shows the maximum drawdown according to eq. 5 and with the depth correction as used in (Uitvoeringsteam WINDOW (IF Technology, TNO, Deltares, KWR) 2020). Even with the depth correction the allowed maximum drawdown is very small: around 1 bar for the depth of 600 to 700 m at which the Brussels Sand is located. Since the depth correction was 'ad-hoc', it is not surprising that it is not likely to be applicable for other cases without adjustment.

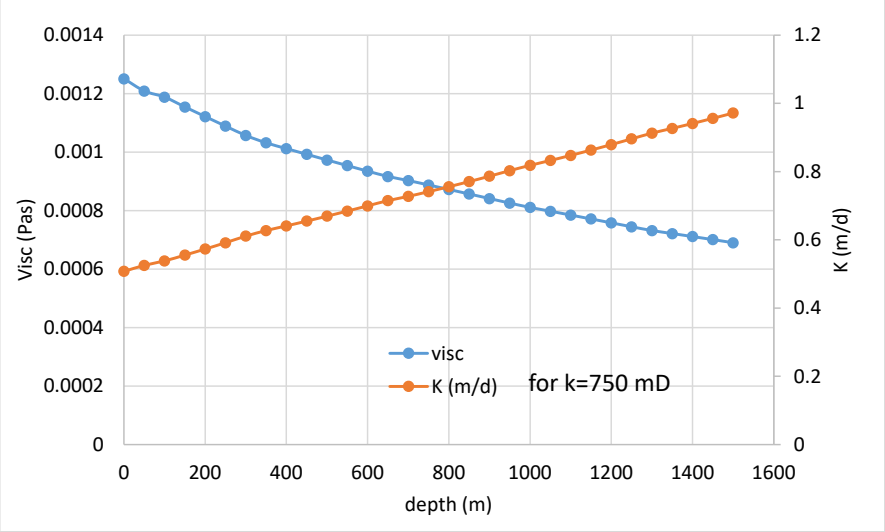

Figure 2-5. viscosity and hydraulic conductivity K with depth. Permeability is 750 mD, salinity increases with depth.

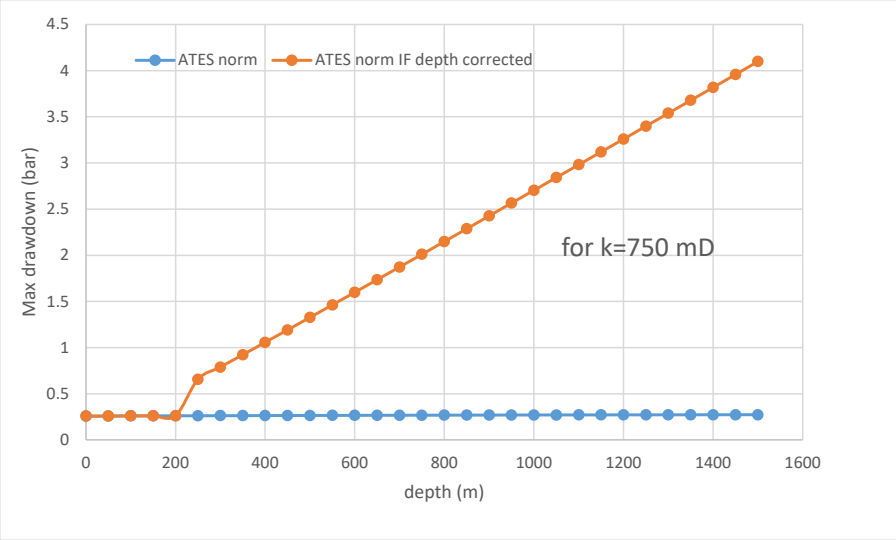

Figure 2-6. High temperature ATES norms for a formation with permeability of 750 mD.

Failure criteria open-hole/perforated

Since the failure criteria proposed by Bellarby and Fjaer do not differ much, only the results from Bellarby are presented. For comparison, the maximum injection pressure according to the SodM (State Supervision of Mines) guidelines (0.135 bar/m* depth) (Protocol bepaling maximale injectiedrukken bij aardwarmtewinning | Publicatie | Staatstoezicht op de Mijnen (sodm.nl)) is plotted in the graph, which is often a limit for deeper geothermal developments. Assuming similar injectivity and productivity (at the same temperature) comparison of the pressure limits shows what would be limiting.

In Figure 2-7 the case for a constant yield strength of 50 bar (5 MPa) is presented as well as the case for an unconsolidated formation with only shear strength (both assuming isotropic stress conditions and a vertical well). For the case with fixed strength, the critical drawdown becomes negative below 400 m, which means that even without drawdown the open hole is not stable and thus will likely produce sand. With increasing depth, the hole becomes less stable. If only shear

strength is accounted for, then the critical drawdown is always negative (and thus sand production is expected). This is because the shear strength resulting from confining stress is relatively small (Figure 2-4).

For the second case, rock strength is assumed to increase with depth as shown in Figure 2-4. The results are presented in Figure 2-8. For the first 200 m it was assumed that the yield strength is very small. In this interval the critical drawdown is negative, which means that a hole is not stable and sand production is likely to occur. After that depth, the yield strength increases and at a depth of 350 m, the critical drawdown becomes positive. At a depth of around 400 m, the critical drawdown becomes larger than the pressure difference allowed for injection. In the case of a doublet with similar injector and producer, that would mean that the pressure limits due to sand production is not likely to be ever reached because the injection limit would be reached first. Also illustrated is the case where the horizontal stress is anisotropic according to equation 2-17. This makes the hole less stable. The anisotropic conditions are also representative for a horizontal well or perforation. This illustrates why orientated perforation are used in many cases to avoid sand production (Hettema, Andrews et al. 2006, Kjorholt, Joranson et al. 1998).

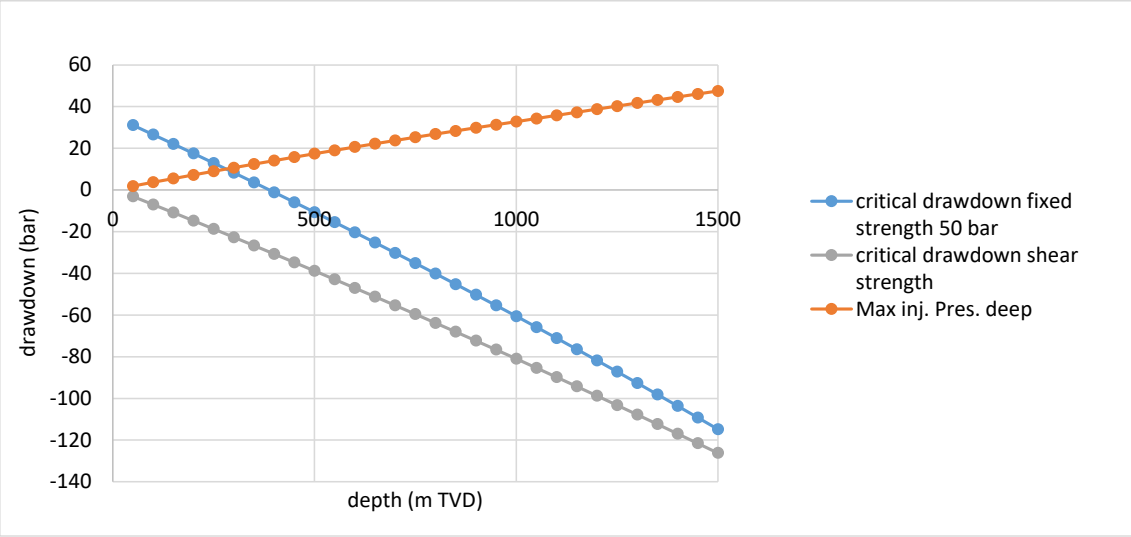

Figure 2-7. Critical drawdown according to eq. 7 for a rock with a yield strength of 50 bar (5 MPa). Also shown is the maximum injection pressure (difference with the hydrostatic pressure).

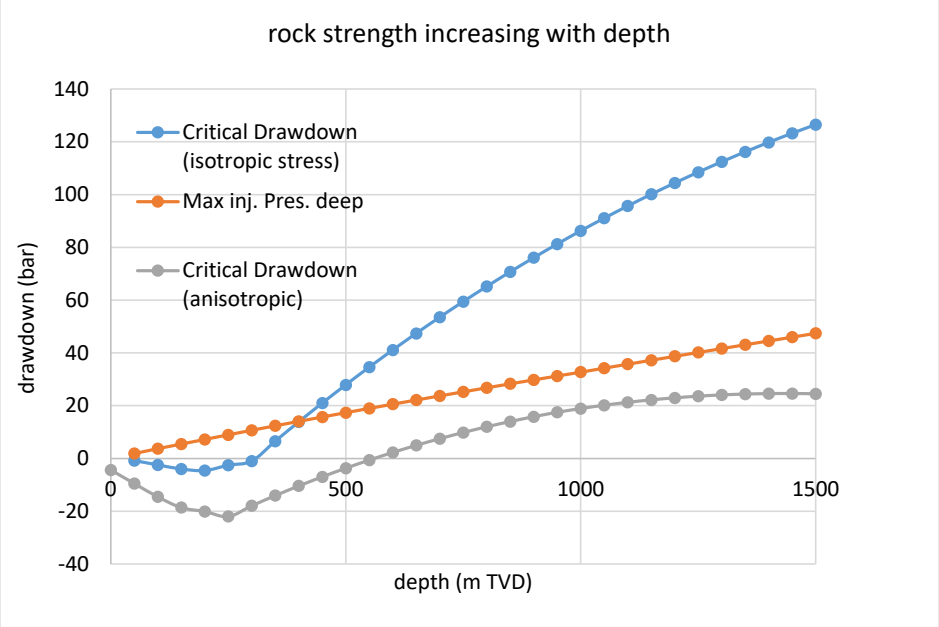

Figure 2-8. Critical drawdown for a vertical well for a formation with increasing yield strength with depth (see Figure 2-4) for an isotropic and anisotropic stress field. Also shown is the maximum injection pressure (difference with the hydrostatic pressure).

Drucker-Prager

The critical drawdown resulting from the Drucker-Prager criterion as proposed by (Buik, N., Bakema 2019) behaves very differently from the other criteria (Figure 2-9). The critical drawdown in Figure 2-9 is for a cohesive strength of zero (resulting in k_d=0 in eq. 10). The maximum amount of drawdown increases with depth. This is because this criterion is for intact rock and not for an open hole and the shear strength increases with depth due to the internal friction (Keaton 2018). The allowed drawdown for a rock with zero cohesion obviously is much higher for this criterion, although still lower than the maximum allowed injection pressure difference.

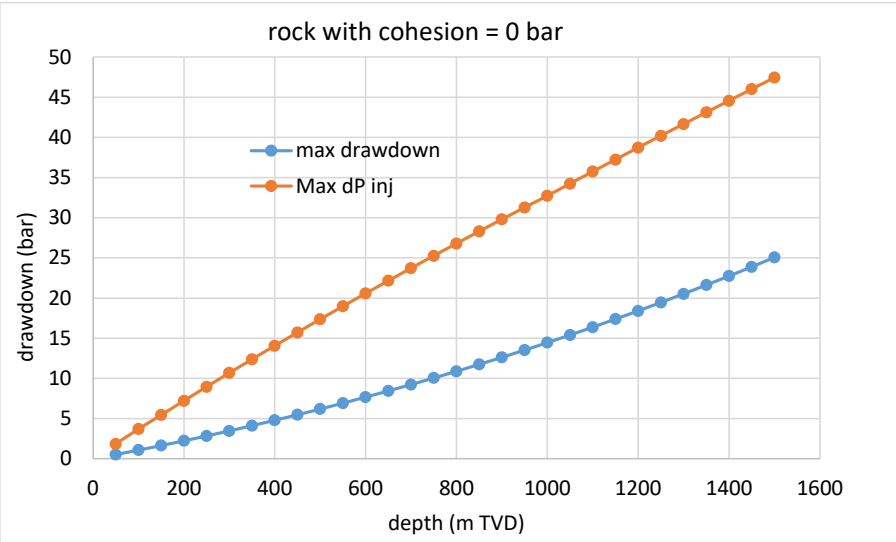

Figure 2-9. Maximum drawdown according to the Drucker-Prager criterion as proposed by (Buik, N., Bakema 2019).

Summary

Although the results vary considerably, the different criteria point in the same direction: the onset of sand production is expected for the mostly unconsolidated formations of the North Sea groups

for perforated or open hole conditions even for very low drawdown. Only if it is assumed that the formation shows some consolidation (more than is expected from the sonic velocity) or is intact (Drucker-Prager criterion following (Buik, N., Bakema 2019)), drawdown is possible. This means that criteria for determining the onset or initiation of sand production are not likely to be useful as design criteria, since they are always exceeded. The Drucker-Prager criterion might be useful for cases in which the completion provides sufficient support to the formation to ensure that the stress situation is not much affected by the open hole (e.g. gravel pack, natural gravel pack, or expandable liner), but it is not clear at this point if and when that condition is met.

If we accept that sand production initiation is unavoidable , the questions become:

- How much sand might be produced over time? This is addressed in the next section.
- Which sand control options are available and are suitable for the local conditions? This is addressed in Chapter 3

2.5 Simulation of sand production rate

In general models for the prediction of sand production can be:

1. Empirical: relate sand production to porosity, flowrate or drawdown.
2. Analytical
3. Numerical

The disadvantage of empirical models models is that they are very locally relevant. The numerical models are complex and require many input parameters which are difficult to quantify. That is beyond the scope of the current study. Therefore the focus is here on an analytical model that can give more insight into the sand production process.

2.5.1 Modelling sand production rate

A relatively simple analytical model for sand prediction was implemented to analyse the sand production process in more detail. Although the model is analytical, and the topic still under development, it does take into account the main aspects controlling sand production: stresses, drawdown, rock strength and production rate.

(Fjaer, Holt et al. 2008) present a simplified analytical model for continuous sand production from a perforation, based on a numerical model by (Papamichos, Vardoulakis et al. 2001). The model describes the rate of sand production from the rock around a cylindrical cavity that has been brought beyond the onset of sand production. Two necessary conditions for sand production are the stress induced damage of the rock (drawdown pressure exceeds the critical drawdown pressure) and the hydrodynamic forces must be strong enough to sustain the erosion process (the fluid flux exceeds the critical fluid flux).

Hydrodynamic forces on the grain cause the erosion process to start, which increases the porosity of the sand producing zone. The sand producing zone is the part of the plastic zone in where the rock has been deformed beyond its critical plastic strain limit (λ_c) (Figure 2-10).

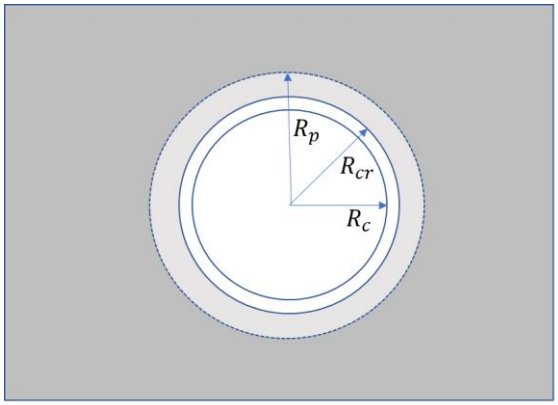

R_p Radius of the plastic zone
R_c Radius of the cavity
R_{cr} Critical radius (@ R_{cr} : drawdown = critical drawdown): boundary of the sand producing zone

Figure 2-10 - Schematic illustration of the plastified zone and the sand producing zone around the cavity based on (Fjaer, Holt et al. 2008).

Consequently, sand production occurs in two steps:

- *Continuous sand production* (when porosity ϕ is smaller than a critical porosity ϕ_{cr})
  The driving mechanism for continuous sand production is the erosion from the plastified material in the surrounding area of the production cavity. Continuous sand production will occur as long as the sand production zone can carry the load.
- *Instantaneous/catastrophic sand production* (collapse, burst) (ϕ => ϕ_{cr})
  When porosity increases, the ability of the cavity to carry load decreases. To account for this erosional-mechanical coupling, the load carrying ability/stiffness of the sand producing zone is assumed to remain constant until the porosity has reached a critical value (ϕ_{cr}). When this occurs, the zone collapses and the remaining sand is produced in one burst.

For the calculation of the continuous sand production, (Fjaer, Holt et al. 2008) derive the following generalised equation for sand erosion based on the hydrodynamic forces acting on the grains. The mass rate of sand produced from a volume element is:

$$\frac{\partial m_{sand}}{\partial t} = \lambda_{sand}\mu_f \frac{1-\phi}{\phi^3}\left(q_{fl} - q_{fl}^{cr}\right) \qquad (2\text{-}21)$$

The following approximate solution is presented by (Fjaer, Holt et al. 2008) for the change in porosity:

$$\phi \approx \phi_0 \left[1 + 4\frac{\lambda_{sand}\mu_f}{\rho_s \phi_0^4}\left(q_{fl} - q_{fl}^{cr}\right)(t - t_0)\right]^{1/4} \qquad (2\text{-}22)$$

Where
λ_{sand} : sand production coefficient (s/m³)
μ_f : fluid viscosity (Pas)
ϕ_0 : porosity at t_0 (-)
ρ_s : density of the sand grains (kg/m³)
q_{fl} : fluid flux (as specified in Darcy's law) (m/s)
q_{fl}^{cr} : critical fluid flux (m/s)

The change in porosity is used to calculated the amount of sand produced over time between bursts. At a burst the remaining sand with the critical radius R_{cr} is assumed to be produced. After the collapse, the radius of the cavity increases, the stresses around the cavity are redistributed and the erosion process starts a new cycle with continuous sand production.

The cumulative amount of sand produced for the example of a single perforation as presented by (Fjaer, Holt et al. 2008) is shown in Figure 2-11, with our results on the right for comparison.

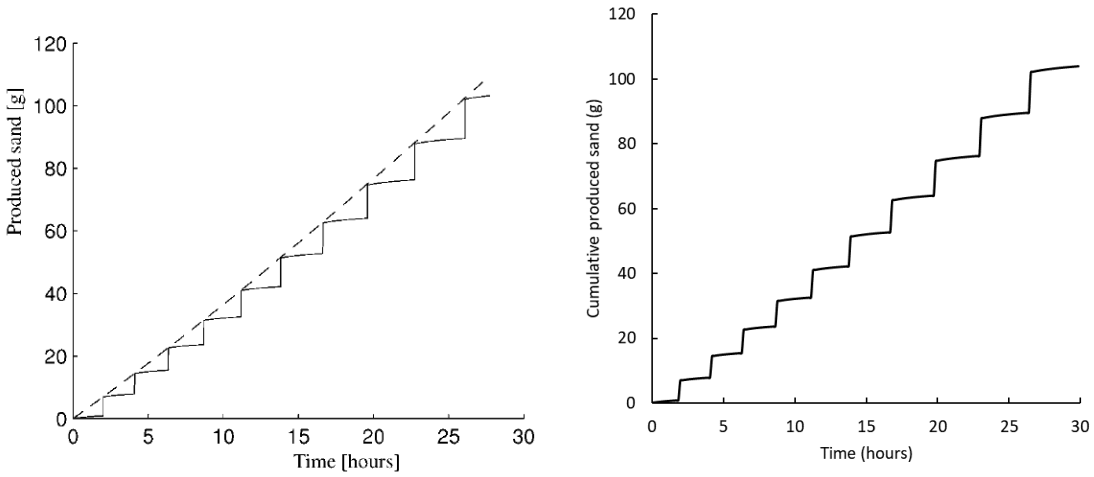

Figure 2-11 – Predicted cumulative sand production from a single perforation. Right: implementation in this report. Left: results presented by (Fjaer, Holt et al. 2008). The dashed line is an approximate average.

The Fjaer et al model is in principle for a perforation. However, unconsolidated or poorly consolidated formations are not usually perforated. Therefore we would like to simulate what the sand production is from an open hole. This is not the sand or fines production which ends up in the well, because the completions would prevent that. Instead this sand production rate can be seen as a measure for the amount of sand/fines that can be mobilized behind the completion (assuming no gravel pack). To adapt the model for open hole, the critical radius of the cavity is now also determined by the critical fluid flux in addition to the stability (drawdown). This is explained in more detail below.

The radius in which sand production R_{cr} can occur due to instability ($p_d > p_d^c$) is given by:

$$R_{cr} = R_c \, e^{\frac{p_d - p_d^c}{C_0}} \qquad (2\text{-}23)$$

R_c : radius of cavity (m)
p_d : drawdown pressure (Pa)
p_d^c : critical drawdown pressure (Pa)
C_0 : uniaxial compressive strength (Pa)

For the implementation for a perforation it is assumed that the critical fluid flux is exceeded within the radius R_{cr}, which is not likely to hold for open hole conditions. The solution to this is to define a second critical radius, namely the radius in which the fluid flux exceeds the critical fluid flux $R_{cr\ q_{fl}^{cr}}$:

$$R_{cr\ q_{fl}^{cr}} = \frac{Q}{2\,\pi\, l\, q_{fl}^{cr}} \qquad (2\text{-}24)$$

Q : flow rate (m^3/s)
q_{fl}^{cr} : critical fluid flux (m/s)
l : length of the inflow zone (m)

We assume that erosion can only occur within the radius in which both the critical fluid flux and the critical drawdown are exceeded.

2.5.2 Results

First the results for two cases are presented with input settings typical for the Brussels Sand in the south of the Netherlands: one for a vertical well with perforations and the second an open hole behind a completion. After that a sensitivity analysis is shown for the input parameters of the model. Based on the results of the previous section, the critical drawdown for the Brussels Sand was set to zero bar. Based on analysis of the well logs of the well Barendrecht-01, which has an extensive set of well logs, a UCS of 5 MPa (50 bar) was estimated for the non-cemented parts of the Brussels Sand (see Section 5.1 for details). From Figure 2-7 (with yield strength 7.5 MPa), the critical drawdown is expected to be negative at the relevant depth (~600 m). The Brussels Sand shows cemented layers (up to 20 to 50 cm thick) throughout the reservoir depth ((Geel, de Haan et al. 2022)). These layers are hard and brittle compared to the rest of the formation. How these hard layers influence the sand production in the well is difficult to predict without detailed simulation. This is beyond the scope of the current analysis.

Table 2-2. Input settings for a vertical well in the Brussels Sand

Input parameter	Perforated vertical well	Vertical well open hole
Initial radius Rc	0.004 m (per perforation)	0.1 m
Flow rate Q	2400 m^3/d*	2400 m^3/d (100 m^3/hr)
Producing length l	0.35 m (per perforation)	50 m
Critical fluid flux q_{fl}^{cr}	0.0005 m/s**	0.0005 m/s
Drawdown p_d	8 bar (based on k=750 mD, μ_f = 1 cP)	11 bar (based on k=750 mD, μ_f = 1 cP) (recalculated after each burst)
Uni-axial compressive strength C_0	50 bar (5 MPa)	50 bar (5 MPa)
Critical drawdown p_d^c	0 bar	0 bar
Initial porosity ϕ	0.3	0.3
Critical porosity ϕ_{cr}	0.38	0.38
Sand production coefficient λ_{sand}	200 s/m^3 (Fjaer, Holt et al. 2008)	200 s/m^3
Density of the sand grains ρ_s	2650 kg/m^3	2650 kg/m^3

* this is distributed over the (open) perforations.

** (Fjaer, Holt et al. 2008) used a value of 0.001 m/s in their example, but because the Brussels Sand has a relatively small particle size (D50 ~ 100-150 µm) a smaller values was selected.

The sand production coefficient and the critical fluid flux cannot be measured directly and are difficult to estimate. These should be based on observations. In particular the critical fluid flux is important for unconsolidated or poorly consolidated formations, since the critical drawdown is often exceeded.

Figure 2-12 shows the cumulative amount of sand produced over a period of 10 days for two perforated cases: one with 500 open perforations and one with 1000 open perforations. Due to the lower fluid flux per perforation in the case of the larger number of perforations, the simulated total amount of sand produced is larger. The average sand production for the 1000 perforations case is 80 kg per day with a concentration of 0.033 kg/m^3. For the case with 500 perforations, this goes up to 198 kg/d with an average concentration of 0.082 kg/m^3. The figure also shows that the bursts become less frequent but larger. Figure 2-12 shows the increase in diameter of the perforation cavity over 10 days. Initially the radius is 4 mm, but that increases to 2 and 4 cm for the 1000 and 500 perforations case respectively. In this model, it is assumed that the sand is only produced by increasing the radius. In reality the cavity could also become longer. For such large diameters, the

perforations might also start to influence each other and overlapping stress zones might break down (Bellarby 2009).

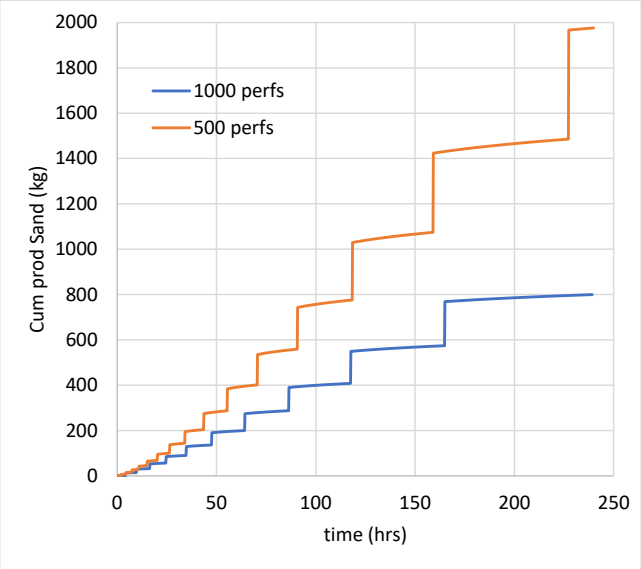

Figure 2-12. Predicted cumulative amount of sand produced (kg) for a perforated vertical well (input see Table 2-2) with 500 open perforations and 1000 open perforations.

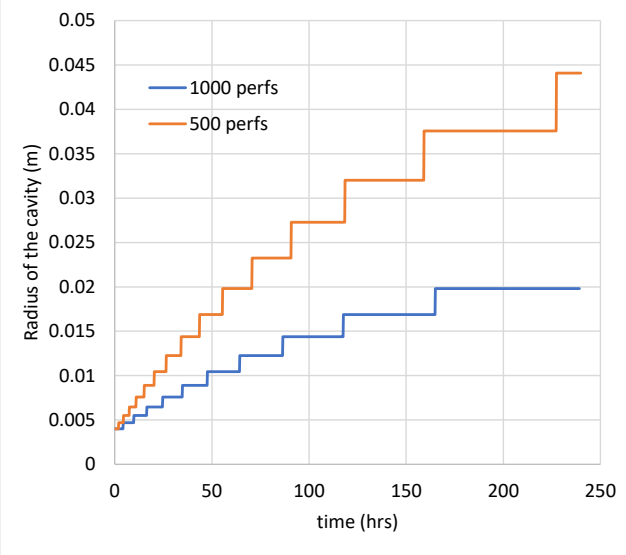

Figure 2-13. Increase in radius of the cavity of the perforations with 500 open perforations and 1000 open perforations.

The second case that is investigated is a vertical, open hole well. The input settings can be found in Table 2-2, right column. Of course, the well would not really be open hole, but would have a screen or liner. Figure 2-14 shows the cumulative sand production over 20 days. For the open hole, the drawdown is recalculated after very burst. The amount of sand that is mobilized is considerably larger than in the perforated case. However most of the sand or fines would be stopped by the completion, which potentially can lead to plugging of the completion. Figure 2-15 shows the development of the radius of the cavity and the fluid flux on the sand face in the same period. Due to the increase in diameter, the fluid flux at the sand face decreases. After the third burst, the fluid flux drops below the critical fluid flux of 5E-4 m/s and sand production stops. In reality, a range in

fluxes would occur due to differences in permeability and the process would be more gradual. In addition, the collapse would probably occur over smaller areas, also making the process more gradual.

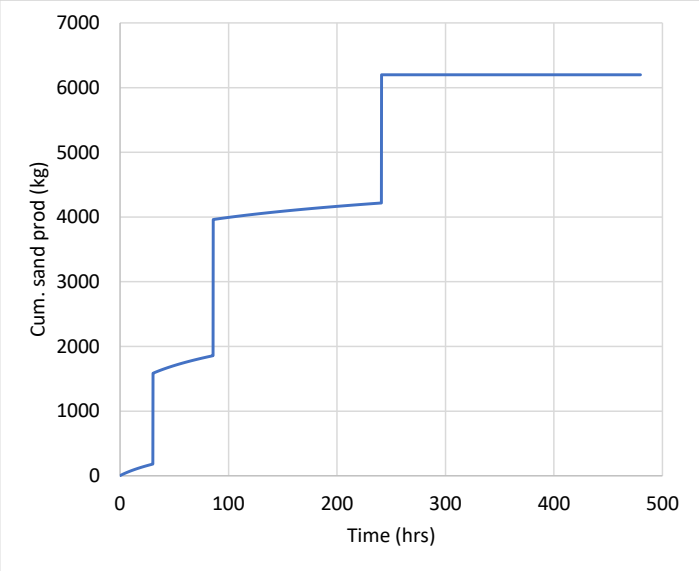

Figure 2-14. Predicted cumulative amount of sand produced (kg) for a vertical well with initial radius of 0.1 m.

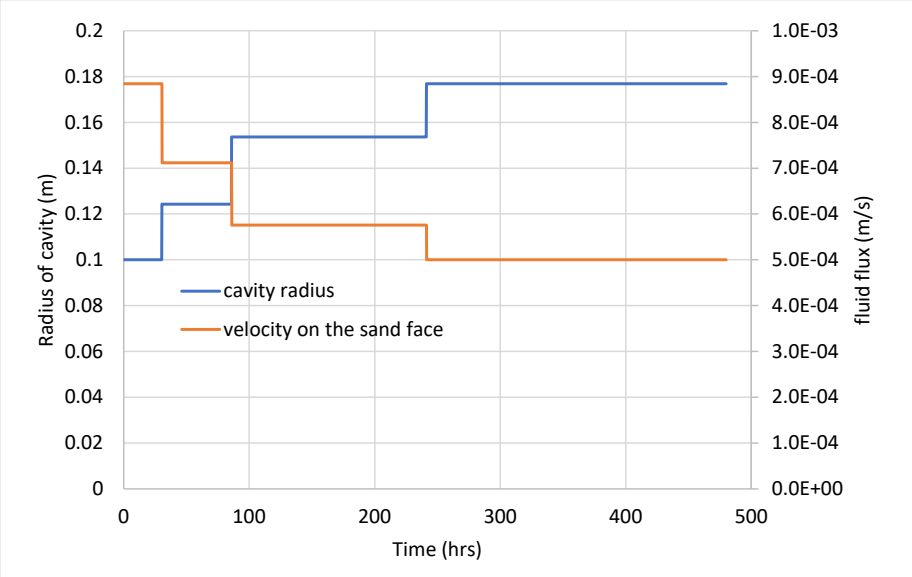

Figure 2-15. Development of the radius of the cavity (well bore in this case) and the fluid flux (m/s) on the sand face during sand production shown in Figure 2-14. The critical fluid flux is 5E-04 m/s.

Sensitivity analysis

A sensitivity analysis has been performed for a perforation and an open hole well. The sensitivity of the model to the different input parameters is shown in Figure 2-16 for the perforation and Figure 2-17 for the open hole. For the perforations the pressure drawdown is fixed and not calculated from the flow rate. For the open hole, the pressure drawdown is calculated from the flow rate and (changing) diameter. The sand production is mainly sensitive to the critical fluid flux and the flow rate. A larger critical fluid flux causes less sand to be produced, and a higher flowrate causes more sand production. For the perforation case also a clear dependency can be seen on the drawdown pressure and critical drawdown pressure. For a larger drawdown pressure, the formation is more

unstable and produces more sand. Also the length of the cavity shows a relation to the amount of sand produced: a longer cavity will produce less sand because the fluid flux decreases (given a fixed flow rate). As long as the fluid flux is smaller than the critical fluid flux, no sand will be produced. For some of the cases a very large amount of sand production is calculated: over 2.5 kg per day from a single perforation, but this is only for very small values of the critical fluid flux.

For the open hole well, the length of the cavity also show a clear sensitivity. In this case the length of the cavity is the total filter length. A larger filter, and therefore larger area, with the same flow rate, will lower the fluid flux, and therefore lower the sand production. The other parameters have a less clear impact on sand production.

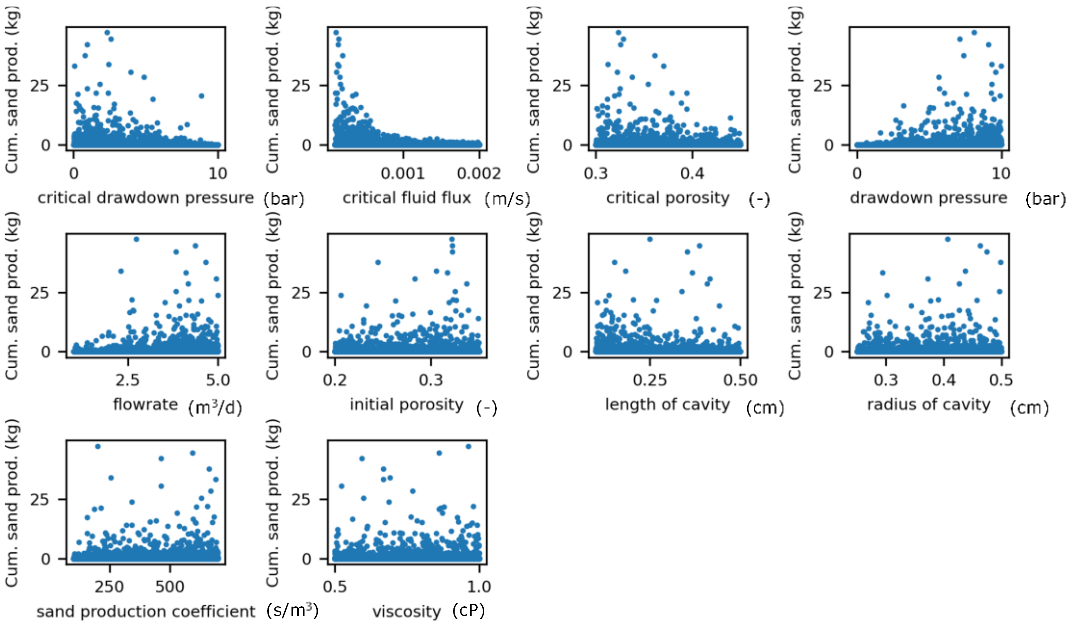

Figure 2-16. Cumulative amount of sand produced for a single perforation (in kg) over a period of 10 days.

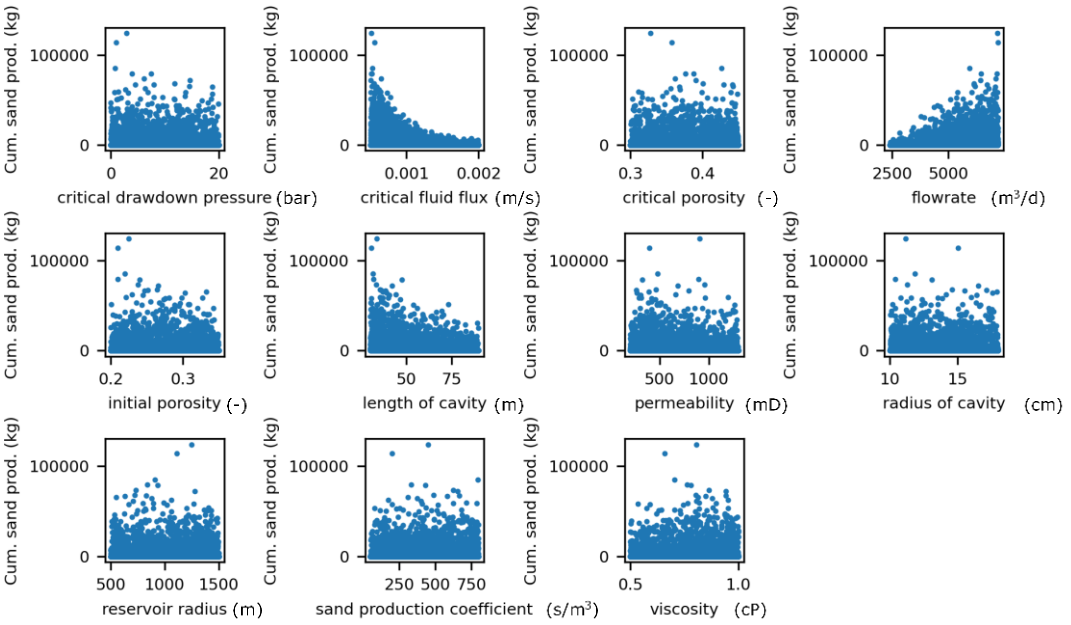

Figure 2-17. Cumulative amount of sand produced (in kg) for an open hole over a period of 10 days.

2.5.3 Discussion

Due to the simplifications and the dependence of the sand production predictions on difficult to quantify properties, it is essential that the predictions form the models are calibrated to observed data from representative wells. Currently, we have no access to information from perforated wells in the Brussels Sand or any other reservoir in the North Sea Groups. We have simulated the settings for the Zevenbergen doublet, which is a doublet with highly deviated wells with screens in the Brussels Sand (Buik, N., Bakema 2019). For the realised rate (~3600 m^3/d), the diameter and the long inflow zone of the deviated wells, the fluid flux is low: ~1E-4 m/s. This is an order of magnitude lower than the critical fluid flux of 0.001 m/s used by (Fjaer, Holt et al. 2008). Thus it is expected that only fines are mobilized. This is consistent with the fact that few fines are produced at surface (Buik, N., Bakema 2019). (Van den Hoek, Kooijman et al. 2000) describe the processes occurring around uncemented slotted liners in horizontal wells based on experimental and field data. The annular space fills up with loose sand and little sand is produced at surface. If the cohesion of the sand bridges around the slots is compromised, for example by introducing a water cut in an oil reservoir, massive amounts of sand can suddenly be produced and even liner collapse can occur.

From the sensitivity analysis it is clear that the sand production is very sensitive to the fluid flux near the well and the critical fluid flux. Since for most North Sea groups the formation is unstable enough to produce sand (Sections 2.3 and 2.4), these are the controlling parameters. For the determining a criterion for limiting the flow rate, thus two main factors are required: the potential to produce sand from the formation and the clogging of the completions (discussed in Chapter 3). For the former, the critical fluid flux appears to be the controlling factor. For comparison, for shallow applications, a maximum flow velocity is defined. For the conditions as presented in Table 2-2, the maximum velocity for the drinking water guidelines would be 9.5E-5 m/s (eq. 2-1) and for the ATES guidelines 1.6E-5 m/s (eq. 4). These values are much lower than the critical fluid flux used above. In addition, the critical fluid flux is a Darcy flux and not the velocity in the pores, which is much higher. This illustrates that choosing a critical fluid flux is not trivial.

Since the forces on a grain depend on its diameter (Fjaer, Holt et al. 2008), it would be expected that the critical fluid flux for a formation depends on the particle size distribution. For erosion and transport of particles in open water, this has long been studied and is usually summarized in a Hjulström curve. An example is reproduced in Figure 2-18. This shows how erosion, transport and deposition depend on flow velocity and grain size. For fines, the difference between the erosion velocity and deposition velocity is very large, because of the cohesive forces between these particles when consolidated. Once suspended, these fines are very slow to settle. The lowest erosion velocity occurs for particles of around 0.1 to 0.2 mm. The flow velocity for which this is expected is 0.2 m/s (this is the velocity in the water body and not the velocity experienced at the erosional interface). The increase in required erosional velocity for very small particles, suggests that the shallow guidelines which are based on the hydraulic conductivity K are valid only when main particle size is > 0.1 mm, because the allowed velocity increases with K and K generally increases with particle diameter.

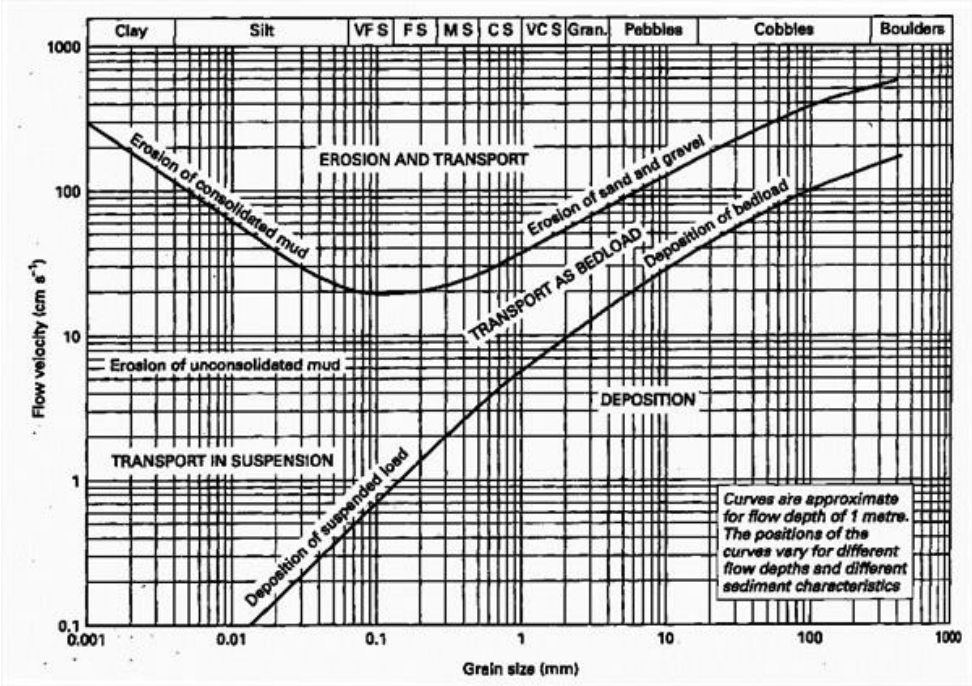

Figure 2-18. An example of the Hjulström curve (source: hjulstrom curve (slideshare.net))

3 Control sand production

Once it has been determined that the reservoir is so unconsolidated that limiting the drawdown and/or rate to avoid sand production is not feasible, the completion can be selected to limit sand production.

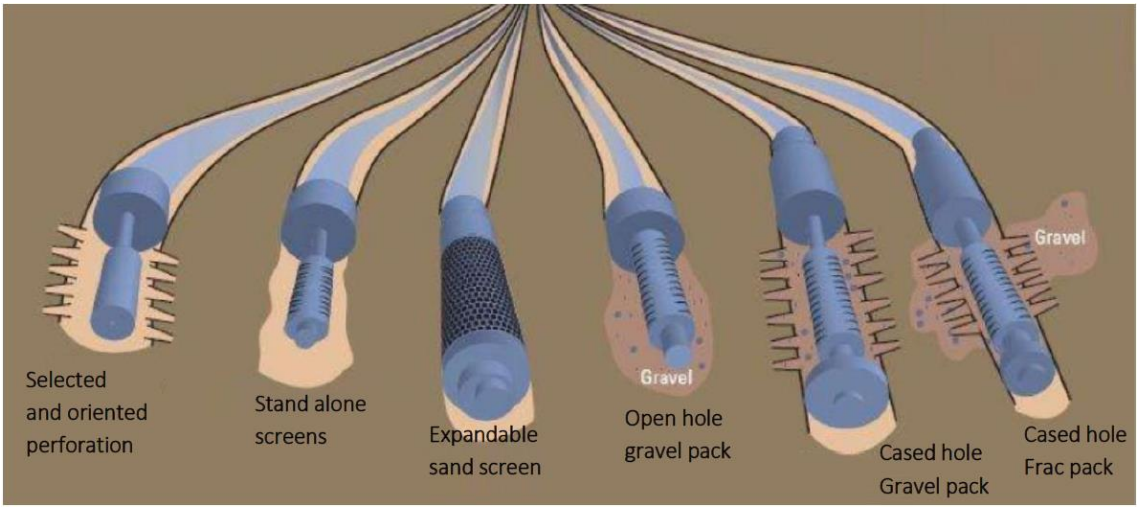

Figure 3-1: An overview of the different possible sand control completions (image taken from (GEOTHERM project 2019)).

In Figure 3-1 an overview of the different sand control mitigation options is presented. Roughly, there are three different types of mitigation: (1) cased hole, (2) using a screen to limit the sand production, or (3) using a gravel pack to limit sand production. In this chapter these alternatives will be considered, and some considerations for the selection of the completion will be given.

3.1 Selected and oriented perforation

In case of a cased hole completion, perforations need to be created downhole. In case of a non-uniform stress distribution in the reservoir it is possible to limit sand production by selecting where and under which angle to create the perforations.

Perforation selection can be used when it is estimated that parts of the reservoir are more consolidated than others. The more consolidated layers allow a larger drawdown before sand production occurs. On the other hand, the more consolidated layers are often less permeable and therefore lead to a more limited production at the same drawdown. Therefore a balance must be found between well permeability and the risk of sand production (Eriksen, Sanfilippo et al. 2001). This technique has been successfully applied to avoid sand production in the Varg field in the Norwegian section of the North sea (Tronvoll, Eek et al. 2004).

Next to limiting the perforations to more consolidated layers of the reservoir, the orientation of the perforations can also be used to limit sand production. In general, the perforations should be directed away from the direction of the minimum horizontal stress. This requires an estimate of the stress field in the reservoir. To estimate the vertical stresses, often density logs are used. Horizontal stresses are more difficult to quantity, but leak-off tests can be used. Furthermore, sonic logs and

core samples can help to determine the stress field. At a particular location along the length of the well two perforations can then be created, 180 degrees apart (Abass, Habbtar et al. 2003). In case of a strongly deviated or horizontal oil well, vertical perforations are preferred as reservoir depletions leads to reductions in the horizontal to vertical stress ratio (Tronvoll, Eek et al. 2004). Oriented perforations have been applied to many wells at a depth of a bit over 2000 meters on the Norwegian Continental Shelf in both oil, gas and injection wells (Andrews, Joranson et al. 2008).

Overall, sand production is limited most by creating many perforations in more consolidated layers of the reservoir and creating fewer perforations with 180 degree phasing in the direction of the maximum stress in less consolidated layers (Tronvoll, Eek et al. 2004). Note, off course that this maximum stress must be sufficient handle the required drawdown. If not, then measures such as screens or gravel packs are required to handle sand production. Since the applicability of selected and oriented perforations is so dependent on the stresses in the reservoir it is difficult to give specific guidelines on when to apply this technique or how much the drawdown and the production will be affected.

3.2 Screens

Screens are used in two different ways: as stand-alone-screens (SAS) in which the screen is the only sand filter between the reservoir and the wellbore, and in combination with a gravel pack where the screen is used to keep the gravel in place. The focus of this section are the stand-alone screens.

Different types of stand-alone (also called bare) screens are available (Ott 2008). The simplest are the slotted liners, which are just cylinders containing rectangular holes. Next, there are the more sophisticated wire-wrapped screens that have a much larger effective inflow area than slotted screens (Lake, Clegg 2007). Many premium screens are also available with custom designs that differ per manufacturer. These screens are typically similar to a wire-wrapped screen in that they contain a base pipe. Around this pipe several layers can be wrapped, each containing a different weave. The term woven screen is also sometimes applied to these screens.

Laboratory tests can be used to evaluate if a specific screen can be used to prevent sand production (often called sand retention tests (Ahad, Jami et al. 2020)). Two different tests are common. The first is a slurry test, in which a flow of water containing a low sand fraction of formation sand (1% or so) is produced through the screen under test. It is then evaluated how much sand is produced along with the water. In these slurry tests, initially there is no sand on the outside of the screen. Therefore, all sand grains smaller than the size of the openings in the screen will be produced. Over time, more large diameter grains are deposited on the screen. These large grains can form bridges that subsequently block the smaller grains as well. The sand production therefore decreases in time until a steady state is reached. If the screen is properly sized, no further sand is produced. Note that the size distribution and even the shape of the particles determine the outcome of the experiment. Therefore, ideally reservoir sand is used in the experiment. If simulated sand is used, it is important that it accurately reflects the properties of the reservoir sand.

In a prepack test, a slurry of a high viscosity liquid containing a lot of sand is first used to create a sand pack around the screen. Subsequently pure water is produced through the screen and it is determined how much of the sand from the sand pack will be produced along with the water.

There are many criteria for selecting the screen opening based on the particle size. An overview is presented by (Ott 2008) and by (Ahad, Jami et al. 2020) depending on the type of screen. Ott (2008) presents an example where the sizing determined by various guidelines is presented superimposed on a particle size distribution. There is a significant difference between the criteria, indicating that the type of screen is important, but also that there is a variation in the criterium even for a single screen type.

Typical quantities used in these criteria are D50 (median particle size), D10 (10% of the particles are larger than this size) and the uniformity coefficient (the ratio of the sieve size through which 60% (by weight) of the material passes to the sieve size that allows 10% of the material to pass). From a set of slurry tests (Chanpura, Hodge et al. 2011) determined that the screen opening should be smaller than D10 in order to obtain an acceptable sand production of 0.12 lbm/ft^2 (0.59 kg/m^2), as shown in Figure 3-2. Note that the units of the sand production are in kg/m^2, as it is the rate of sand production per area of the screen. The acceptable limit is not universal, as it depends on the flow rate at which liquid flows through the screens.

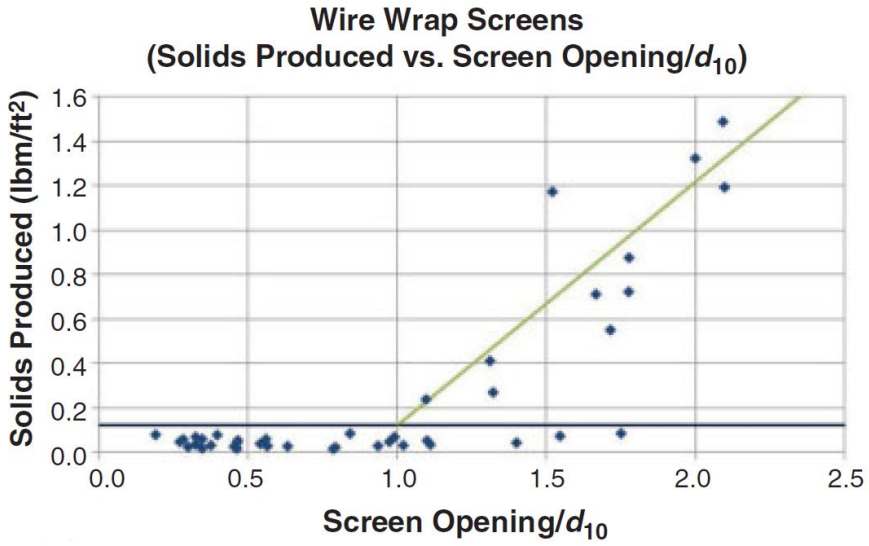

Figure 3-2: Solid production as a function of the screen opening in slurry tests with stand-alone-screens (Chanpura, Hodge et al. 2011).

(Wu, Choi et al. 2016) also provide an overview of the different sizing guidelines for different screen designs. The guidelines are different, also because the experiments used to create these guidelines are very different. In the experiments the sand types, flow rates, acceptable pressure losses and flow areas vary significantly, which also results in different guidelines. The authors then perform experiments with different screen coupons that are similar to wire wrapped screens. They obtain two correlations: one for the sand production (S in lbm/ft^2) through the mesh, and one for the permeability of the mesh (K in Darcy):

$$S = 0.4895\left(\frac{D_r W}{d_{10}}\right)^{5.9972} ; K = 7.993\left(\frac{RU_c d_{50}}{W}\right)^{-2.398} \qquad 3\text{-}1$$

In these equations D_r is the fractal dimension of the particle roughness, W is the size of the screen opening, U_c is the uniformity coefficient, and R is the roundness of the particle. This work shows that there is not a general guideline for the required size of the screen opening. Furthermore, the required opening depends on the shape of the sand particles, such as the roundness and the

roughness fractal dimension. These can be determined using image analysis, but they are not taken into account in many rough guidelines.

The unclogged permeability of any sand prevention completion (and therefore also of stand-alone-screens) is much higher than that of the reservoir (Hodge, Burton et al. 2002). The size of the openings in the screen are based on the largest sand grains, while the pores in the formation sand are to a much greater extend determined by the small sand grains. However, for the screen to function, a sand pack must be formed around the screen. This sand pack often clogs the screen to some extent. Examples of screen permeability after prepack experiments were collected by (Chanpura, Hodge et al. 2011). In this set of 304 tests, in only 2 cases the retained permeability was less than 4% (basically the two measurement points at the bottom-left corner of the figure), while in 17% of the cases sand production was not stopped by the screen (the points above the horizontal line in Figure 3-2. Therefore the results suggest that for typical values of particles size distributions and screen openings selected in the petroleum industry, unacceptable solids retention is more likely than unacceptable clogging.

Expandable screens are a particular type of sand screens where the filter overlap during installation, such that the screen can be expanded after which the filter still spans the circumference of the wellbore (Kuncoro, Ulumuddin et al. 2001). By expanding the screen, the annulus between the filter and the reservoir sand will be closed. As a result, shear failure and disaggregation of the material around the wellbore: the material is kept in place by the screen. (Nouri, Vaziri et al. 2005) performed laboratory experiments in which they used a fine-mesh metal stiffener to emulate an expandable screen. They found that the compaction of the sample by the stiffener reduced the porosity and the permeability compared to an open hole completion. However, the support allowed for a greater drawdown without formation collapse. No sand was produced when the aperture size of the mesh was 4.2 times the maximum grain diameter and 8 times the mean grain diameter. Note that this is a larger opening than suggested by (Chanpura, Hodge et al. 2011) for wire wrap screens. However, these authors performed more experiments and used a different experimental setup, so it is difficult to compare the two.

3.3 Gravel packs

A gravel pack is a downhole filter consisting of sand with a larger diameter than the formation sand. The gravel pack is typically held in place by a screen and can be applied in both open-hole and cased-hole completions. The selection of the grain size of the gravel pack sand determines how effective the pack is. When the gravel pack sand is too fine the permeability of the gravel pack is too low. When the gravel pack sand is too coarse reservoir sand can flow into the gravel pack, leading to sand production and a potential reduction of the permeability. These effects are illustrated in Figure 3-3.

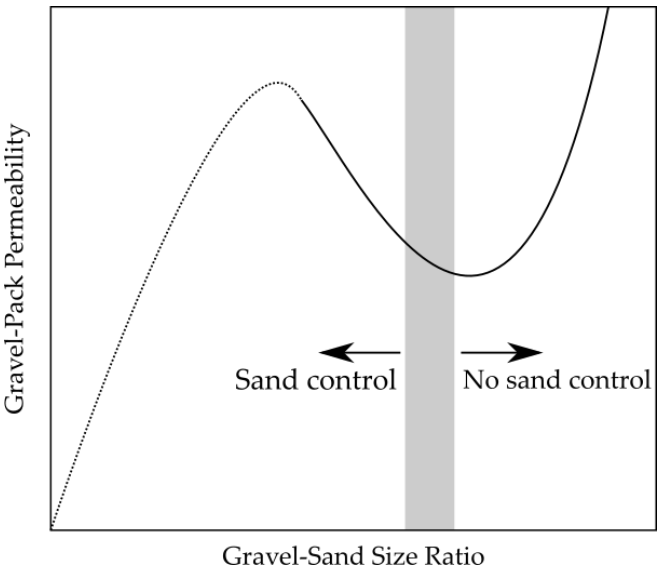

Figure 3-3: Rough illustration of the effect of the gravel pack sand grain size on the permeability and the sand production (Lake, Clegg 2007).

The classic procedure to select the sand used in a gravel pack is given by (Schwartz 1969). He indicates 6 parameters that are relevant for the selection of the gravel size: *D10*, *D40*, *D70*, *D90*, *C = D40/D90*, and the inflow velocity *v*. Then the following relations hold:

$$\begin{aligned} C < 5 \;\&\; v < 1.5\frac{\text{cm}}{\text{s}} \quad &: D_{10,gravel} = 5D_{10} \\ 5 < C < 10 \mid v > 1.5\frac{\text{cm}}{\text{s}} \quad &: D_{40,gravel} = 5D_{40} \\ C > 10 \quad &: D_{70,gravel} = 5D_{70} \end{aligned} \tag{3-2}$$

For these relations, it is assumed that the grain size of the gravel is relatively uniform, and that the shape of the gravel particles is spherical. A simpler relation found in the literature to determine the grain size of the gravel pack is (Hodge, Burton et al. 2002):

$$D_{50,gravel} = 6D_{50} \tag{3-3}$$

These relations indicate that the grain size of the gravel is significantly larger than that of the reservoir sand. As the permeability tends to scale with the square of the grain size, this means that the permeability of the gravel is much larger than the permeability of the reservoir sand. However, as indicated by (Tiffin, King et al. 1998) there is often intrusion of fines and sand into the gravel pack. This is illustrated in Figure 3-4. In an extreme case, (Hodge, Burton et al. 2002) mention a gravel pack in which the ratio of the gravel grain size and the formation grain size is very large ($D50_{,gravel}$ = 21.9 D50). The subsequent intrusion of formation sand into the gravel pack reduces the gravel-pack permeability to only 0.3% of its original value. Note, however, that even after this reduction the gravel pack is still more permeable than the reservoir sand. (Tiffin, King et al. 1998) also indicate that a relatively coarse gravel pack can be applied in two situations: (1) when the reservoir sand is relatively uniformly distributed (in line with the work by (Schwartz 1969) and (2) when a lot of fines are present. These fines can clog gravel packs with a relatively small grain size. Applying a coarse gravel pack in combination with a screen through which the fines can pass then at least does not clog the well. Note that fines production will occur in this case.

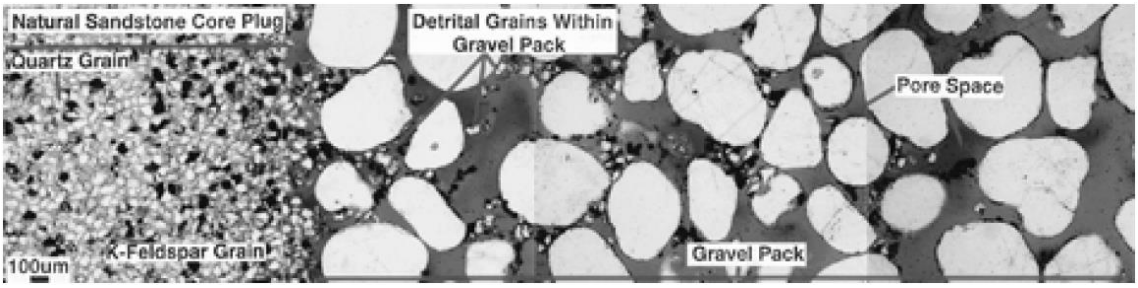

Figure 3-4: Intrusion of fines and sand into a gravel pack (Tiffin, King et al. 1998).

For shallow applications, generally the following rule of thumb is used for heat/cold storage: the average size of the gravel should be 4 times the D50 of the finest sand layer (Buik, N., Bakema 2019, van der Schans, Meerkerk 2019). This is finer than the guidelines by (Hodge, Burton et al. 2002). Norms from the drinking water industry will not further be discussed because (Buik, N., Bakema 2019) already concluded that the norms generally used for drinking water wells are less appropriate because in the Netherlands they are generally in much coarser formations.

Clogging of gravel packs is a very relevant topic for shallow applications, although it affects drinking water wells more than deeper wells used for heat storage (Bloemendal, Lopik et al. 2020). Based on samples from the borehole wall, accumulation of fine particles from the formation is one of the major causes of clogging, often in combination with scaling, cake resulting from incomplete cleaning of drilling mud and less often biofilm (Bloemendal, Lopik et al. 2020). Simulation of the clogging process is challenging (De Zwart 2007) because of the different transport mechanisms involved: diffusion, interception and gravitational sedimentation. These simulation approaches would need to be adjusted for deeper applications to account for different temperature, pressure and fluid properties.

3.4 Criteria for selecting the sand control method

Some rough criteria exist to determine whether a only a screen can be used, or whether a combination of a screen and a gravel pack is required to avoid sand production. According to (Tiffin, King et al. 1998) any bare sand control screen can be used for the following reservoir sand properties: D10/D95 < 10, D40/D90 < 3, sub 44 µm < 2%. A bare screen with “new technology” (that is, by the standards of 1998), such as a woven or wire-wrapped screen can be used for: D10/D95 < 10, D40/D90 < 5, sub 44 µm < 5%. A very similar criterion for the application of screens was presented by (Latiff 2011): D10 > 175 µm, D40/D90 < 5, sub 44 µm < 5%.

From the work of (Tiffin, King et al. 1998) these is also a limit to the use of gravel packs. For D10/D95 > 20, D40/D90 > 5, sub 44 µm > 10% there are so many fines and small sand particles that the gravel pack will lose too much of its permeability at the gravel-sand interface. In this case, it might be required to enlarge the wellbore (e.g. through fracturing) to allow production. This information is presented in a more visual way in Figure 3-5.

Weatherford (Weatherford 2012)(https://www.weatherford.com/documents/brochure/products-and-services/completions/sand-screen-selector/) uses a combination of criteria to select open hole completions: D50, uniformity coefficient (D40/D90) and sorting coefficient (D10/D95). Gravel packs are advised for very fine (< 50 µm) and very poorly sorted sands. The thresholds for the uniformity and sorting coefficient depend on the D50, with increasing sorting required for finer formations to

allow screens (wire-wrap or mesh). Expandable screens are suitable for all levels of sorting, but not for very fine sands (< 50 µm).

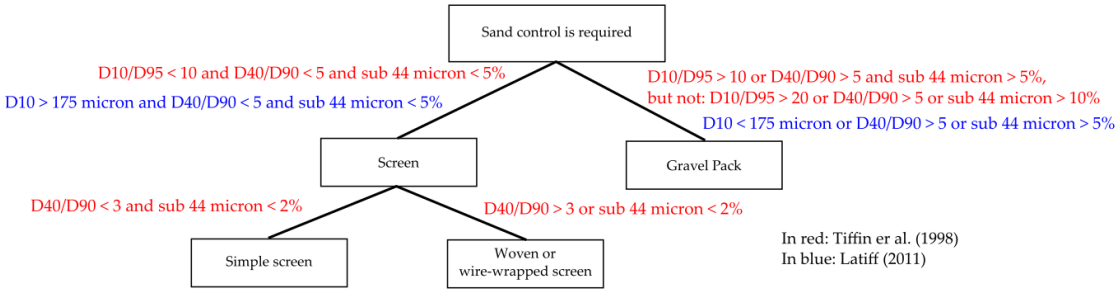

Figure 3-5: Overview of the criteria for selecting sand screens or gravel packs to control the sand production. Note that it should be determined whether sand control is required before performing this screen selection.

Note that there is a difference between these criteria determined by the oil-and-gas industry and the experience in very shallow systems, as described by Buik and Bakema (2019). In these shallow systems a 'natural gravel pack' is used in poorly sorted formations. It is basically a screen which prevents the largest sand particles from moving through. The natural gravel pack that forms at the screen in this way is then able to prevent the finer sand particles from reaching the wellbore. Different completions impact the expected development of the productivity differently. In the presentation below this is neatly summarized for different possible completions.

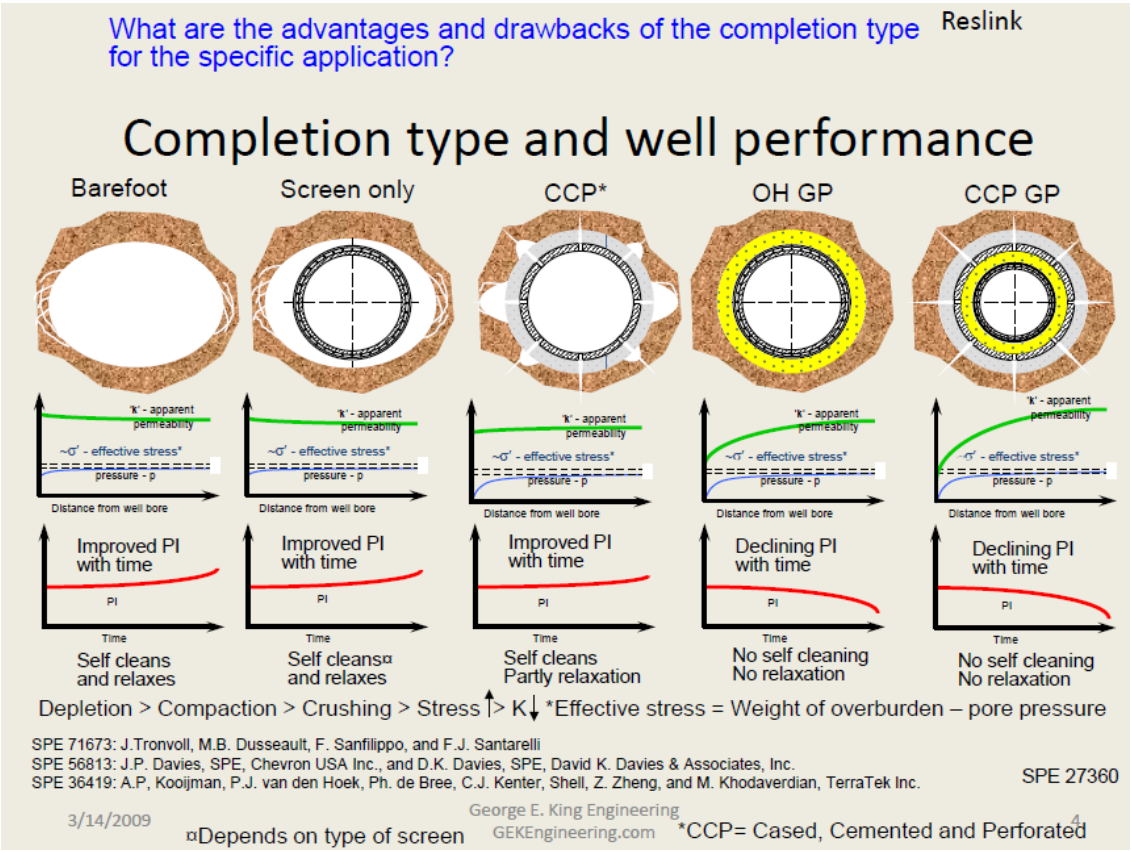

Figure 3-6. Overview of different completions (from G.E. King Engineering, GEKEngineering.com (King 2009))

Overall, it is clearly not an exact science to determine which sand control technique should be used. Furthermore, it is not obvious how the overall permeability is affected by the sand control.

There is a large dependence of the grain size distribution of both the sand and the gravel. Furthermore, the shape of the gravel particles also plays a role in the likelihood of sand and fines being trapped in the gravel. The shape of the sand particles also plays a role in determining whether sand control is effective. It is possible, once the grain size distribution of the reservoir is known, to recommend a screen or a gravel pack.

It might not always be feasible to perform an analysis of the sand particles before installing the sand control method. In this case, an estimate may be possible based on previous measurements of sand particle size measurements in similar formations. Furthermore, as clogging of a screen is not occurs at significantly lower screen openings than sand production (see Figure 3-2), there is room to install a mesh that is on the conservative side (i.e. a smaller screen opening then required). Finally, cost can also be a criterion. As screens are cheaper than gravel packs, it might be more cost-efficient to install a screen and live with some remaining sand production then it is to install a gravel pack.

4 Handle sand production

Once the sand enters the well, it needs to be transported upwards along with the liquid in the production well and along the top-side facilities and pipeline. The transport of sand in the pipelines is a function of several parameters such as mixture velocity, pipe diameter and inclination, fluid properties and particle properties (such as concentration, density and size distribution). The interaction between lift, drag and inter-particle forces will determine the sand transport regime, as an example given in Figure 4-1. Lowering the fluid velocity further than illustrated in the figure will lead to the sand deposition. Furthermore, the presence of the sand causes erosion of the wall of the pipeline. In this section, these two issues will be discussed and simple calculations and simulations are preformed to estimate the severity of these issues. Note that in most of the simple calculations pure water is used as an example. The water in most wells is salty, having properties more like sea water. However, using sea water leads only to a 3-4% increase in density and a 6% increase in viscosity. This will not matter much in these example calculations (the viscosity changes much more with temperature).

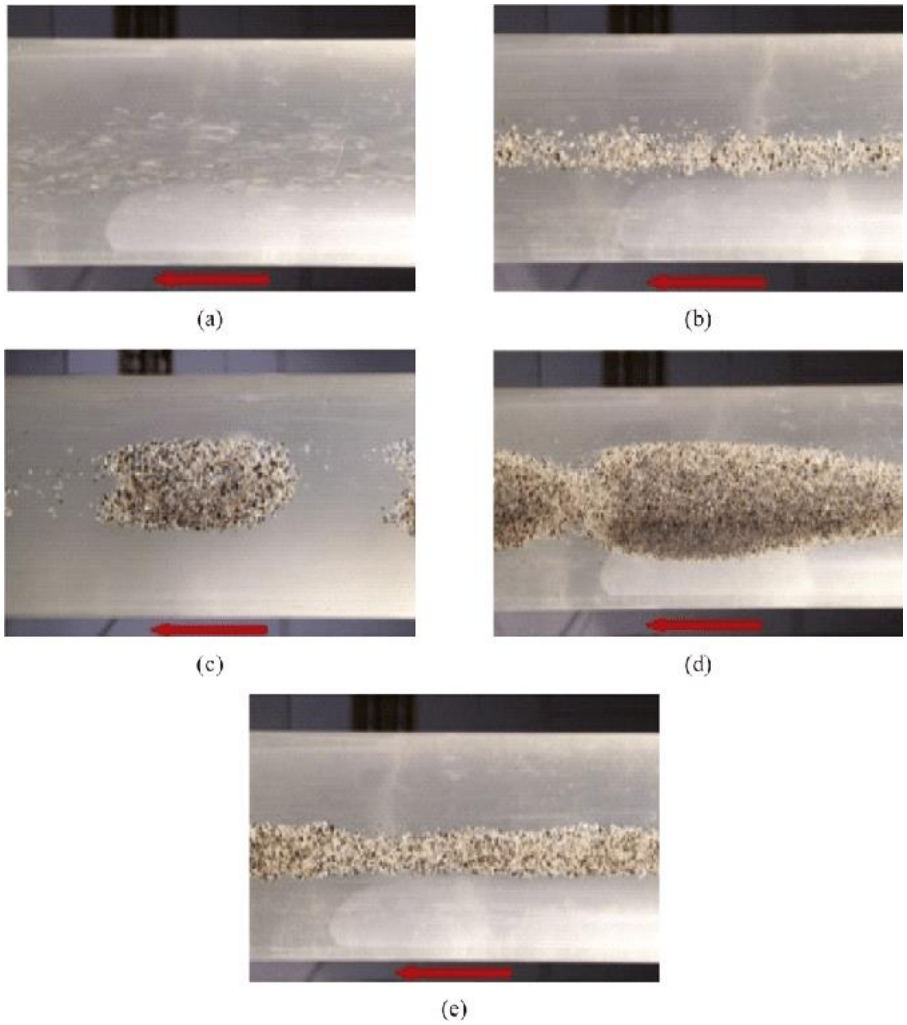

Figure 4-1: different regimes of sand transport (a) suspension, (b) moving bed, (c) and (d) moving dunes and (e) stationary bed ordered by the reduction in the flow velocity (Leporini, Marchetti et al. 2019)

4.1 Sand in the well

In case the sand is transported through a vertical well, the typical velocity of the sand particles with respect to the liquid is the terminal velocity. For a sand particle with diameter *d* the terminal velocity v_t is determined from the following relation:

$$\frac{1}{4}\pi d^2 \frac{1}{2}\rho_l v_t^2 C_D = \left(\rho_p - \rho_l\right)\frac{1}{6}\pi d^3 g \qquad (4\text{-}1)$$

Here ρ_l is the density of the liquid, ρ_p is the density of the particle, g is the gravitational acceleration, and C_D is the drag coefficient. For small particles it is equal to 24/Re, where the Reynolds number is equal to $\rho_l v_t d/\mu_l$ where μ_l is the liquid viscosity. For sand particles with a diameter of 100 µm and a density of 2400 kg/m^3 in water (40°C) this leads to a terminal velocity of 0.01 m/s.

This analysis above shows that in vertical wells, where the vertical velocity component of the liquid flow is typically much larger than 0.01 m/s, the sand will be easily produced from the well. However, geothermal wells may have a horizontal section in the reservoir in which the production of sand may be an issue. For instance, in the commercial software LedaFlow a model by (Oroskar, Turian 1980) is used to estimate the velocity below which a stationary sand bed may form. It is given by the following equation:

$$v_c = \nu^{-0.09} d^{0.17} s^{0.55} D^{0.47} \qquad (4\text{-}2)$$

In this relation ν is the kinematic viscosity, s is the specific gravity and D is the pipe diameter. For example, take a pipe with a diameter of 25 cm, in combination with 100 µm particles with a density of 2400 kg/m^3 in water with a kinematic viscosity of 0.7e-6 m^2/s (for water at a temperature of 40°C). This leads to a critical velocity of 0.4 m/s. It is significantly larger than the terminal velocity of the sand particles in the liquid.

To look into the presence of sand in the wellbore further, some simulations with the OLGA Dynamic Multiphase Flow Simulator (version 2018.1.0) were performed. In OLGA the following relation is used for the slip velocity:

$$\begin{aligned} Re < 3 \qquad & v_s = 0.32673\left(\rho_p - \rho_l\right)\left(\frac{d^2}{\mu_l}\right) \\ 3 < Re < 300 \qquad & v_s = 0.7086 d\left(\rho_p - \rho_l\right)^{0.667}(\rho_l \mu_l)^{-0.333} \\ Re > 300 \qquad & v_s = 2.9452\left(\frac{d\left(\rho_p - \rho_l\right)}{\rho_l}\right)^{\frac{1}{2}} \end{aligned} \qquad (4\text{-}3)$$

As an example, let's consider the 100 µm particles with a density of 2400 kg/m^3 in water at 40 °C (density 992 kg/m^3, viscosity 6.5e-4 Pa s). Then a slip velocity of 0.01 m/s is obtained, for a Reynolds number of 1.

In OLGA the effect of the sand on the viscosity of the liquid is also modelled using the following relation:

$$\frac{\mu_l}{\mu_{l,0}} = \left(1 - \frac{\phi}{0.75}\right)^{-2.0025} \qquad (4\text{-}4)$$

Here $\mu_{l,0}$ is the dynamic viscosity of the pure liquid, μ_l is the dynamic viscosity of the liquid with sand and ϕ is the volume fraction of the sand in the liquid. Note that even when the volume fraction of the sand is 1%, which is a lot in vertical flow, this leads to a viscosity increase of only 2.7%. The change in viscosity due to the sand is only significant in sand beds.

Some simple simulations were performed in OLGA. These simulations were performed in four simple pipe geometries, illustrated in Figure 4-2. The parameters of these simulations are specified

in Table 4-1. To simplify the simulations, the temperature in the entire well is 40 °C, there is no heat lost to the environment.

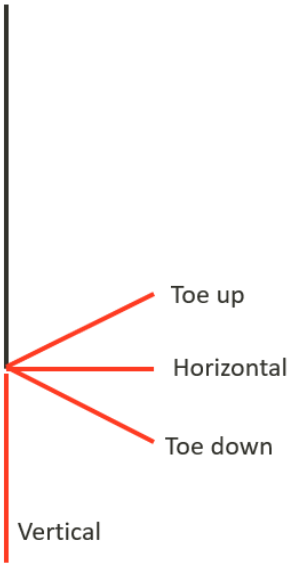

Figure 4-2: Illustration of the 4 simple geometries in the OLGA simulations.

Table 4-1: Parameters used in the OLGA simulations.

Quantity	Value
Internal pipe diameter	8” (0.2032 m) (both vertical section and toe)
Total flow rate	10 kg/s (u_{sl} = 0.31 m/s)
Length of horizontal section	500 m
Length of vertical section	1000 m
Water injection points	10, injecting 1 kg/s each, distributed at equal distance along the tubing
Liquid	Pure water (no dissolved gasses)
Water temperature	40°C
Sand particle size	100 µm
Sand particle density	2400 kg/m^3
Sand particle mass fraction	0.5%
Deviations of the toe	0° (vertical) 84.3° (toe down) 90° (horizontal) 95.7° (toe up)
Size of each grid cell	50 m

In each of the simulations, the well is initialized with stagnant water at a temperature of 40 °C. Next, the injection is started and the simulation is run until a steady state is reached after 30 days. As there are relatively few grid cells in the system, it is quick to simulate for such a long time (although a shorter simulated time would have sufficed).

In Figure 4-3 the sand holdup is shown for the four different toe configurations considered. As soon as the toe is upwards inclined, such as in the toe down and vertical configurations, no sand is accumulated in the wellbore. As the slip velocity is very low (0.014 m/s) and this velocity is already reached at the first injection point/grid cell, it makes sense that the liquid can quickly drag the sand upwards. Only in the horizontal and toe up configurations a sand bed is formed in the first 200

meters of the toe. However, the OLGA result do not show a significant additional frictional pressure gradient due to the sand bed, compared to the hydrostatic pressure of the vertical well.

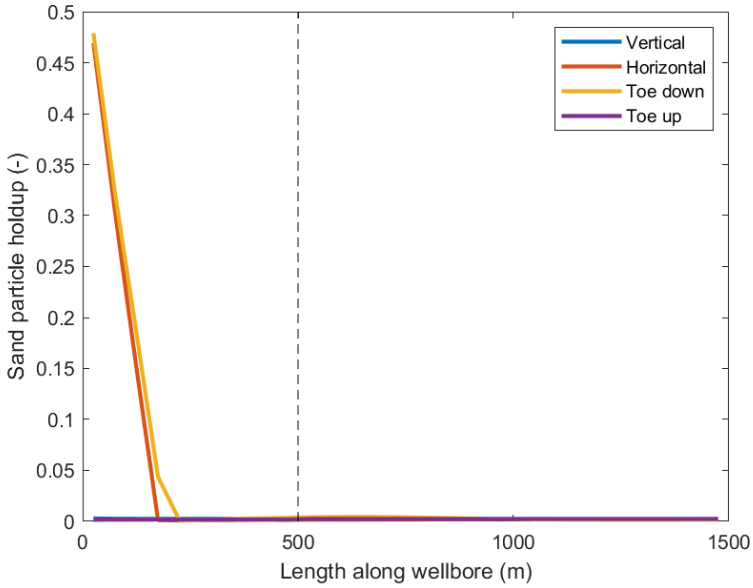

Figure 4-3: Sand particle holdup for the simulations specified in Table 4-1.

To show the effect of the particle diameter, a simulation with 1000 µm particles was run for the horizontal toe. The resulting sand particle holdup is shown in Figure 4-4. For the large particles a sand bed forms along the entire horizontal section, and in the vertical section the sand fraction is over 10 %. Note that it requires a sand particle size that is much larger than would realistically be found in reservoirs to have a large impact on the flow in the well.

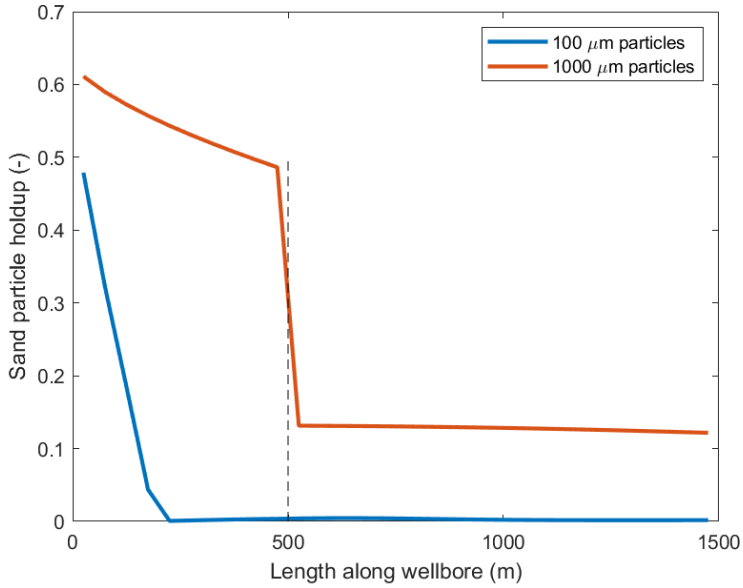

Figure 4-4: Sand particle holdup from the OLGA simulations for two very different particle sizes.

In Figure 4-5 the sand fraction is shown for three different flow rates. The injection always occurs at 10 positions uniformly distributed along the toe (at each position 10% of the flow is injected). The results show that at low flow rates, a significant sand bed can form along the entire toe.

However, in the OLGA simulations this sand bed is removed when the flow rate is increased once again. These results show that sand accumulation in the toe can occur when starting up or shutting down the system. Using vertical or toe down well designs would reduce the risk of such accumulation.

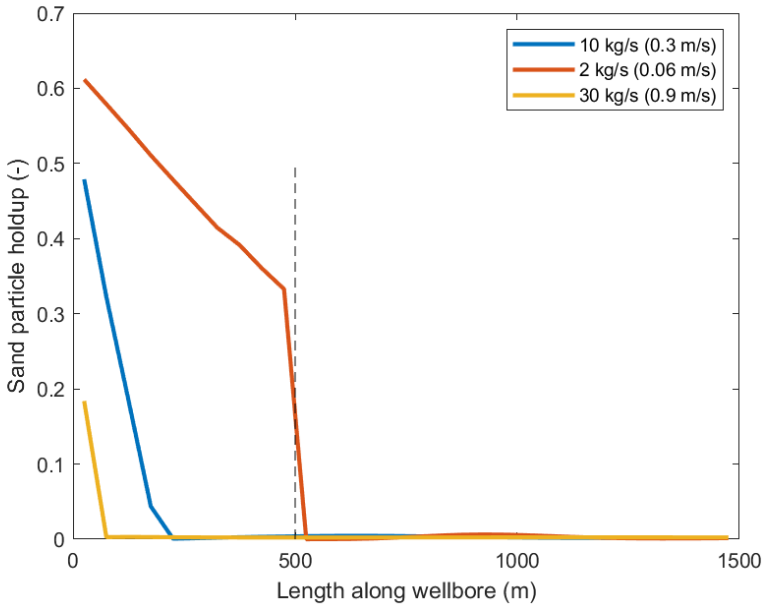

Figure 4-5: Sand particle holdup from the OLGA simulations for three different flow rates.

Note that in the OLGA simulations above a very low liquid flow rate was used. The velocity in the pipeline was 0.31 m/s, an order of magnitude lower than is typical in a geothermal system. Figure 4-5 shows that at realistic velocities no sand bed would be obtained at all. Sand beds would therefore only occur during transient operation, i.e. when the system is just started up or undergoes a shutin.

Overall, it is the formation of a sand bed that should be avoided. The OLGA simulations above showed the formation of such a bed in horizontal sections at low flow rates. The formation of a sand bed can also be predicted by empirical models that categorize the dispersion of sand in water. In the work of (Swamy, Díez et al. 2015), some of these empirical models have been compared to the results of CFD simulations for a horizontal pipe. A map of the flow patterns is presented in Figure 4-6. In the simulations presented above a particle size of 100 µm is considered, which leads to a transition between a stationary and a moving bed at a liquid velocity of 0.23 m/s. In the OLGA simulations, this velocity is obtained as well: OLGA predicts a stationary bed below this velocity, but no moving bed above this velocity as the particle concentration is too low. This velocity is much lower than the velocity typically found in geothermal systems.

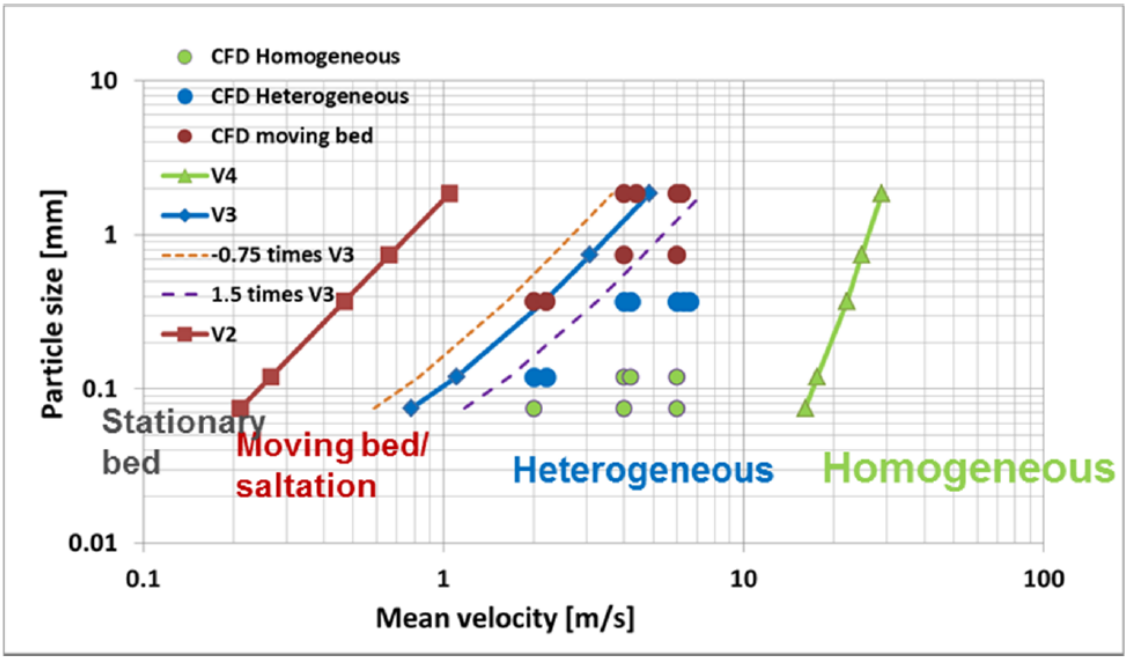

Figure 4-6: Flow pattern map of slurry flow taken from (Swamy, Díez et al. 2015).

These results indicate that it is not likely that sand will accumulate in the wellbore, even when the velocity of the geothermal well is reduced. Especially when sand control is in place, and the remaining sand that is produced has a small grain size. Reducing the velocity in the well leads to a decrease of sand production, and an increased risk of sand depositing in the well. However, the ESP typically cannot operate at such low flow rates, so it is unlikely that wells are at risk of sanding up. In the topside separator, however, the flow velocity is very low. As a result, it is likely that sand will accumulate in the separator and filters when sand is produced.

4.2 Erosion

The chance of bed formation due to the presence of sand might not be large, there might still be a risk of erosion of sand in the wellbore and top-side facilities. The erosion rate does not only depend on the parameter impacting the sand transport, but also the hardness of the particles, tubing materials, particle impact velocity and angle and potential interaction with scaling and corrosion. In this section, several correlations from the literature to estimate erosion are compared. Since the flow topology has an impact on the erosion rate, the effect on the erosion of a change in pipe diameter, as occurs in the production well, is considered. Finally the considerations with respect to erosion of other components in the well, such as ESP and sand screens are provided.

4.2.1 Erosion correlations

There are two types of correlations which can be used to estimate the risks associated with the erosion issue. The first type is estimating critical erosional velocity which describes the criteria for the velocities which has no erosion issues. The second type of the correlations focusses on estimating the erosion rate (e.g. in terms of mm/yr). Since erosion depends both on the geometry and the material of the geothermal well and on the material, shape and size distribution of the sand particles, these correlations necessarily leave out many factors and provide a rough estimation of the erosion for a particular geometry (usually either a straight pipe or an elbow). To make a comparison between the different correlations, either a straight pipe or a wide elbow are

selected as the geometry. This does mean that the erosion rate is likely higher / critical erosional velocity is likely lower in very sharp bends. Erosion can also be worse in valves, pumps and other obstructions to the flow.

The most common standard to estimate erosion in the petroleum industry is the API RP 14E standard created by the American Petroleum Institute (American Petroleum Institute 1991). It predicts a maximum velocity (V_e) above which erosion might occur, given by:

$$V_e = \frac{c}{\sqrt{\rho_m}} \qquad (4\text{-}5)$$

Where ρ_m is the mixture density (approximately equal to the liquid density for low sand fractions), and *c* is a constant. In the standard, values for this constant are suggested: 100 for corrosive and 150-200 for non-corrosive liquids. Alternate values of *c* have been suggested by e.g. Total (Sani, Huizinga et al. 2019):

C < 100 for fluids containing significant amounts of solid particles
C = 100 160 for corrosive fluids
C = 200-300 for non-corrosive fluids

As indicated by several authors (Sani, Huizinga et al. 2019; Svedeman, Arnold 1994; Salama 2000) the API RP 14E is typically conservative. This makes sense, as it hardly contains any specifics of the system. The calculated critical erosional velocity should be at or below the actual critical velocities for many different systems. An accurate, non-conservative, value of c in this standard would be based on the specifics of the systems, hardness of the materials and particles and can only be applicable to a fixed geometrical conditions. Due to its simplicity, this standard is easy to use, but conservative.

Another simple rule of thumb that can be used as an alternative to the API RP 14E standard is the NORSOK P-002 (NORSOK 2014) standard. For both carbon steel and stainless steel, the maximum velocities in this standard are presented in Table 4-2. Note that sand does not have a large impact on the erosion velocity in this standard.

Table 4-2: Example of the maximum velocities in the NORSOK P-002 standard for both carbon steel and stainless steel.

Fluid	V_e CS (m/s)	V_e SS (m/s)
Liquids	6	7
Liquid with sand	5	7
Untreated seawater	3	7

Next, there is the correlation be (Svedeman, Arnold 1994), which explicitly includes the sand flow rate when calculating the erosional velocity:

$$V_e = \frac{K_S D}{\sqrt{Q_s}} \qquad (4\text{-}6)$$

In this equation Q_s is the sand flow rate in cubic feet per day, D is the pipe inner diameter in inches, and K_s is a fitting erosion constant, that depends on the geometry, the material and the flow regime. A typical value of the constant K_s for a ASTM A234 carbon steel long-radius elbow in gas-liquid flow with solids is 1.34. It is typical to calculate erosion rates for elbows, as the erosion rate is larger in bends than in straight pipes: it will be flow in elbows that limits the flow rate. This correlation is based on measurements by Bourgoyne (1989) for gas-solid, gas-liquid-solid and liquid-solid systems. This does mean it is a very generic correlation, where a lot of details are implicitly included in the fitting constant.

A comparison of the three standards is made in Table 4-3. Note that only in the (Svedeman, Arnold 1994) correlation the erosional velocity changes depending on the diameter and the sand concentration. The effect of the sand erosion in the work by Svedeman and Arnold is based on experiments by (Bourgoyne 1989), who performed experiments with sand fractions of up to 0.12%. In the work, he indicates that at the largest sand fractions considered the erosion is no longer proportional to the sand fraction. The large effect of the sand fraction obtained in Table 4-3 is therefore likely much larger than in reality. It also shows that at more realistic sand fractions (0.005% sand) the correlations that do not include the sand flow rate become conservative.

Table 4-3: Comparison of the three presented correlations for the erosional velocity. For Svedeman and Arnold a K_s value of 1.34 is used.

	V_e(m/s)		
Model	7" pipe 0.5% sand	10" pipe 0.5% sand	7" pipe 0.005% sand
API RP 14E	3.8	3.8	3.8
NORSOK P-002	5	5	5
Svedeman and Arnold	0.7	1.1	7.4

These three previous standards only yield an erosional velocity, that should be considered an upper limit below which the erosion rate is deemed acceptable. There is also a set of correlations in which the erosion rate (ER, typically given in mm/year) is calculated. Three common correlations will be described here.

In the DNV GL-RP-0501 guideline (DNV 2015), the erosion rate is given by the following equation:

$$ER = KU_p^n F(\alpha) m_p \qquad (4\text{-}7)$$

For common materials used in well completions, such as carbon steel, stainless steel or Inconel the material coefficient K((m/s)$^{-n}$) is equal to 2e-9 and the velocity exponent *n* is equal to 2.6. The particle impact velocity (U_p)is equal to the mixture velocity (m/s). m_p (kg/s) is the mass flow rate of the sand particles (in the Svedeman and Arnold correlation it was the volumetric flow rate of the sand that was used). The impact angle function for ductile materials is equal to:

$$F(\alpha) = 0.6\,[\sin(\alpha) + 7.2(\sin(\alpha) - \sin^2(\alpha))]^{0.6}[1 - \exp(-20\alpha)] \qquad (4\text{-}8)$$

In this equation the impact angle α is given in radians. The erosion rate is then given in kg/s, and needs to be converted to mm/y:

$$ER_{\left\{\frac{mm}{y}\right\}} = ER \cdot \frac{T_c}{A_t \cdot \rho_w} \qquad (4\text{-}9)$$

Where T_c is the conversion factor between mm and years, ρ_w (kg/m^3) is the density of the pipe and A_t (m^2) is the area exposed to erosion, given by:

$$A_t = \frac{A_{pipe}}{\sin(\alpha)} \qquad (4\text{-}10)$$

Where A_{pipe} (m^2) is the cross-sectional area of the pipe (Det Norske Veritas 2007).

Next, there is the Tulsa erosion model (Zhang, Y., Reuterfors et al. 2007). There are several variants of this model, but one of these variants is as follows:

$$ER = C\frac{m_p}{\rho_{pipe} A_{pipe}} \sin(\alpha) H_b^{-0.59} F_s U_p^n F(\alpha) \qquad (4\text{-}11)$$

In this equation m_p is the mass flow of the sand particles (kg/s), ρ_{pipe} is the density of the pipe material (kg/m^3), A_{pipe} (m^2) is the cross-sectional area of the pipe, α is the particle impact angle, H_b (GPa) is the Brinell hardness of the pipe material, F_s is the particle shape factor (1: sharp angular, 0.53: semi-rounded, 0.2: fully rounded). U_p (m/s) is the particle impact velocity, and this time the function $F(\alpha)$ is equal to (for α in radians):

$$F(\alpha) = 5.4\alpha - 10.11\alpha^2 + 10.93\alpha^3 - 6.33\alpha^4 + 1.42\alpha^5 \qquad (4\text{-}12)$$

The constant C is equal to $2.17 \cdot 10^{-7}$.

A third common correlation is the Salama model (Salama 2000). It is based on empirical research of flow in pipe bends, and states that the erosion rate is equal to:

$$ER = \frac{1}{S_m}\frac{Q_s V_m^2 d}{D^2 \rho_m} \qquad (4\text{-}13)$$

In which S_m is a geometrical constant equal to 5.5 for a elbows (with radii of 1.5-5 D). Q_s is the sand flow rate in kg/day, V_m is the mixture velocity in m/s, d is the sand particle diameter in µm, D is the pipe diameter in mm and ρ_m is the mixture density in kg/m^3.

There are some differences between these three correlations: in the Salama model, there is a pre-factor that takes into account the geometry, while the Tulsa and DNV GL-RP-0501 models explicitly contain the particle impact angle, which is also affected by the geometry of the system. The material of the pipes is also differently included into the model: for the DNV GL-RP-0501 there is a single constant and an exponent that differ depending on the selected material. In the Tulsa model actual material properties are used: the hardness of the material and its density. Finally, the Salama model does not include the pipe material at all: the correlation is based on a set of experiments in steel pipes so that is implicitly included.

In the DNV and Tulsa models the geometry can be included through the impact angle of the particles. In the Salama model this is not possible: experiments have been performed for particular geometries and the correlation can only be applied to those. As erosion is most severe in bends and Tees, the experiments are limited to those geometries. Unlike the correlations for the critical velocity, the predictions of the erosion rate all consider the sand flow rate, but only the Salama correlation contains the particles size, and only the Tulsa model contains the shape of the particles.

In Table 4-4 a few example calculations are performed for the three models that were presented. For the impact angle 40 degrees is selected, which is the worst case for ductile materials. Steel is selected as the material. The flow rate is 300 m^3/h in all calculations. In the DNV and Tulsa correlations low erosion rates are obtained, while the Salama correlation predicts a problematic erosion rate for the 7”pipe, with a 0.5% mass fraction of sand and a particle size of 150 µm. Note that these sand flow rates are unrealistically high. A more realistic case is considered in section 5.2. Note that if a wall thickness of 17.5 mm is assumed and the lifetime of a doublet is 30 years, then the erosion rate must be (significantly) lower than 0.58 mm/y. In the table, all erosion rates, even for the high sand fraction, are lower this. From these correlations, it seems that erosion is not a problem for straight pipes and large radius bends. Considering the composition of the brine in geothermal systems, corrosion is probably a much greater risk than erosion. Note that corrosion can also increase erosion as the material properties of the pipe change.

Table 4-4: Example calculation of the erosion rate for the three considered models.

	Erosion rate (mm/y)			
Model	7”pipe, 0.5% sand, 150 µm	10”pipe, 0.5% sand, 150 µm	7”pipe, 0.005% sand, 150 µm	7”pipe, 0.5% sand, 15 µm
DNV	0.008	5.93e-4	7.70e-5	0.008
Tulsa	0.010	8.9e-4	1.0e-4	0.010
Salama	0.35	0.0068	5.83e-4	0.006

4.2.2 Erosion simulations

In the previous section, correlations were considered in which the geometry was only considered through an empirical constant, or by assuming an impact angle. The local fluid velocities, turbulent levels and particle impact angle has a significant impact on the erosion rate which cannot be

captured by simplified models above. By performing computational fluid dynamic (CFD) simulations, the flow in the geometry is simulated and the impact angle can be determined with much greater accuracy. This is especially true when recirculation zones are present or when the flow changes direction, e.g. in the bends.

In this section an example is presented in which the diameter of the casing increases. A schematic of the geometry is presented in Figure 4-7. A similar approach can be used to determine the areas with a higher chance of erosion due to flow profiles and topology, such as valves, inlet of ESPs, etc. The pipe widens from an internal diameter of 17.8 cm (7”) to a diameter of 25.0 cm (9 5/6”). Note that the pipe is vertical in reality (gravity acts from left to right in the figure. To solve the flow a RANS (Reynolds Averaged Navier Stokes) method is used. In a RANS method, only the average velocity field is solved and all of the eddies in the turbulent flow are not resolved. This significantly reduces the time required to run the calculations. To model the turbulence a k- ω SST (shear stress transport) model is used in which equation for the turbulent kinetic energy (k) and the specific rate of energy dissipation (ω) are solved. The resulting flow is axisymmetric and a two-dimensional solver can be used. Solving the equations occurs on a computational grid, shown in the bottom of the figure. To solve the flow, ANSYS Fluent is used, which is a commercial software program for CFD simulations. As boundary conditions, a fully developed turbulent flow is set at the inlet. At the outlet an outflow boundary condition is specified (fixed pressure). In the simulations the properties of water at a temperature of 20°C are used, and it is assumed that the water is incompressible.

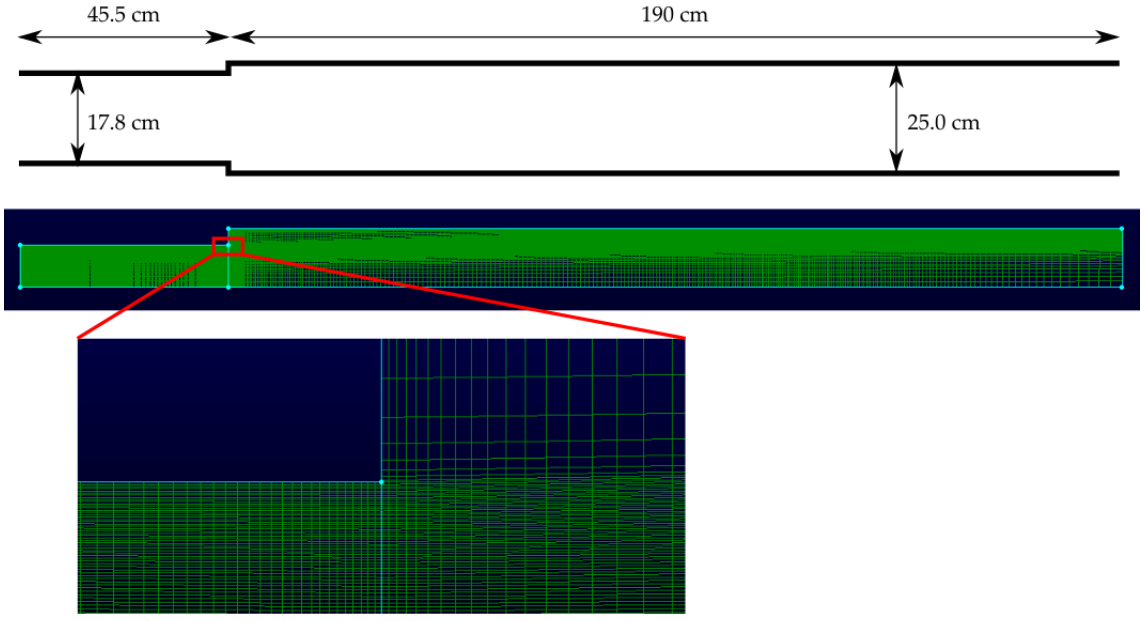

Figure 4-7: The geometry used in the calculation (top), followed by the mesh that is used (middle), and a detail showing the fine mesh near the change in diameter (bottom). Note that the pipe is actually vertical and has been rotated 90 degrees to fit better on the page. Gravity therefore acts from right to left.

In the calculation, first 100 seconds of flow is simulated with time-steps of 1 second in order to obtain a steady state. A flow rate of 300 m^3/h is applied, which results in a velocity of 3.35 m/s in the 17.8 cm section and a velocity of 1.71 m/s in the 25.0 cm section. The resulting flow after this steady state simulation is presented in Figure 4-8. The contours show that in the corner, where the pipe is widening, the axial velocity is almost zero and there is a small radial velocity inwards: this indicates a recirculation zone where an accumulation of sand can occur.

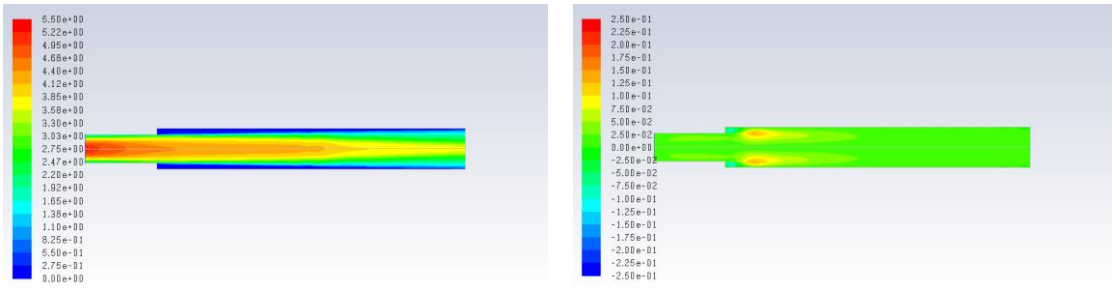

Figure 4-8: Contours of the axial velocity (left) and the radial velocity (right) in the widening pipe.

Next, the sand is introduced at the inlet in the steady state flow. The initial velocity of the sand particles is equal to the local flow velocity. The sand mass flow rate is 0.45% of the liquid mass flow rate and the sand particles have a diameter of 100 µm and are made of dolomite (density 2872 kg/m^3). Note that dolomite is chosen here as a worst case (heavy particles can cause more erosion and have a larger relative velocity with respect to the fluid) and for the practical reason that this material is included in Fluent by default. Off course, this sand fraction and particle diameter would lead to a huge amount of particles being injected every second (about 700 billion). Therefore, 100 particles are injected every second, which represent the much larger number of particles. Note that the number of injected particles is independent of the mass flow rate of the sand: each particle in the computation just represents a different number of actual particles. As the average velocity in the pipe is solved, the particles would mainly move straight ahead and there would be no erosion. Therefore, the particles are subjected to a Discrete Random Walk Model and a Random Eddy Lifetime of 0.15 such that they move according to the local turbulence properties.

Even after solving the flow and tracking a representative set of particles an erosion model needs to be selected. Many erosion models have a velocity exponent which cannot be determined from the CFD simulations. The way in which the material properties are included should also be addressed in an erosion model. In the current example the McLaury model is used, which was developed at the University of Tulsa based on experiments with sand in water. The default parameters in Fluent are selected. The results are presented in Figure 4-9.

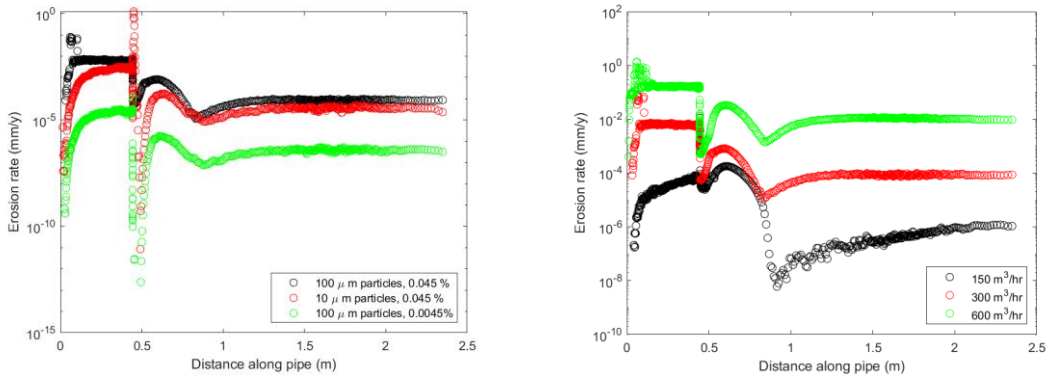

Figure 4-9: Erosion rate determined using the Fluent simulations using the McLaury model. Variations in the flow rate (right figure) and in the particle size and particle mass fraction are considered.

These results show a large dependence of the erosion rate to the flow rate of the liquid. This is in line with the erosion models discussed earlier, that both the mass flow rate of the particles and the impact velocity, which both increase with increasing liquid flow rate, also increase the erosion rate. For all but one of the considered cases, the erosion rate is lower at the change in diameter than in

the pipe with the smaller diameter. Only when small 10 µm particles are considered does the erosion rate actually increase at the pipe diameter change. Note that such a large mass fraction of such small particles is not likely to occur in reality, so this should not be a problem in the actual geothermal wells. Overall, these results show that a diameter change in which the diameter widens does not lead to problematic erosion if that erosion was not already problematic in the smaller diameter pipe. In other words, during the steady production of the geothermal well, the casing erosion risks can be well estimated by the erosion rate in the section with the smallest diameter. The situation might be different during the transient effects, such as well start-up or shut-in. Well shut-in might lead to sand accumulation in several areas of the casing and those sand piles can be produced during the well start-up

CFD can be a good tool to improve erosion estimation, but it does come at a higher computational cost. For an empirical erosion model, performing a calculation to estimate erosion takes almost no time. However, CFD calculations require (1) creating a model of the geometry, (2) creating a computational grid, (3) performing a time-consuming CFD calculation. And even then, the proper erosion model with proper parameters needs to be selected. It is therefore important to investigate what is likely to be the place where the worst erosion will occur (i.e. the sharpest bend or the place with the highest flow velocity) and performing the calculation only for that part of the system. For both empirical and CFD models, a calibrated erosion model is required. The impact of several parameters on the erosion rate trends can be quantified using these models but the absolute value of the erosion rate can only be achieved after calibrating the models based on a representative set of experiments or field data monitoring data, if available.

4.2.3 Erosion in ESPs

Perhaps the most critical component for erosion is the ESP. Due to high velocities, turbulence and rapid changes in the flow directions in the internals of the ESP at different stages, the risk of erosion is higher. As an example, considering an 6.75" impeller at 60 Hz, a point on the impeller's edge has a velocity of 34 m/s with a corresponding high shear rate caused by this high velocity and change in the flow direction (dictated by blade design). Erosion can occur in different components of the ESP such as blades, vanes and shrouds which can cause a lower performance of the pump or a complete failure. A significant amount of research on ESP erosion is being performed at the University of Tulsa, for instance in the work of (Zhu, Zhang et al. 2019). In this work, results from CFD calculations in Fluent are compared to actual experiments in which paint is applied to an ESP, which is then eroded away. This makes the erosion easily visible. An example of their results is shown in Figure 4-10. Depending on the volumetric rates, sizing of the ESP and particles sizes and fraction, different areas of the ESP internals which are more susceptible to erosion was identified. The area inside the impeller blades were most exposed to the erosion risks. From another study by (Morrison, Carvajal et al. 2015), it was found that the erosion processes are more obvious from the second stage onwards.

There are no simple empirical correlations available to estimate the erosion inside an ESP. Much also depends on the ESP design. The closest to a guideline is possibly the work of (Pirouzpanah, Morrison 2014). They calculate an erosion fraction based on the sand volume fraction α_s, the near wall sand velocity V_s and the turbulent kinetic energy *k:*

$$EF = \alpha_s^{0.08} V_s^{0.07} k_w^{1.25} \qquad (4\text{-}14)$$

And then calculate the erosion rate as follows:

$$ER = A \cdot EF^2 + B \cdot EF \qquad (4\text{-}15)$$

Where the coefficients *A* and *B* are given by 0.0163 and 0.8774, respectively. The experiments and computations (Pirouzpanah, Morrison 2014) performed were in a 8.15" ESP with a flow rate of 331

m^3/h, sand particles of 180 µm and 2 g/l of sand. Note that the turbulent kinetic energy is not known a priory, so CFD is probably still required to use the correlation. The simulation then does not require particle tracking, which is also time consuming: the erosion behavior of the particles can be calculated from the equation above. From the correlation, Pirouzpanah and Morrison obtained maximum erosion rates of 5-40 µm/h. When using the Salama model, the erosion with these parameters would be 0.01 µm/h. This is a very large difference, which clearly indicates that the standard erosion models are insufficient to estimate the erosion in ESP and pump systems. Unlike for the straight pipes and large radius bends, erosion might be a problem for the ESP, especially in the first stage.

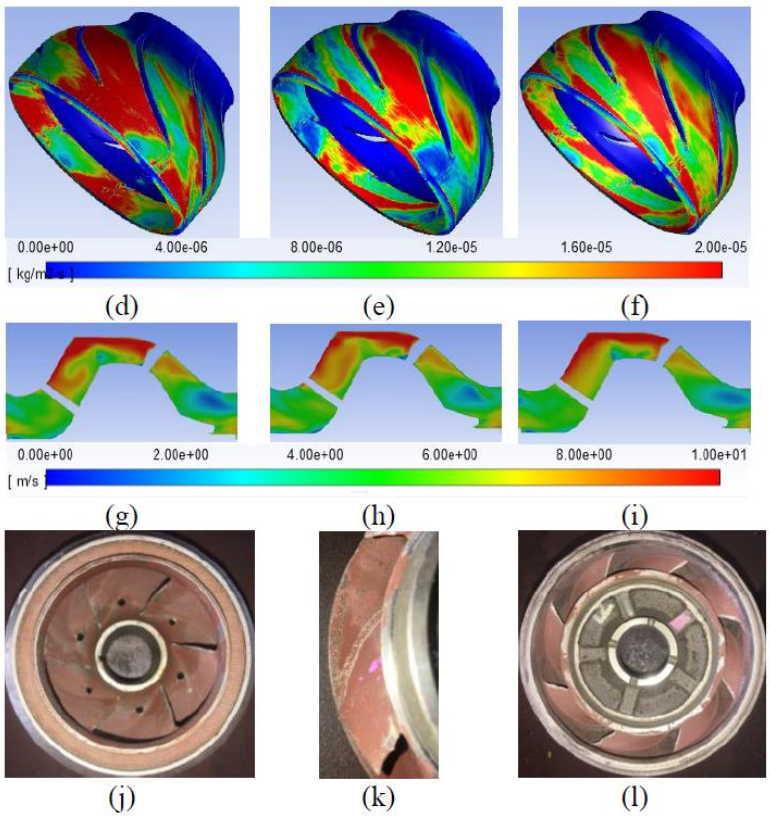

Figure 4-10: Results taken from the paper by Zhu et al. (2019), showing the results from CFD calculations (top) and from experiments (bottom). The top row shows the erosion contour (kg/m^2s) from the CFD simulations, the middle row shows the average velocity contours and the bottom row shows the results from the experiments, in which the paint has been removed through erosion at at the impellers and at several other locations.

4.2.4 Erosion in sand control screens

Sand control screens typically contain a weaved mesh which is used to filter the sand from the liquid. This mesh is also subject to erosion, especially when there are many fines present in the liquid.

There is a typical limit suggested in the literature of 0.27 ft/s (0.082 m/s) for the aperture velocity in a sand screen (Cameron, Jones 2007). Below this limit, erosion should be avoided and the screen should not fail. In an open hole completion it should not be a problem to stay below this limit: the surface area between the reservoir and the bottomhole is very large. However, in cased hole completions where the screen is placed inside the casing the aperture velocity might be significantly higher, as most of the flow occurs at the position of the perforations. Furthermore, even for open hole completions the inflow is generally not uniform, due to the presence of low permeability streaks or local high skin. As a result, erosion might occur unexpectedly. This could

explain why the typical limit in the literature is so low. Production logging tools (PLTs) can be used to monitor erosion of the sand control screen during production.

Several authors suggest that the 0.27 ft/s limit is conservative. (Gillespie, Beare et al. 2009) indicate that erosion is unlikely up to 0.5 ft/s, whereas (Procyk, Gou et al. 2015) indicate an upper limit of 0.65 ft/s. They found that this is the lowest aperture velocity at which failure of a sand screen was observed in an actual gas well. An even larger maximum velocity of 1 ft/s has been advised by (U.S. Filter 1998).

Several authors created a correlation to predict the erosion in a sand screen. (Procyk, Gou et al. 2015) created an empirical equation for the amount of mass (in grams) lost from the screen:

$$\Delta \mathrm{M} = 1.63 \cdot 10^{-4} \cdot F \cdot HR^{0.56} \cdot d \cdot \left(\frac{SE_r}{V_r^{2.7}}\right) \cdot \left(\frac{V_f}{\zeta}\right)^{2.7} \cdot V_f \cdot A \cdot T \cdot C \cdot \rho \qquad (4\text{-}16)$$

In this equation *F* is a tuning factor equal to 1.48, *HR* is the Vickers hardness ratio between particle and screen (~10 for steel and sand), *d* is the particle diameter (µm), SE_r is the reference specific erosion (equal to $7.6 \cdot 10^{-6}$g/g), V_r is the face velocity (ft/s), ζ is the flow velocity multiplier (equal to 0.22), A is the screen exposure area (ft^2), T is the time (hr), C is the particle concentration (mg/kg) and ρ is the carrier fluid density (lb/ft^3). The factor $1.63 \cdot 10^{-4}$ is there for all the unit conversions.

A similar correlation was proposed by (Cameron, Jones 2007), who created the correlation specifically for cased completions:

$$M_{loss} = k \cdot \frac{1}{4} \cdot \pi \cdot d_{perf}^2 \cdot v_a \cdot k_{sf} \cdot \rho_s \cdot N \cdot SE_r \cdot t \qquad (4\text{-}17)$$

In this equation d_{perf} is the perforation diameter in feet, v_a is the fluid velocity at the exit of the perforation (ft/s), k_{sf} is the particle shape factor (1 for sharp angular particles, 0.2 for round particles and 0.53 for semi-rounded particles), ρ_s is the sand density (g/cc), *N* is the sand volume fraction and *t* is the time (in seconds). *k* is again a constant to correct for the different units. Unfortunately, the authors only indicate the specific erosion rate in graphs where the vertical axis does not contain numbers. Note however, that this equation still requires a model of the specific erosion rate SE_r, which depends on the impact angle of the particles. It therefore differs depending on screen design.

(Zhang, R., Hao et al. 2020) performed CFD simulations in order to validate the correlation by (Procyk, Gou et al. 2015). From the simulations, the flow field through the wire wrapped screen can be nicely observed, as shown in Figure 4-11. However, in order to compare the resulting erosion rate to the equation by (Procyk, Gou et al. 2015) the specific erosion rate was chosen such that the predicted and simulated mass loss match exactly for one of the simulations. If that is done, the other simulations at other flow rates also match the equation.

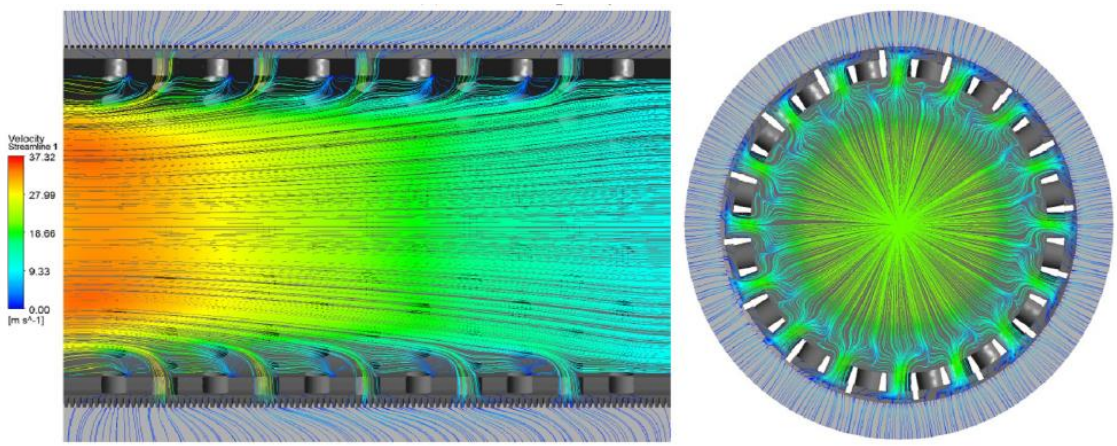

Figure 4-11: Results of CFD simulations through a wire-wrapped screen taken from (Zhang, R., Hao et al. 2020).

Overall, there is a rule of thumb for the maximum velocity through the screen that is on the conservative side. There are some models available to predict the mass loss in the screens, but they are somewhat difficult to use. First an estimate of the acceptable mass loss should be made, and then there needs to be an estimate of the specific erosion, which is not at all straightforward. The specific erosion should depend on the actual geometry of the weave, which is complex in itself.

From the erosion research summarized in this chapter, it can be concluded that in the straight sections and the large radius bends in a geothermal system the risk of erosion is small. The existing guidelines for erosion estimation are great simplifications that do not take into account many of the parameters that determine the erosion rate. However, they do all indicate that erosion is not a problem in the straight sections and large radius bends in geothermal wells. And, as the literature indicates that these correlations, especially API RP 14E, tend to be on the conservative side, it is unlikely that erosion will occur. If erosion occurs, it is likely to happen at the ESP, where the relative velocity between the fluid and the rotors is very large. It is also possible that erosion occurs at the sand control screen, or in places at the topside where the direction of the flow varies quickly. At those locations it is very difficult to estimate the erosion, since the flow follows a complex pattern which can lead to large variations in the impact angle and the impact velocity of the sand particles on the geometries. CFD is an option in such cases, although it still requires a calibrated model of the specific erosion rate. Therefore, monitoring the performance of the ESP, and monitoring erosion at the sand screen using production logging tools can help to determine whether erosion is becoming problematic in well operation.

5 Example case: Brussels Sand shallow geothermal application

In this chapter, we will illustrate sand control options for the Brussels Sand, in particular in the area around Zwijndrecht which was selected as one of the pilot regions in WarmingUp. The focus will be on selecting sand control completions, since it was already concluded in Chapter 2 that some form of sand control is required. The steps as presented in the Weatherford sand screen selector are largely followed (Weatherford 2012):

A. Characterization (Section 5.1): the particle sizes, the expected productivity/injectivity in the area, which determines the drawdown and rate and geomechanical parameters of the formation. These inputs are used to estimate sand production using the method from section 2.5.1.
B. Asses sand control options (criteria discussed in section 3.4).
C. Testing of the selected option using sand or slurry retention tests (discussed in section 3.2; skipped in this case).
D. Refine the sand control selection by choosing opening sizes (not included here).
E. Consider consequences for completion design: erosion and reservoir performance (in terms of pressure drop) in this case.

5.1 Characterization of the Brussels sand

Particle Size

In the framework of WarmingUp, particle size distributions (PSD) of cuttings were estimated for several wells in The Netherlands (Veldkamp, Geel et al. 2022). Here the PSD of the well closest to Zwijndrecht is presented: Barendrecht-01 (short name: BRT-01) in Figure 5-1. Only the samples of the main reservoir depth are presented. The lower part of the formation has more fines. The data in Figure 5-1 is plotted as the percentage coarser than the given size. In this report, we follow the convention for plotting the cumulative PSD summing up from the coarsest fraction. Thus, Dxx should be interpreted as xx% of the particles are larger than this size.

These data were observed using laser diffraction, which generally results in larger particle sizes than sieve data (Zonneveld 1994, Veldkamp, Geel et al. 2022). In addition, due to the pre-processing of the cuttings, the fines fraction is probably underrepresented: the mud fraction was separated from the observations by fitting Gaussian distributions. Due to the underrepresentation of the fines, it is likely that the sorting is somewhat overestimated, depending on the definition of the sorting. For a more extensive discussion of the processing and interpretation of the cuttings see (Veldkamp, Geel et al. 2022). It should be noted that the results presented here are earlier results than those presented in (Veldkamp, Geel et al. 2022). Later processing included improved representation of the silt fraction and resulted in more fines included in the PSD. Also nearby well HEI-01 was showed somewhat coarser grain size, but similar sorting. Because this does not materially change the results, here these preliminary PSDs are used.

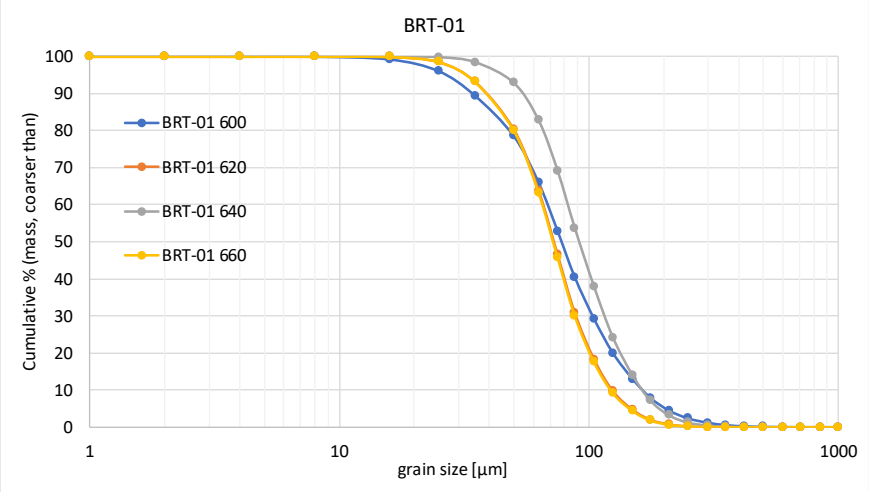

Figure 5-1. PSD observed in sampled cuttings from BRT-01 at four different depth values (laser PSD, cumulative weight coarser than given size) (Veldkamp, Geel et al. 2022).

Production

In the expected production rates for different well orientations at the location of Zwijndrecht were presented. The main productivity results are presented in Table 5-1. One of the main uncertain factors is the vertical permeability. The vertical permeability is low due to tight, calcite-cemented streaks (Geel, de Haan et al. 2022). From a sensitivity analysis for the vertical permeability, it was shown that the variability in the productivity of the horizontal well was very large. For the simulations, a total maximum pressure differential of 24 bar was assumed (14 bar on the injector and 10 bar on the producer), a maximum rate of 150 m^3/hr and an injection temperature of 8°C. The injectivity/productivity of the horizontal wells is similar to the injectivity observed at the doublet in Zevenbergen namely ~20 m^3/hr/bar at 30°C (Buik, N., Bakema 2019). The injectivity corrected for viscosity would be higher at 26.6 m^3/hr/bar, the productivity is lower. The difference between the injector and producer is caused by the fact that the properties improve in southerly direction (Geel, de Haan et al. 2022).

Table 5-1: Overview of the productivity/injectivity (m^3/hr/bar) for a doublet of vertical, deviated and horizontal wells after 20 years for a well diameter of 0.19 m (source: (Geel, de Haan et al. 2022)[1]).

Well type	Producer	Injector (@ 8°C*)
Vertical	9.2 m^3/hr/bar	7.2 m^3/hr/bar
Deviated (400 m @ 75°)	12.9 m^3/hr/bar (41% increase)	11.0 m^3/hr/bar (52% increase)
Horizontal (500 m length)	17.2 m^3/hr/bar (88% increase)	16.0 m^3/hr/bar (120% increase)

* viscosity at 8°C is 1.4 cP and at 0.9 cP at the production temperature of 30°C.

The well distance at reservoir depth in the simulations in (Geel, de Haan et al. 2022) is 1250 m, which is more than enough to avoid thermal breakthrough in 20 years. Additional simulations indicate that 850 m distance at reservoir depth is enough to limit the thermal breakthrough to ~1 degree in 30 years. The simulations were done using the fine scale model (1-m vertical resolution).

[1] Please note that the values used here for productivity and injectivity are slightly different from the values given in (Geel, de Haan et al. 2022) because these are based on an earlier version of the simulations.

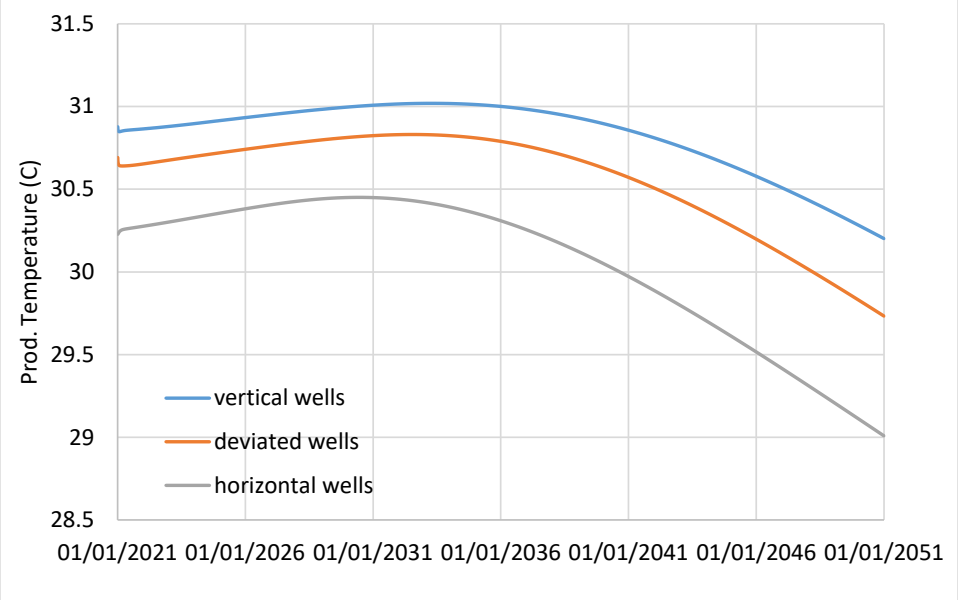

Figure 5-2. Production temperature for a doublet of vertical, deviated and horizontal wells over 30 years of production for a well distance of 850 m at reservoir level (at the heel of the wells).

Rock strength

To get an estimate of the rock strength of the Brussels Sand, an analysis was done for the nearby well BRT-01 which will geologically be fairly similar to the location Zwijndrecht as it is only 10 km away along strike, is roughly at the same depth, and has the same thickness. Moreover, BRT-01 has a good quality suite of logs: GR, SP, DT, RHOB and DIL. See (Geel, Foeken 2021) for a discussion of the petrophysical analysis of the well. The interpretations were done with the computer program Interactive Petrophysics (IP), version 4.6 (2019) from Lloyd's Register Digital Products Limited.

Unfortunately, well BRT-01 does not have a shear sonic log, which is important for estimating rock mechanical properties. Therefore, first a shear sonic log was created based on the sonic log (DT). This can be done in IP based on the volumes of sandstone, limestone, dolomite and shale. For each of these an equation relating v_s (shear velocity) to v_p (compressional velocity) needs to be specified:

$$v_s = av_p^2 + bv_p + c \qquad (5\text{-}1)$$

The constants *a*, *b* and *c* need to be estimated on data from other wells. In this case, the constants were estimated based on a DSI (Dipole Shear Sonic Imager) run in well A15-03, which is one of the few wells in the Netherlands which has this information for unconsolidated sands and shales, in this case deltaic sands and shales of Pliocene and Pleistocene age. Limestone is used to represent the calcite cement, dolomite is not present. The used values are listed in Table 5-2. In Figure 5-3, the fit to the data is shown for sand, which is poor. This adds to the uncertainty in the estimated values.

Table 5-2: Input values for the estimation of a shear sonic log

	a	b	C
Sandstone / sand	0	0.67	-0.58
Limestone	-0.05508	1.01677	-1.03049
Shale/clay	0	0.5	-0.25

Based on this input data, Poisson's ratio, bulk and shear modulus, Young's modulus and C_0 (uniaxial compressive strength) are estimated. The estimate of C_0 is based on Sarda et al. (1993) and Horsrud (2001).

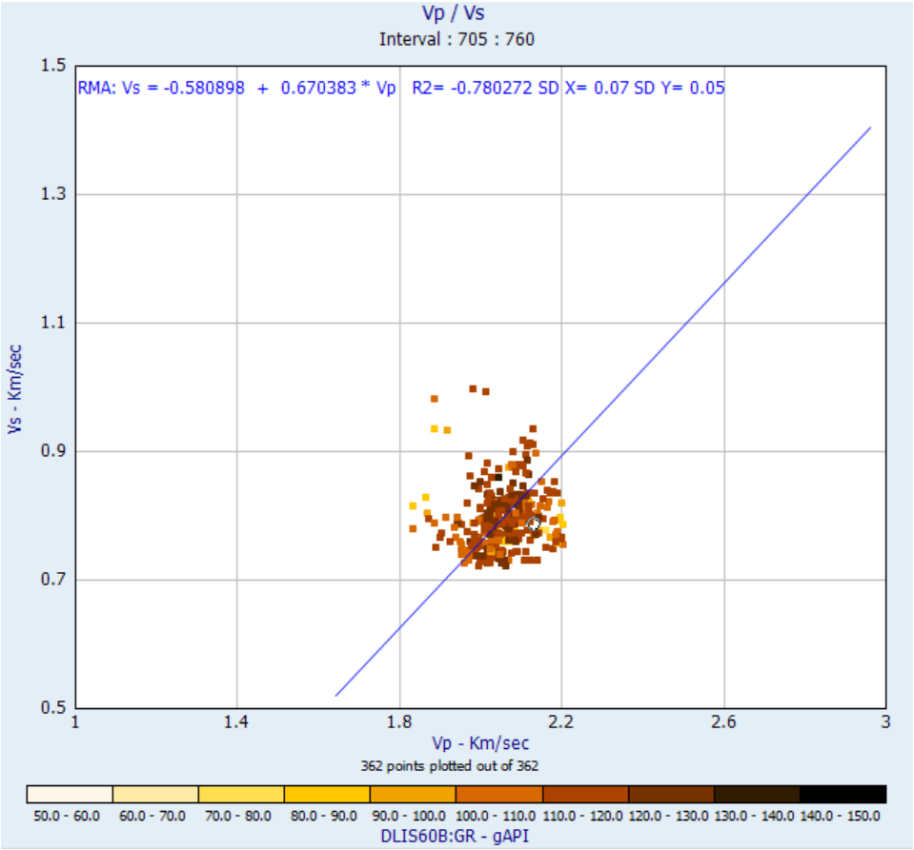

Figure 5-3. Vp versus Vs for well A15-03 including the characteristics of the fitted line at top of the figure.

The resulting estimations are shown in Appendix A and Table 5-3. The thin spikes are caused by the calcite cemented layers. For the sandy, non-cemented intervals C_0 varies between 3 and 10 MPa, and is on average estimated to be 6.8 MPa (68 bar). The interval 590-605 m has low values for C_0: around 3 MPa. For sand production, the weakest intervals determine the risk. However, in the simplified models used in this work, the variability in depth is not included, so using the minimum value would result in a gross overestimation of the sand production. Therefore for the simulations, a value between the minimum and the average was used: 5 MPa. Sensitivity scenario's with weaker (3 MPa) and stronger (10 MPa) rock are run for comparison.

Table 5-3. Average values for the main geomechanical parameters of the Brussels Sand in well BRT-01 (see Appendix A)

Lithology	Poisson ratio	E (Young's Modulus)	Mu (Shear Modulus)	KB (Bulk Modulus)	UCS
All lithologies	0.42	3.90	1.39	7.34	7.89
Calcite-cemented streaks excluded	0.42	3.20	1.13	6.90	6.77
Calcite-cemented streaks only	0.37	8.34	3.08	10.16	15.02

Sand production

To understand the impact of the diameter and selected flow rate on the sand production, we estimate the amount of mobilized sand for a vertical producer (open hole) for the first 100 days using the model described in section 2.5.1. The results are illustrated in Figure 5-4. The amount of mobilized sand ranges from 3000 to 15,000 kg. The time period over which this sand is mobilized varies: therefore the amounts cannot be interpreted in terms of concentration. The flow rate has a larger impact on the amount of sand mobilized then the diameter. The results in Figure 5-4 are for C_0 (uni-axial compressive strength) of 5 MPa (50 bar) (average over the sandy interval). For comparison also the mobilized sand for the upper and lower end of the estimated C_0 range is estimated. The results for the stronger rock (C_0 = 10 MPa) are presented in Figure 5-5 and for the weaker rock (C_0 = 3 MPa) in Figure 5-6. For the high flow rate cases (which also have higher drawdown), sand production is very similar for all three cases, also for the stronger rock. However, for the low flow rates, sand mobilization reduces clearly for the stronger rock compared to the weaker rock. This suggests that for a stronger rock type, reduction of the flow rate is much more effective.

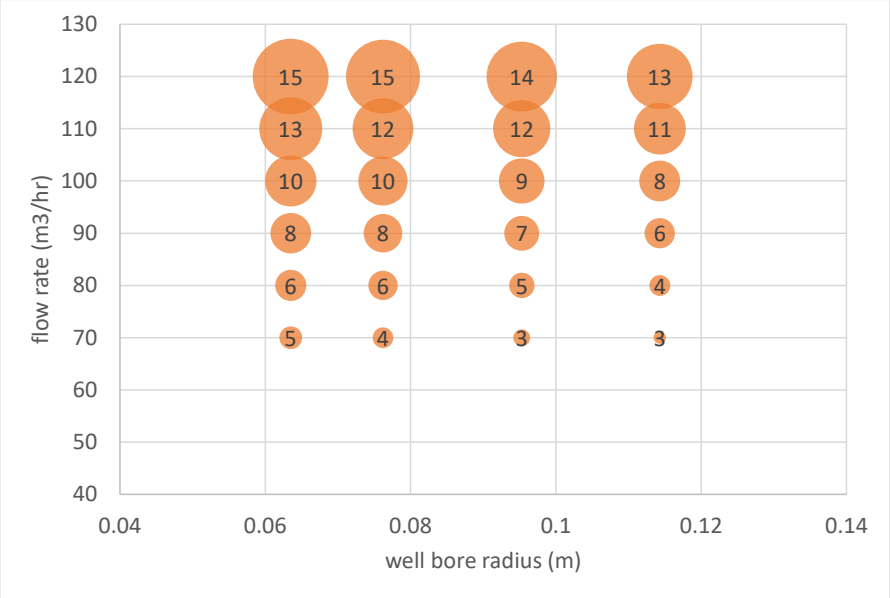

Figure 5-4. Estimated amount of mobilized sand in the first 100 days for a vertical, open hole well as a function of diameter and flow rate (**C_0 = 5 MPa**, T=31 Dm, viscosity = 0.9 cP, critical fluid flux = 5E-4 m/s). Bubble size indicates amount of sand in 1000 kg.

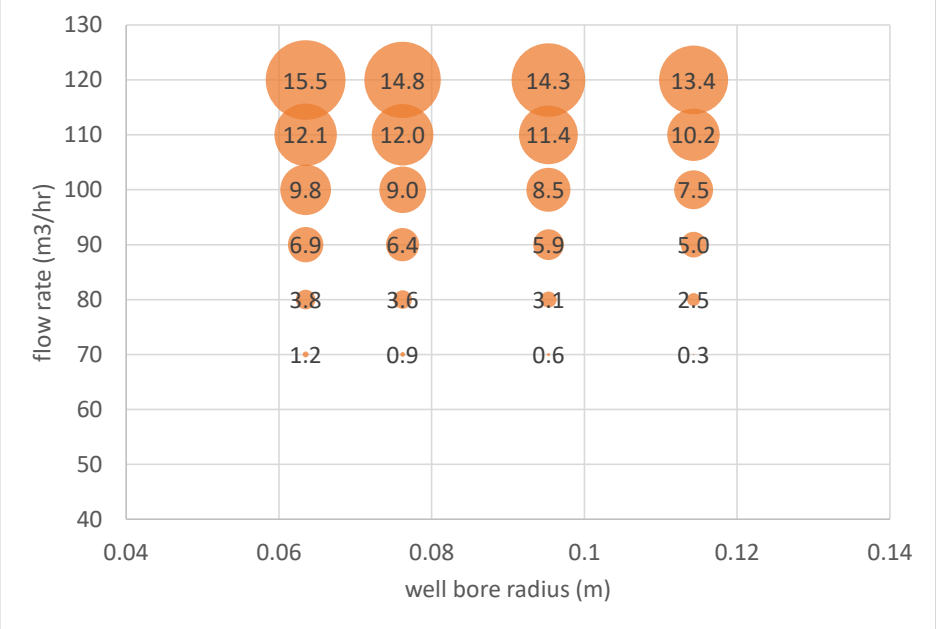

Figure 5-5. Estimated amount of mobilized sand in the first 100 days for a vertical, open hole well as a function of diameter and flow rate (**C_0 = 10 MPa**, T=31 Dm, viscosity = 0.9 cP, critical fluid flux = 5E-4 m/s). Bubble size indicates amount of sand in 1000 kg.

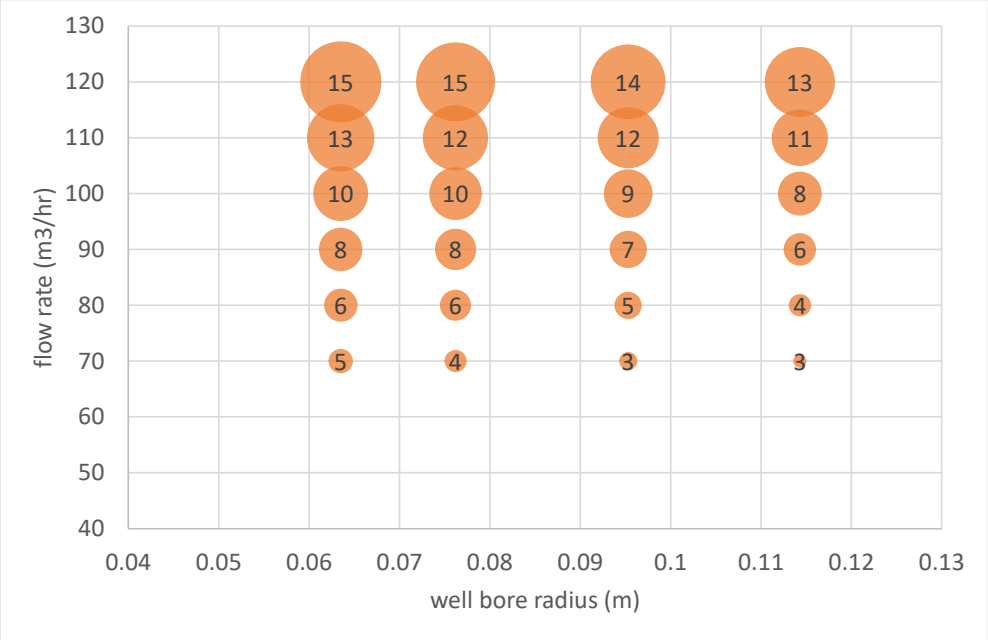

Figure 5-6. Estimated amount of mobilized sand in the first 100 days for a vertical, open hole well as a function of diameter and flow rate (**C0 = 3 MPa**, T=31 Dm, viscosity = 0.9 cP, critical fluid flux = 5E-4 m/s). Bubble size indicates amount of sand in 1000 kg.

For the estimation of erosion and possible accumulation of sand on the well bore, also the concentration of sand is important. To estimate the concentration, the cumulative amount of sand produced presented above in Figure 5-4 could be divided by the time period during which sand production occurs. This time period is show in Figure 5-7 and is highly variable. This is because for some cases, a small final burst of sand occurs which makes the time period much longer. For all cases, however, the bulk of the sand production occurs in the first 10 to 15 days. Therefore the average concentration during the first 10 days is reported in Figure 5-8. The concentration ranges from 0.08 kg/m^3 to 0.5 kg/m^3.

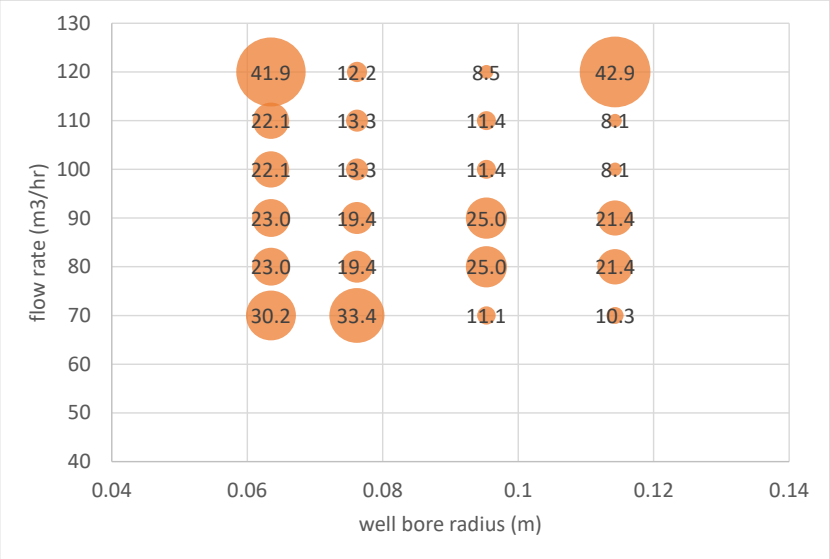

Figure 5-7. Time until sand production stops (in days indicated by bubble size and the numbers) for the simulations shown in Figure 5-4 for C_0 = 5 MPa.

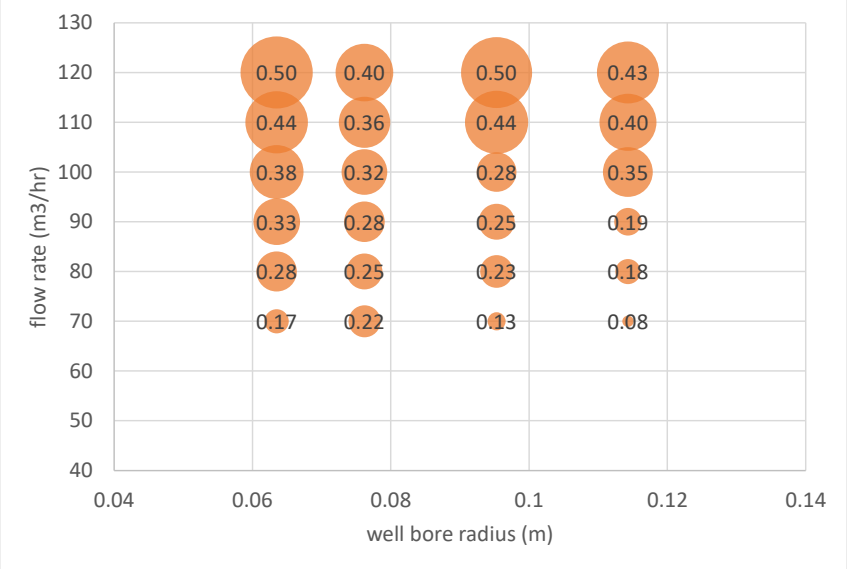

Figure 5-8. Average concentration during the first 10 days (in kg/m^3 indicated by the bubble size and numbers) for the simulations shown in Figure 5-4.

5.2 Impact for completions

In this section, three questions will be addressed:
1. Based on the particle size distribution estimated for the Zwijndrecht area, what would be the best sand control method according to Figure 3-5?
2. What would be the velocities and pressure gradients in the well, depending on the wellbore radius that is selected?
3. If no sand control method would be used, what would be the erosion rates in the wellbore?

To answer question 1, the average of the particle size distributions from Figure 5-1 are selected. This results in the data presented in Table 5-4. It should be realized that the PSD on which these values are based, were derived from unwashed cuttings from which the contributions of the mud and formation was estimated by fitting curves (see (Veldkamp, Geel et al. 2022) for more details). Thus uncertainty is high. When comparing the Dxx quantities with the work of (Tiffin, King et al. 1998), the results would suggest that a simple screen is possible. However, the sub 44 µm fraction is higher than allowed even for a gravel pack completion. It should be noted however, that due to the fact that the particle size distribution was derived from cuttings, the fines fraction is highly uncertain. Please see (Veldkamp, Geel et al. 2022) for a full discussion. When comparing with the work by (Latiff 2011, Geel, de Haan et al. 2022) a gravel pack completion would be selected based on the low value of D10. According to the Weatherford sand selector (Weatherford 2012), a gravel pack is not required: an expandable screen or metal-mesh screen would be sufficient due to the relatively good sorting. A simple wire-wrap is not recommended because of the fine sand. (Blinovs, van Og 2022) also advised a metal-mesh screen for a well design at Zwijndrecht in the Brussels Sand. Based on this data, for the considered criteria the selection of the completion is therefore not obvious, although overall a gravel pack does not appear to be required. In either possible completion, there is a risk of clogging of the system by the small fines. It is very difficult to predict clogging, also since the shape of the particles plays a role in the clogging process.

For the well ZVB-GT-01 at Zevenbergen, also a shallow geothermal well in the Brussels sand, a similar analysis was performed by Buik and Bakema (2019). The sand properties they found were similar, but they used a different criterium for the sand control selection from the drinking water industry. From this criterion, a gravel pack was selected as the best applicable method, mainly because of the low diameter of the sand particles. However, it proved financially unfeasible to place a gravel pack in the horizontal wells that were created. Therefore a premium screen with a mesh size of 100 µm was selected, which corresponds approximately to D50. The reason given for not selecting a finer mesh size was that it was not possible to remove mud or sand from behind the screen when required. The selected sand control method was therefore not in line with any recommendations in the literature, but seems to perform well in the first results.

Table 5-4: Properties of the approximate particle size distribution for the Zwijndrecht location (based on cuttings from well BRT-01; see (Veldkamp, Geel et al. 2022)).

Property	Values BRT-01
D10	146 µm
D40	87 µm
D90	40 µm
D95	32 µm
Sub 44 µm	11%
D10/D95	4.6
D40/D90	2.17

To look at the pressure losses and the velocities in the well, a well design should be selected. In this section a very simple well-design will be assumed. The vertical section of the well has a depth of 600 m, after which either a 500 m horizontal section, a 400 m 75° deviated section, or a 104 m vertical section is placed in which the production occurs. The production occurs through a lined casing with a fixed diameter, given by the wellbore radius in section 5.1. 300 meters below the surface the ESP is placed. The ESP flows into a tubing that has an internal diameter that is 65% of the internal diameter of the liner. The flow rate is 100 m^3/h.

From this, the numbers from Table 5-5 and Table 5-6 follow. A water temperature of 40 °C is assumed, and with a sand concentration of < 0.5 kg/m^3 (< 0.05 % by mass) the sand will not affect the fluid properties significantly. The pipe roughness is estimated at 500 µm. The results show that the pressure losses in the system are more determined by the diameter and the hydrostatic pressure gradient than by the inflow for the well completions considered.

Table 5-5: Rough estimates of the pressure losses in the Zwijndrecht geothermal producing well.

Wellbore radius	ΔP inflow (bar)	ΔP liner (300 m) (bar)	ΔP tubing (300 m) (bar)
0.064 m	10.9	33.2	44.5
	7.8		
	5.8		
0.114 m	10.9	29.4	30.0
	7.8		
	5.8		

Table 5-6: Rough estimates of the velocity in the Zwijndrecht geothermal producing well.

Wellbore radius (m)	Velocity liner (m/s)	Radius tubing (m)	Velocity tubing (m/s)
0.064	2.16	0.042	5.11
0.114	0.68	0.074	1.61

Finally, the erosion is estimated. The worst case erosion in the straight pipes will occur in the tubing downstream of the ESP, where the velocity is highest. Considering the DNV and Salama models, in combination with the largest possible sand concentration of 0.5 kg/m^3, the erosion rates in Table 5-7 are obtained in the pipe flows. For the particle diameter the average of 78 µm is used. None of the erosion rates are problematic, mainly due to the smaller particle size and the lower sand fraction compared to the earlier calculations.

Table 5-7: Erosion rates estimated for the simple completions

Wellbore radius (m)	Erosion rate in the tubing (mm/y) (Salama)	Erosion rate in the tubing (mm/y) (Tulsa)
0.064	0.0048	0.0016
0.114	1.5e-4	2.5e-5

Overall, the erosion of the casing should not be a problem in the straight liner/tubing sections of the pipe. However, larger fluid velocities occur at the ESP, in valves, or in sand screens. If erosion occurs, it would occur there. Since the large amount of fine grains makes it difficult to select a sand control method, it is possible that sand would be produced during well operation. Therefore, the risk of ESP erosion should be taken into account. Furthermore, the topside facilities should be able to handle the production of sand.

6 Summary, conclusions and recommendations

6.1 Summary and conclusions

Sand production is a complex process which depends on many aspects of the subsurface, the well completions and operational schemes: in situ stress conditions, consolidation of the sand, size distribution and shape of the particles and the (transient) flow velocity of the fluids are important aspects. This makes prediction and even translating experience from one well to the next challenging.

Three main options to deal with potential sand production where investigated with focus on the relatively shallow formations of the North Sea Groups: limit flow rate/drawdown, control the inflow of particles through completions or handle in the well.

For limitation of the drawdown/flow rate as a sand control method, design criteria that predict the onset of sand production are often used. These criteria indicate that for the very weak rocks (unconsolidated or poorly consolidated) expected in the North Sea groups some form of sand control is required. Thus design criteria based on well bore or perforation stability are not likely to provide useful design criteria. Design criteria limiting the flow rate below the erosion rate are also not likely to be useful: geothermal wells need to operate at considerable rates to be economically viable. The criteria from shallow applications (< 500 m) such as heat storage, which assume sand control (generally a gravel pack) and identify the maximum velocity on the borehole wall, appear to be overly conservative. In general, the guidelines and experience from shallow applications (< 500 m) is less relevant: drilling techniques, well completions, formations (grains size, consolidation), water quality, legal constraints: all are more similar to deeper applications.

To really understand if sand production will be a problem, approaches that can predict the amount of sand production over time are more useful. However predictive models for both onset and amount of sand produced need to be tuned to the local conditions, which is mostly done using sand production data and experience in existing wells. However, available experience of shallow geothermal production is very limited. A simple sand production model by (Fjaer, Holt et al. 2008) was implemented, which showed that the flow velocity at which particles can be moved is an important, but very uncertain parameter.

Completions for sand control are mainly different types of screens and gravel packs. The criteria for choosing a particular type of completion are sometimes different for different sources, also because different criteria are used, such as sorting or the sub 44 µm fraction. Clogging of the completions can always be an issue, but some level of clogging can be acceptable before the inflow is significantly affected as the pores in the gravel pack and the screens are typically much larger than the pores in the reservoir.

For handling particles in the well, sand hold up and erosion were investigated. Due to the relatively high flow rates in geothermal wells, sand deposition in the well is not likely to be an issue. The risk of erosion is small in the straight sections and the large radius bends. The most likely place for

erosion is the ESP, however erosion in the ESP is difficult to simulate and no simple correlations exist.

For the Brussels Sand Mb a detailed analysis was done at the location of Zwijndrecht. For this formation, information was collected in the WarmingUP project. Sand control in the form of metal mesh screens appears to be the most appropriate. Alternatively expandable screens might be an option. There is some disagreement however between the different methods for determining the type of sand control: the sand fraction is reasonably well sorted, but the formation also has a relatively large sub 44 µm fraction. The reasonable sorting typically leads to the advice of a metal-mesh screen. In some methods, the relatively large sub 44 µm fraction leads to the advice of a gravel pack.

Due to the relatively large amount of fines, which are predominantly present in the lower parts of the formation, clogging is possibly an issue and some fines will be produced. Careful startup and shutin procedures are required to ensure stability of the formation and the 'natural gravel pack' that will likely develop around the screen. At this point, it is not clear whether a limitation on the flow rate is advisable to avoid clogging of the screens, because it is difficult to determine the risk of clogging of the gravel packs and metal-mesh screens. For the Brussels Sand Mb, the formation productivity/injectivity is not very large and limits due to pressure constraints appear to be more important than due to sand production issues.

The results of the analysis for the Brussels Sand Mb cannot be applied easily to other shallow formations, because of differences in depth, PSD, reservoir quality and rock strength. However, some conclusions hold more widely because most aquifers in the lower and middle North Sea Groups are relatively unconsolidated and fine grained:

- All formations are likely to require some form of sand control because of low rock strength.
- Many formations of the Middle and Lower North Sea Group are of marine origin and relatively fine grained (Buik, N., Bakema 2019, Rijks Geologische Dienst 1985, Veldkamp, Geel et al. 2022) and with moderate permeability unlike the really shallow formations of the Upper North Sea Group. Thus pressure constraints are more likely to be limiting than flow rate constraints like for the Brussels Sand Mb.

6.2 Knowledge gaps and recommentations

The following knowledge gaps were identified:

- Little information is available on the geomechanical characteristics of the aquifers in the North Sea groups.
- Information on particle size distribution and particle shapes of the North Sea groups is available but sparse: a start on providing this information has been made in the NOA (Nationaal Onderzoeksprogramma Aardwarmte) program in the 1980s (Rijks Geologische Dienst 1985). More details on the Brussels Sand Mb are provided in (Veldkamp, Geel et al. 2022). This document also includes a summary of the NOA data.
- Public information on sand retention and clogging of screens, liners and gravel packs for relevant PSDs, fluid properties and flow rates is a scarce, because the majority of the information is for either for petroleum or shallow (groundwater, heat storage) applications. This holds both for measured data and simulations. Simulation of clogging for

shallow, groundwater applications is also not directly applicable due to differences in conditions (e.g. (De Zwart 2007)).
- The erosion rates in straight pipes and in pipe bends can be calculated with many different models. However, it is much more difficult to determine the erosion of the ESP. There are no correlations that can easily predict it.
- There is a lack of guidelines in how to deal with produced sand.

Recommendations

Below, a number of activities is proposed that could improve predictions of sanding issues and proposals for completions. Most of the activities will also benefit other developments in Paleogene and Neogene formations, and other types of applications including heat storage.

- Estimation of geomechanical rock parameters is of key importance, including rock strength. Since it is expensive to do geomechanical tests (even more so when it is done on cores), methods to estimate geomechanical characteristics from more easily available data should be developed. For example, drilling data could give relevant information on rock strength. However, first a dataset should be created which can be used to develop and test such methods. The data set should preferably also include measurements of sand and fines produced from the well, so that relevant geomechanical data can be linked to sand production. Specific geomechanical tests for sand production for consolidated formations have been developed (Fjaer, Holt et al. 2008), but are not likely to be useful for poorly or unconsolidated shallow formations.
- To facilitate the knowledge developments, it is recommended that samples of produced sand and fines are collected from newly drilled wells whenever possible.
- Dedicated sand retention tests for relevant PSDs, fluid properties and proposed screens would be very useful to reduce the risks of geothermal development in these formations, for example following (Ma, Deng et al. 2020). The data can be used to enhance our understanding and improve model approaches.
- Some existing rules-of-thumb, like erosional limits for screens, appear to be overly conservative. It is recommended to study under which conditions these rules-of-thumb can be relaxed.
- For the Brussels Sand specifically detailed simulations of the stresses around different well orientations and with different completions to understand the impact of the hard, calcite cemented layers on sand production. It could be investigated whether oriented perforations could be an option if they are placed near these layers.
- Development of methods to estimate the risk of sand production for different operational strategies.

Acknowledgements

The constructive comments of the reviewers Pieter Bruijnen and Marc Hettema (EBN) and Nick Buik (IF Technology) are gratefully acknowledged. Visser & Smit-Hanab BV is gratefully acknowledged for access to the data from the Zevenbergen doublet.

References

ABASS, H., HABBTAR, A. and SHEBATALHAMD, A., 2003. Sand control during drilling, perforation, completion and production, *Middle East Oil Show* 2003, OnePetro.

AHAD, N.A., JAMI, M. and TYSON, S., 2020. A review of experimental studies on sand screen selection for unconsolidated sandstone reservoirs. *Journal of Petroleum Exploration and Production Technology,* **10**(4), pp. 1675-1688.

AL-AWAD, M.N., EL-SAYED, A.H. and DESOUKY, S.E.M., 1999. Factors affecting sand production from unconsolidated sandstone Saudi oil and gas reservoir. *Journal of King Saud University-Engineering Sciences,* **11**(1), pp. 151-172.

AMERICAN PETROLEUM INSTITUTE, 1991. Recommended Practice for Design and Installation of Offshore Production Platform Piping Systems. *Recommended Pratice 14E.* 5th edn. American Petroleum Institute, .

ANDREWS, J.S., JORANSON, H. and RAAEN, A.M., 2008. Oriented Perforating as a Sand Prevention Measure. Case Studies from a Decade of Field Experience Validating the Method Offshore Norway, *Offshore Technology Conference* 2008, Offshore Technology Conference.

BELLARBY, J., 2009. *Well completion design. Developments in Petroleum Science vo. 65.* Amsterdam, The Netherlands: Elsevier.

BLINOVS, A. and VAN OG, G., 2022. *Feasibility study. WarmingUP Doublet Theme T4A, potential location Zwijndrecht.* Hoogeveen (NL): Well Engineering Partners.

BLOEMENDAL, M., LOPIK, J.V., JANSEN, F., DRIJVER, B., BERGEN, F.V., KOENEN, M., CORINA, A.N., POTHOF, I., VAN DER MOST, L. and KHOSHNEVIS, N., 2020. *C1 - Literatuurstudie brontechniek.* WINDOW fase 1, KWR 2020.145. The Netherlands: KWR.

BOURGOYNE, A.T., 1989. Experimental study of erosion in diverter systems due to sand production, *SPE/IADC drilling conference* 1989, OnePetro.

BUIK, N. and BAKEMA, G., 2019. *Geothermie putten in ondiepe fijnzandige formaties. Literatuuronderzoek en ervaringen uit de olie/gas-, drinkwater- en WKO-sector.* 65163/RDx/20191218. IF Technology.

BUIK, N.A. and WILLEMSEN, A., 2002. Clogging rate of recharge wells in porous media. In: P.J. DILLON, ed, *Management of Aquifer Recharge for Sustainability. Proceedings of the 4th International Symposium on Artificial Recharge of Groundwater, Adelaide, September 2002.* Routledge Talylor and Francis Group, pp. 195-198.

CAMERON, J.A. and JONES, C., 2007. Development, verification and application of a screen erosion model, *European Formation Damage Conference* 2007, OnePetro.

CHANPURA, R.A., HODGE, R.M., ANDREWS, J.S., TOFFANIN, E.P., MOEN, T. and PARLAR, M., 2011. A review of screen selection for standalone applications and a new methodology. *SPE Drilling & Completion,* **26**(01), pp. 84-95.

DAKE, L.P., 1983. *Fundamentals of reservoir engineering.* Elsevier.

DE KLER, R., NEELE, F., NIENOORD, M., BROWNSORT, P., KOORNNEEF, J., BELFROID, S., PETERS, L., VAN WIJHE, A. and LOEVE, D., 2016. *Transportation and unloading of CO2 by ship - a comparative assessment. CATO WP 9 final report CO2 shipping.* CCUS-T2013-09-D08.

DE ZWART, A.H., 2007. Investigation of clogging processes in unconsolidated aquifers near water supply wells.

DNV, 2015. *DNVGL-RP-O501, recommended practice: managing sand production and erosion.* Det Norske Veritas.

ERIKSEN, J.H., SANFILIPPO, F., KVAMSDAL, A.L., FLINT, G. and KLEPPA, E., 2001. Orienting live well perforating technique provides innovative sand-control method in the North Sea. *SPE Drilling & Completion,* **16**(03), pp. 164-175.
FATTAHPOUR, V., MOOSAVI, M. and MEHRANPOUR, M., 2012. An experimental investigation on the effect of rock strength and perforation size on sand production. *Journal of Petroleum Science and Engineering,* **86**, pp. 172-189.
FJAER, E., HOLT, R.M., HORSRUD, P., RAAEN, A.M. and RISNES, R., 2008. *Petroleum related rock mechanics.* 2nd Edition edn. Elsevier.
GEEL, C.R. and FOEKEN, J., 2021. *Formation evaluation of the Brussels Sand Member in the Netherlands (WarmingUP).* Utrecht: TNO.
GEEL, C.R., DE HAAN, H.B. and PETERS, E., 2022. *Characterisation and production of the Brussels Sand Member near Zwijndrecht Zuid.* Utrecht: TNO.
GEOTHERM PROJECT, 2019. *Best practice guide for the design of new geothermal plants. Task 5.5 - GEOTHERM project.* Denmark: GEOOP.
GILLESPIE, G., BEARE, S.P. and JONES, C., 2009. Sand control screen erosion-when are you at risk? *8th European Formation Damage Conference* 2009, OnePetro.
HETTEMA, M.H., ANDREWS, J.S., PAPAMICHOS, E. and BLAASMO, M., 2006. The relative importance of drawdown and depletion in sanding wells: Predictive models compared with data from the Statfjord field, *SPE International Symposium and Exhibition on Formation Damage Control* 2006, OnePetro.
HODGE, R.M., BURTON, R.C., CONSTIEN, V. and SKIDMORE, V., 2002. An evaluation method for screen-only and gravel-pack completions, *International Symposium and Exhibition on Formation Damage Control* 2002, OnePetro.
HORSRUD, P., 2001. Estimating Mechanical Properties of Shale From Empirical Correlations. *SPE Drilling & Completion,* (June),.
HUISMAN, L., 1969. *Stromingsweerstanden in leidingen.* KIWA Mededelingen nr. 14. Rijswijk: KIWA.
IF TECHNOLOGY, 2012. *Ontwerpnormen fijnzandige aquifers. Deelrapport Werkpakket I.* 26.723/61335/RW. Arnhem: IF Technology.
IF TECHNOLOGY, 2001. *Ontwerpnormen voor bronnen voor koude-/warmteopslag.* 1/9805/GW. Arnhem, The Netherlands: IF Technology.
KEATON, J.R., 2018. Angle of Internal Friction. In: P.T. BOBROWSKY and B. MARKER, eds, *Encyclopedia of Engineering Geology.* Springer, .
KHAMEHCHI, E. and REISI, E., 2015. Sand production prediction using ratio of shear modulus to bulk compressibility (case study). *Egyptian Journal of Petroleum,* **24**(2), pp. 113-118.
KING, G.E., 2009-last update, Sand control methods. Available: https://documents.pub/document/sand-control-overview-558446fbbf5f6.html [5/26, 2021].
KIRSCH, C., 1898. Die theorie der elastizitat und die bedurfnisse der festigkeitslehre. *Zeitschrift des Vereines Deutscher Ingenieure,* **42**, pp. 797-807.
KJORHOLT, H., JORANSON, H., MARKESTAD, P., RAAEN, A. and VIKEN, R., 1998. Advanced sand prediction in a user friendly wrapping, *SPE/ISRM Rock Mechanics in Petroleum Engineering* 1998, OnePetro.
KUNCORO, B., ULUMUDDIN, B. and PALAR, S., 2001. Sand control for unconsolidated reservoirs. *Proceding Simposium Nasional IATMI Yogyakarta,* , pp. 3-5.
KWR, 2011. *Kennisdocument Putten(velden) Ontwerp, aanleg en exploitatie van pomp- en waarnemingsputten.* KWR 2011.014. Nieuwegein: KWR Watercycle Research Institute.
LAKE, L.W. and CLEGG, J.D., 2007. Petroleum engineering handbook: production operations engineering, vol IV. *Society of Petroleum Engineers, Richardson,* .

LATHAM, J.P., FARSI, A., XIANG, J. and CHEN, B., 2019. *The Horizon 2020 Project SURE: Deliverable 7.2 Report on Laterals Stability Modelling ,* Potsdam: GFZ German Research Centre for Geosciences, DOI:.
LATIFF, A., 2011. Assessment and Evaluation of Sand Control Methods for a North Sea Field.
LEPORINI, M., MARCHETTI, B., CORVARO, F., DI GIOVINE, G., POLONARA, F. and TERENZI, A., 2019. Sand transport in multiphase flow mixtures in a horizontal pipeline: An experimental investigation. *Petroleum,* **5**(2), pp. 161-170.
MA, C., DENG, J., DONG, X., SUN, D., FENG, Z., LUO, C., XIAO, Q. and CHEN, J., 2020. A new laboratory protocol to study the plugging and sand control performance of sand control screens. *Journal of Petroleum Science and Engineering,* **184**, pp. 106548.
MOHD JAMIL, N.F., 2011. PRODUCTION ENHANCEMENT FROM SAND CONTROL MANAGEMENT.
MORITA, N., WHITFILL, D., FEDDE, O. and LEVIK, T., 1989. Parametric study of sand-production prediction: analytical approach. *SPE Production Engineering,* **4**(01), pp. 25-33.
MORITA, N., WHITFILL, D., MASSIE, I. and KNUDSEN, T., 1989. Realistic sand-production prediction: numerical approach. *SPE Production Engineering,* **4**(01), pp. 15-24.
MORITA, N., DAVIS, E. and WHITEBAY, L., 1998. Guidelines for solving sand problems in water injection wells, *SPE Formation Damage Control Conference* 1998, OnePetro.
MORRISON, G., CARVAJAL, N., SALEH, R. and BAI, C., 2015. The Measured Impact of Erosion on the Rotodynamic and Performance Characteristics of a Mixed Flow ESP, *Proceedings of the 31st International Pump Users Symposium* 2015, Turbomachinery Laboratories, Texas A&M Engineering Experiment Station.
MUKERJI, T. and MAVKO, G., 2006. Understanding the Rock Physics Links Between Geologic Processes and Seismic Signatures. *Recent Advances in Rock Physics and Fluid Substitution,* **31**(special),.
NORSOK, 2014. *Process system design (Revision 1).* Standards Norway.
NOURI, A., VAZIRI, H.H., KURU, E. and ISLAM, M.R., 2005. A Laboratory Study of the Effect of Installation of Reticulated Expandable Liners on Sand Production in Weakly Consolidated Sandstone Formations, *SPE Annual Technical Conference and Exhibition* 2005, OnePetro.
NVOE, 2006. *NVOE-richtlijnen ondergrondse energieopslag.* NVOE.
OROSKAR, A.R. and TURIAN, R.M., 1980. The critical velocity in pipeline flow of slurries. *AIChE Journal,* **26**(4), pp. 550-558.
OTT, W.K., 2008. *Selection and Design Criteria for Sand Control Screens.* SPE Distinguished Lecturer Series.
PAPAMICHOS, E., 2018. Sand Production in Isotropic and Anisotropic Stress Tests, *52nd US Rock Mechanics/Geomechanics Symposium* 2018, American Rock Mechanics Association.
PAPAMICHOS, E., 2020. Analytical models for onset of sand production under isotropic and anisotropic stresses in laboratory tests. *Geomechanics for Energy and the Environment,* **21**, pp. 100149.
PAPAMICHOS, E., VARDOULAKIS, I., TRONVOLL, J. and SKJAERSTEIN, A., 2001. Volumetric sand production model and experiment. *International Journal for Numerical and Analytical Methods in Geomechanics,* **25**(8), pp. 789-808.
PIROUZPANAH, S. and MORRISON, G.L., 2014. Predictive erosion modeling in an ESP pump, *Fluids Engineering Division Summer Meeting* 2014, American Society of Mechanical Engineers, pp. V01BT10A004.
PLUYMAEKERS, M.P.D., DOORNENBAL, J.C. and MIDDELBURG, H., 2017. *Velmod-3.1.* TNO 2017 R11014. Utrecht: TNO.

PROCYK, A., GOU, X., MARTI, S.K., BURTON, R.C., KNEFEL, M., DRESCHERS, D., WIEGMANN, A., CHENG, L. and GLATT, E., 2015. Sand Control Screen Erosion: Prediction and Avoidance, *SPE Annual Technical Conference and Exhibition* 2015, OnePetro.
RAHMATI, H., JAFARPOUR, M., AZADBAKHT, S., NOURI, A., VAZIRI, H., CHAN, D. and XIAO, Y., 2013. Review of sand production prediction models. *Journal of Petroleum Engineering,* **2013**.
RIJKS GEOLOGISCHE DIENST, 1985. *Permeabiliteit, porositeit en kleigehalte van Tertiaire en Onder-Kwartaire afzettingen in Nederland.* 84KAR13EX. Haarlem: Rijks Geologische Dienst.
SALAMA, M.M., 2000. An alternative to API 14E erosional velocity limits for sand-laden fluids. *J.Energy Resour.Technol.,* **122**(2), pp. 71-77.
SANI, F.M., HUIZINGA, S., ESAKLUL, K. and NESIC, S., 2019. Review of the API RP 14E erosional velocity equation: Origin, applications, misuses, limitations and alternatives. *Wear,* **426**, pp. 620-636.
SANTARELLI, F., SKOMEDAL, E., MARKESTAD, P., BERGE, H. and NASVIG, H., 2000. Sand production on water injectors: how bad can it get? *SPE Drilling & Completion,* **15**(02), pp. 132-139.
SARDA, J., KESSLER, N., WICQUART, E., HANNAFORD, K. and DEFLANDRE, J., 1993. Use of porosity as a strength indicator for sand production evaluation, *SPE Annual Technical Conference and Exhibition* 1993, OnePetro.
SCHWARTZ, D.H., 1969. Successful sand control design for high rate oil and water wells. *Journal of Petroleum Technology,* **21**(09), pp. 1193-1198.
SICHARDT, W., 1928. Das Fassungsvermogen von Rohrbrunnen und seine Bedeutung fur die Grundwasserabsenkung, insbesondere fur großere Absenkungstiefen. *Berlin, Germany: Julius Springer,* .
SPIVEY, J.P., MCCAIN, W.D. and NORTH, R., 2004. Estimating Density, Formation Volume Factor, Compressibility, Methane Solubility, and Viscosity for Oilfield Brines at Temperatures From 0 to 275° C, Pressures to 200 MPa, and Salinities to 5.7 mole/kg. *Journal of Canadian Petroleum Technology,* **43**(7), pp. 52-61.
SVEDEMAN, S. and ARNOLD, K., 1994. Criteria for Sizing Multiphase Flowlines for Erosive. *Corrosive Service, SPE,* **26569**.
SWAMY, M., DÍEZ, N.G. and TWERDA, A., 2015. Numerical modelling of the slurry flow in pipelines and prediction of flow regimes. *WIT Trans Eng Sci,* **89**, pp. 311-322.
TIFFIN, D., KING, G., LARESE, R. and BRITT, L., 1998. New criteria for gravel and screen selection for sand control, *SPE Formation Damage Control Conference* 1998, OnePetro.
TRONVOLL, J., EEK, A., LARSEN, I. and SANFILIPPO, F., 2004. The effect of oriented perforations as a sand control method: A field case study from the Varg Field, North Sea, *SPE International Symposium and Exhibition on Formation Damage Control* 2004, OnePetro.
U.S. FILTER, 1998. *Threshhold velocities for screen erosion.* U.S. Filter / Johnson Screens.
UITVOERINGSTEAM WINDOW (IF TECHNOLOGY, TNO, DELTARES, KWR), 2020. *Verkenning HTO Heerhugowaard.* KWR 2020.140.
VAN DEN HOEK, P.J. and GEILIKMAN, M.B., 2006. Prediction of Sand Production Rate in Oil and Gas Reservoirs: Importance of Bean-Up Guidelines, *SPE Russian Oil and Gas Technical Conference and Exhibition* 2006, Society of Petroleum Engineers.
VAN DEN HOEK, P.J. and GEILIKMAN, M.B., 2005. Prediction of sand production rate in oil and gas reservoirs: field validation and practical use, *SPE Annual Technical Conference and Exhibition* 2005, Society of Petroleum Engineers.
VAN DEN HOEK, P.J. and GEILIKMAN, M.B., 2003. Prediction of sand production rate in oil and gas reservoirs, *SPE annual technical conference and exhibition* 2003, Society of Petroleum Engineers.

VAN DEN HOEK, P.J., KOOIJMAN, A.P., DE BREE, P., KENTER, C.J., ZHENG, Z. and KHODAVERDIAN, M., 2000. Horizontal-wellbore stability and sand production in weakly consolidated sandstones. *SPE Drilling & Completion,* **15**(04), pp. 274-283.
VAN DER SCHANS, M.L. and MEERKERK, M.A., 2019. *Putten en puttenvelden ten behoeve van drinkwater. Deel 2: Ontwerp.* KWR PCD 13-2. Nieuwegein: KWR Watercycle Research Institute.
VAN EIJS, R.M.H.E., 2015. *Neotectonic stresses in the Permian Slochteren Formation of the Groningen Field.* EP201510210531. Assen: NAM.
VARDOULAKIS, I., STAVROPOULOU, M. and PAPANASTASIOU, P., 1996. Hydro-mechanical aspects of the sand production problem. *Transport in Porous Media,* **22**(2), pp. 225-244.
VEEKEN, C., DAVIES, D., KENTER, C. and KOOIJMAN, A., 1991. Sand production prediction review: developing an integrated approach, *SPE annual technical conference and exhibition* 1991, Society of Petroleum Engineers.
VELDKAMP, J.G., GEEL, C.R. and PETERS, E., 2022. *Characterization of aquifer properties of the Brussels Sand Member from cuttings: particle size distribution and permeability.* WarmingUP report Theme 4A. Utrecht: TNO.
VERWEIJ, J.M., SIMMELINK, H.J., UNDERSCHULTZ, J. and WITMANS, N., 2012. Pressure and fluid dynamic characterisation of the Dutch subsurface. *Netherlands Journal of Geosciences,* **91**(4), pp. 465.
VRIJLANDT, M.A.W., STRUIJK, E.L.M., BRUNNER, L.G., VELDKAMP, J.G., WITMANS, N., MALJERS, D. and VAN WEES, J.D., 2019. ThermoGIS update: a renewed view on geothermal potential in the Netherlands, *European Geothermal Congress*, 11-14 June 2019 2019.
WAN, R., LIU, Y. and WANG, J., 2006. Prediction of volumetric sand production using a coupled geomechanics-hydrodynamic erosion model. *Journal of Canadian Petroleum Technology,* **45**(04),.
WEATHERFORD, 2012. *Sand screen selector: open hole.* Weatherford.
WOJCIECHOWSKI, M., 2018. A note on the differences between Drucker-Prager and Mohr-Coulomb shear strength criteria. *Studia Geotechnica et Mechanica,* **40**(3), pp. 163-169.
WONG, G.K., DRIA, D.E., GEILIKMAN, M.B. and STEWART, D.R., 2005. Bean-up guidelines for sand-control completions, *SPE Annual Technical Conference and Exhibition* 2005, Society of Petroleum Engineers.
WU, B., CHOI, S., FENG, Y., DENKE, R., BARTON, T., WONG, C., BOULANGER, J., YANG, W., LIM, S. and ZAMBERI, M., 2016. Evaluating sand screen performance using improved sand retention test and numerical modelling, *Offshore Technology Conference Asia* 2016, OnePetro.
ZARE-REISABADI, M. and SAFARI-BEIDOKHTI, M., 2014. Sand Production Prediction and Well Completion Optimization. **2**(4), pp. 361-374.
ZHANG, R., HAO, S., ZHANG, C., MENG, W., ZHANG, G., LIU, Z., GAO, D. and TANG, Y., 2020. Analysis and simulation of erosion of sand control screens in deep water gas well and its practical application. *Journal of Petroleum Science and Engineering,* **189**, pp. 106997.
ZHANG, Y., REUTERFORS, E., MCLAURY, B.S., SHIRAZI, S. and RYBICKI, E., 2007. Comparison of computed and measured particle velocities and erosion in water and air flows. *Wear,* **263**(1-6), pp. 330-338.
ZHU, H., ZHANG, J., ZHU, J., RUTTER, R. and ZHANG, H., 2019. A Numerical Study of Turbulence Model and Rebound Model Effect on Erosion Simulations in an Electrical Submersible Pump (ESP), *Fluids Engineering Division Summer Meeting* 2019, American Society of Mechanical Engineers, pp. V03BT03A041.
ZOBACK, M.D., 2007. *Reservoir Geomechanics.* Cambridge University Press.
ZONNEVELD, P.C., 1994. *Vergelijkend onderzoek korrelgroottebepaling (zeef/malvern).* OP 6500. Rijks Geologische Dienst.

Appendix A

Geomechanical properties determined from well logs. Well BRT-01. Tracks: 1) Depth (m); 2) Stratigraphy (WarmingUp); 3) Gamma-ray log [GRAPI]; 4) Caliper and Bit size; 5) Poisson Ratio [-/-]; 6) Young's modulus [GPa]; 7) Shear Modulus [GPa]; 8) Bulk Modulus [GPa]; 9) Unconfined Compressive Strength [MPa]: UCS_Sarda_phi for sand, UCS_Horsrud_DT for shale, UCS_Sarda_Horsrud is a combined log.

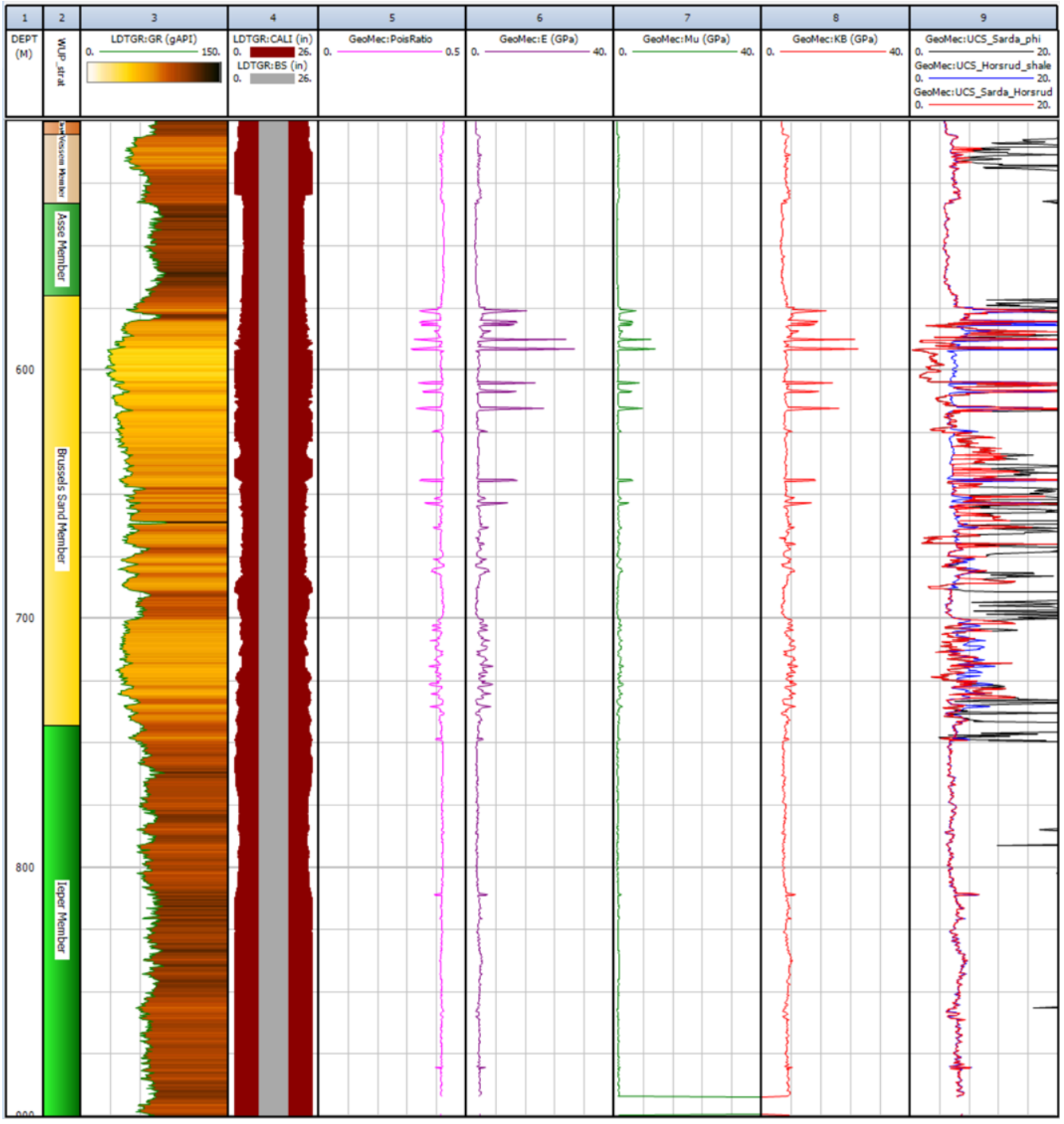

WARMINGUP
Innovatief Duurzaam Warmtecollectief

Adres
Princetonlaan 6
3584 CB Utrecht

Postadres
Postbus 80015
3508 TA Utrecht

Telefoon
088 866 42 56

E-mail
contact@warmingup.info

Website
www.warmingup.info

V1.0 6 oktober 2022